The kinetics of the heterogeneous alkaline isomerization of carbohydrates

THE KINETICS OF THE HETEROGENEOUS ALKALINE ISOMERIZATION OF CARBOHYDRATES

J.A.W.M. BEENACKERS

THE KINETICS OF THE HETEROGENEOUS ALKALINE ISOMERIZATION OF CARBOHYDRATES

THE KINETICS OF THE HETEROGENEOUS ALKALINE ISOMERIZATION OF CARBOHYDRATES

PROEFSCHRIFT

TER VERKRIJGING VAN DE GRAAD VAN DOCTOR IN DE TECHNISCHE WETENSCHAPPEN AAN DE TECHNISCHE HOGESCHOOL EINDHOVEN, OP GEZAG VAN DE RECTOR MAGNIFICUS, PROF. IR. J. ERKELENS, VOOR EEN COMMISSIE AANGEWEZEN DOOR HET COLLEGE VAN DEKANEN IN HET OPENBAAR TE VERDEDIGEN OP OP VRIJDAG 2 MEI 1980 TE 16.00 UUR

DOOR

JOHANNES ADRIANUS WALTHERUS MARIA BEENACKERS

GEBOREN TE BAVEL, GEMEENTE NIEUW GINNEKEN

DRUK WIBRO HELMOND

Dit proefschrift is goedgekeurd door de promotoren

Prof.drs. H.S. van der Baan

en

Prof.dr.ir. H. van Bekkum

aan mijn ouders

aan Ling

CONTENTS

CHAPTER 1

Introduction

1.1. CHEMURGY

The word *chemurgy* was coined by William J. Hale, and was first used in his book *The Farm Chemurgic* in 1934 (1). It was derived from the Greek words *chimia* (chemistry) and *ergon* (work) and was used for industrial utilization of farm products. A more modern and general definition might be the use of renewable resources for materials and energy (2,3). Among these renewable resources, carbohydrates rank first.

Carbohydrates are produced every year in large quantities by photosynthesis. The overall production is high in spite of a low efficiency. Only 0.8% of the solar energy that reaches the earth is used for fotosynthesis. One can hardly believe that this efficiency will not be further improved in the future (54). The annual production in terms of energy is 3.10^{21} J, while the world's annual energy consumption is presently only 3.10^{20}J (4).

Since the report of the Club of Rome was published, the interest in alternatives for energy and chemical feedstock is growing (5). Due to the enormously increased price of oil the economic attractiveness of processes based on carbohydrates instead of oil is increasing too (6-13). The most important potential resources in this respect are cellulose from wood ($0.8.10^{12}$ kg a^{-1}), sugar from cane and beet ($1.2.10^{11}$ kg a^{-1} in 1978) and starch from cereal crops, maize, potatoes and cassava (10^{12} kg a^{-1}) (13,14). *Cellulose* in the form of wood is applied as a construction material and as a fuel (15-17). Estimates regarding its present contribution to the annual energy consumption are 6 and 15% (18,4). Only about 10% of the cellulose is converted to paper, cellulose fibres and films, or to other commodities (19-24). *Sucrose* is mostly used directly in foods and allied products (25-28). Alcohol from sucrose containing materials as an supplementary alternative fuel and as a feedstock for chemical industry is becoming

important (29-31). *Starch* is mainly applied in food, paper, textiles and adhesives (32-36). About 10% is hydrolysed to glucose. From the monosaccharides obtained by hydrolysis, *glucose* is the most important as a base material for the chemical industry. Nowadays already a number of products can be produced from glucose at a commercial scale such as fructose, sorbitol and mannitol, ethanol, gluconic acid, lactic acid, glycerol and glycol (37-40). *Lactose* is one of the few carbohydrates from animal origin, which is produced in large quantities. It is prepared from whey, a by-product in the manufacture of cheese (41,42). Lactose is mainly used in pharmaceutical products.

This thesis deals with the kinetics of the heterogeneous alkaline isomerization of carbohydrates. In particular, the isomerization of glucose, fructose and mannose as well as lactose and lactulose, catalyzed by strongly alkaline ion exchangers has been studied.

1.2. ECONOMIC ASPECTS OF THE ISOMERIZATION PROCESS

Isomerization of glucose yields a mixture of glucose and fructose and small amounts of mannose. This mixture is known by many names, e.g. isoglucose, isomerose, fructo glucose, HFS (High Fructose Sirup). The sweetness of isoglucose (glucose : fructose $\tilde{\sim}$ 1 : 1) is about equal to that of sucrose, which makes it a good alternative for sucrose. Its application is somewhat limited because isomerose cannot be crystallized.

The development of the isoglucose production is strongly influenced by agro-political circumstances. Because the U.S.A. is the largest maize producer in the world, while it has to import sucrose, it was economically attractive to start the isoglucose production there as soon as the appropriate technology was developed in 1967 (47). In 1975 the annual production in the U.S.A. was already $0.45.10^9$ kg while in the E.E.C. the production then still had to be started. Due to the strong position of the farmers in the Common Market the E.E.C. Council of Agriculture Ministers decided to impose a lery on the manufacture of isomerose, taking effect as from 1 July 1977. On 25 October 1978, however, the European Court in Luxemburg repealed in fact this decision, so that for the near future an increased interest in the isomerization product of glucose can be expected (48,49).

Isoglucose as a feedstock for other processes opens up new fields of applications. The dehydration gives hydroxymethylfurfural (HMF) and levulinic acid (40) while by hydrogenation the important products sorbitol and mannitol are obtained (50).

The isomerization product of lactose can as such be used as a medicine against constipation and special forms of liver trouble (51, 52). Hydrogenation of the lactose gives lactitol and epilactitol (53), and oxidation gives lactobionic acid (101).

1.3. ISOMERIZATION OF CARBOHYDRATES

1.3.1. SURVEY

Since the work of Peligot (102,103) in 1838 and the important article of Lobry de Bruin and Alberda van Ekenstein (55) many articles have been published on the isomerization of carbohydrates*. The aldo-keto conversion is not only important for the glucose-fructose and the lactose-lactulose isomerization. According to the same mechanism we also can consider the isomerization of xylose to xylulose, galactose to tagatose, maltose to maltulose, melibiose to melibiulose and many others (56).

The glucose-fructose conversion can be carried out with two different kinds of catalysts:
- the enzyme glucose isomerase;
- alkaline catalyst, with or without additives.

These catalysts can be used in homogeneous as well as in heterogeneous reaction systems (57).

1.3.2. ENZYMATIC ISOMERIZATION

In 1957 Marshall and Kooi were the first to isolate an enzyme that converts glucose to fructose (58). Hardly ten years later a process based on this enzyme was applied in a commercial plant of the Standard Brands Company in the U.S.A. (47).

* In appendix 1 a survey of the structural formulas of various sugars and sugar-acids is given.

The most important characteristics of the process are (59):

- the selectivity is high;

  In Figure 1.1 $k_{GF} >> k_{GD}$ and $k_{FG} >> k_{FD}$;

- the catalyst costs are high.

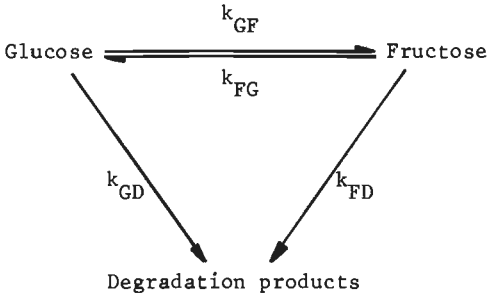

Figure 1.1. Simplified scheme of the isomerization and degradation of glucose and fructose.

When high purity of the glucose-fructose mixture as an endproduct is important, the enzymatic conversion will be the most preferable process (39). For all the other isomerizations, mentioned in section 1.3.1, no enzymes have been found yet, but all these reactions can be catalyzed by alkali.

1.3.3. ALKALINE ISOMERIZATION

Because alkali is the oldest isomerization catalyst in carbohydrate chemistry, many articles have been published about this subject. In chapter 5 a detailed literature survey will be given. The most important characteristics are (39):

- the selectivity is low;
- the catalyst costs are low;
- the process is simple.

The alkaline isomerization can be carried out homogeneous e.g. with NaOH as well as heterogeneous e.g. with ion exchangers. In case the isomerization is only the first step of a reaction sequence, the selectivity as well as the conversion can be increased to a great extent. By combining isomerization with e.g. a hydrogenation, the

fructose formed can be hydrogenated straight away to sorbitol (systematic name is glucitol) and mannitol, so that the fructose concentration remains relatively low. Because the degradation products are faster formed from fructose (in Figure 1.2: $k_{FD} \tilde{\sim} 3\ k_{GD}$), the total degradation will decrease and the selectivity will increase.

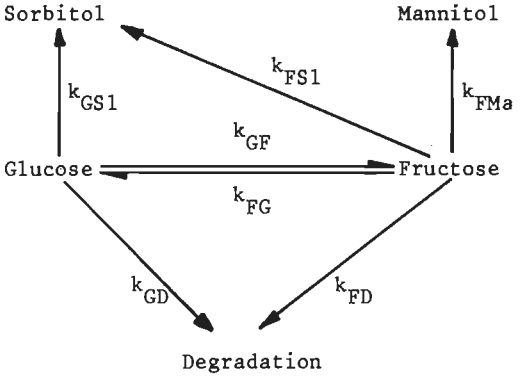

Figure 1.2. Simplified scheme of the isomerization, hydrogenation and degradation of glucose and fructose.

A second advantage is that the hydrogenation reaction is generally irreversible, so that the glucose conversion is not limited to the thermodynamic equilibrium value of about 50%. By combining both catalytic functions on the same catalyst carrier, little diffusional transport from the one type of site to the other is required. By depositing platinum on a strongly alkaline ion exchanger, and adding hydrogen to the reaction mixture, the isomerization of glucose and the hydrogenation reactions can both take place on such a bifunctional catalyst, so that sorbitol and mannitol are produced in one process step (246).

Vellenga (39) has shown that the hexose anion can be considered to be the active species in the isomerization reaction. Schematically the reaction system for the interconversion of glucose and fructose can be presented as in Figure 1.3.

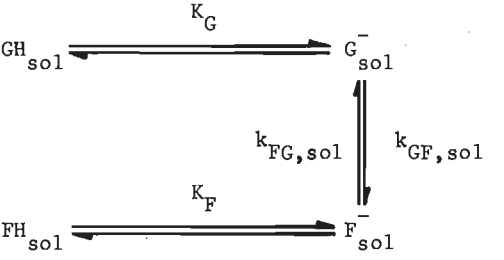

Figure 1.3. Kinetic description of the homogeneous isomerization of glucose to fructose. The index 'sol' refers to solution.

The molecular glucose in the solution GH_{sol}* will deprotonate, depending on the hydroxyl concentration and the ionization constant K_G. The ionized glucose G^-_{sol} will react to the fructose ion, which in turn is in equilibrium with non-dissociated fructose.

For the heterogeneous isomerization the same reaction is supposed to occur inside the catalyst. The hydroxyl groups in the alkaline ion exchanger deprotonate the adsorbed glucose:

$$GH_{ie} + OH^-_{ie} \overset{K_G}{\rightleftharpoons} G^-_{ie} + H_2O_{ie}$$

The isomerization products desorb from the catalyst by diffusion. In Figure 1.4 the process is shown schematically. This scheme shows that the following steps have to be taken into account to describe the isomerization process:

- *dissociation*
  The dissociation in the solution and in the ion exchanger determine the concentrations of the hexose ions in these two regions.
- *homogeneous isomerization*
  Because the pH in the solution is relatively low (pH < 8) the homogeneous isomerization can be neglected.

* For all sugars (S) the next notation will be used:
SH = molecular sugar;
S^- = ionic sugar;
S = all sugar ($S = SH + S^-$).

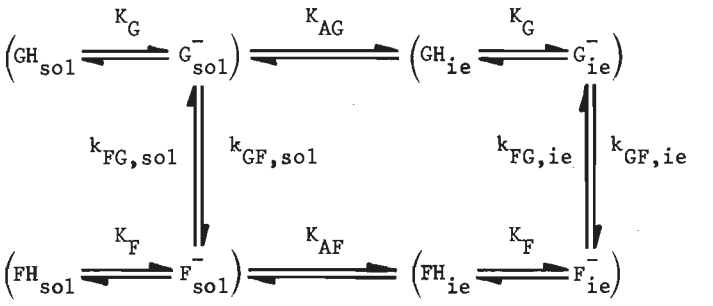

Figure 1.4. Kinetic description of the heterogeneous isomerization of glucose to fructose. The indices "ie" and "AS" refer to ion exchanger and adsorption of sugar, respectively.

- *adsorption*
  The equilibrium between the concentration of a sugar in solution and its concentration in an ion exchanger can be described by an adsorption constant (for gluclose: K_{AG}).
- *diffusion*
  When an ion exchanger is added to a glucose solution, diffusion of the glucose to the active sites in the catalyst occurs, and in the same way the isomerization products will diffuse to the solution where the concentration is lower.
- *heterogeneous isomerization*
  In an ion exchanger the hydroxyl concentration is very high. This gives a high degree of dissociation for the hexoses in the ion exchanger, so that isomerization can take place.

For the isomerization of lactose or other carbohydrates the same description applies.

1.3.4. ALKALINE ISOMERIZATION WITH ADDITIVES

The conversion of glucose to fructose is limited by the thermodynamic equilibrium between glucose and fructose in the solution. By adding a complexing agent selective for fructose, it is possible to reach a much higher conversion to the complexed product. It is clear that this higher yield must be paid for by a more complex and costly operation.

In 1960 Mendicino (60) reported a conversion of 80-85% to fructose for an alkaline isomerization in the presence of borate ions, but this high conversion has not yet been reproduced by other investigators (61-66).

A similar effect can also be reached by using sodium or potassium aluminate (68-78). In this way Shaw and Tsao (79,80) could reach a conversion to fructose of 70%. Almost no mannose has been found but the conversion to psicose was relatively high. These authors assumed that the complexed sugars were the active intermediates in the isomerization.

Recently Rendleman and Hodge (81) reported on this isomerization with the aid of an ion exchanger resin, treated with sodium aluminate:

$$NaAlO_2 + 2\ H_2O + Cl^-_{ie} \rightleftharpoons NaCl + Al(OH)_4^-{}_{ie} \qquad (1.1)$$

They found that the isomerization is catalyzed by hydroxyl, while the aluminate only complexes the fructose produced:

$$Al(OH)_4^-{}_{ie} \rightleftharpoons OH^-_{ie} + Al(OH)_{3\ ie} \qquad (1.2)$$

$$GH_{sol} + OH^-_{ie} \rightleftharpoons G^-_{ie} + H_2O \qquad (1.3)$$

$$G^-_{ie} \rightleftharpoons F^-_{ie} \qquad (1.4)$$

$$F^-_{ie} + Al(OH)_{3\ ie} \rightleftharpoons F\text{-}Al(OH)_3^-{}_{ie} \qquad (1.5)$$

The complexation of glucose and mannose appeared to be very low. Rendleman and Hodge found in an ion exchanger without borate the equilibrium constant $K_{GF} = k_{GF}/k_{FG} = 1.4$. With aluminate this constant was found to be 21. These data make it possible to calculate the equilibrium distribution between glucose and fructose in the ion exchanger. When the complexation of glucose can be neglected and we consider only glucose and fructose, we calculated:

G^-_{ie} = 4.5%
F^-_{ie} = 6.5%
$F\text{-}Al(OH)_3^-{}_{ie}$ = 89 %

For the isomerization of lactose and other oligo saccharides, the same effect is published (75,247-253). In chapter 5 we will come back to the isomerization of sugars.

1.4. AIM AND OUTLINE OF THIS THESIS

After the first publication of Rebenfeld and Pascu (82) many papers have been published on the heterogeneous alkaline isomerization of carbohydrates. See also chapter 5 for literature data. Besides the experimental data only data on the amount of fructose obtained or the measured D.E.-value* have been presented.

Recently, however, Rendleman and Hodge (81) published the first paper about the kinetics of the heterogeneous isomerization. Their measurements were carried out with a large excess of ion exchanger by injecting 0.1-0.2 mmol of hexose into a column of 3-4 cm^3 resin. After immersing the column in a constant-temperature batch for a chosen period of time, the sugars were washed from the column with 0.5-1.0 dm^3 of water and analyzed. All their experiments were carried out under the same conditions at 300 K with Bio-Rad AGZ-X8.

The main aim of this thesis was to study the kinetics of a heterogeneous alkaline isomerization process which can be applied directly for industrial purposes. For this reason the experiments were carried out with an excess of sugar instead of an excess of catalyst. This leads to special problems because under these circumstances not all the sugar can be adsorbed. When the excess of sugar is not too high, the catalyst will only be partly covered by adsorbed sugar. This coverage can be determined by adsorption experiments. Again in order to make our results applicable in industry we only used commercially available resins. Several factors were studied:

- the catalyst; about 20 resins were tested;
- the ion-form of the catalyst;
- the particle diameter of catalyst;
- the temperature;
- the concentration of the sugar in the solution and in the ion exchanger;

* D.E.-value (dextrose equivalence) = reducing ability based on dry material, relative to the reducing ability of glucose.

- the regeneration of the ion exchange resin.

Kinetic studies were carried out in a stirred tank reactor and a tube reactor. The experiments with the tube reactor will not be discussed in this thesis.

In chapter 2 the analysis of the various reaction mixtures is discussed. Two analytical systems based on ion exchange chromatography were used for the analysis of the isomerization products of glucose and lactose. A special colour reaction was developed to determine relatively low concentrations of ketoses in an aldose solution. Sugar acids were determined with the aid of isotachophoresis.

In the solution as well as in the ion exchanger the dissociated sugar are subject to isomerization (39,83,84). While in the ion exchanger the sugar concentrations are relatively high, the solvation can play an important role. For these reasons in chapter 3 the dissociation and solvation in not-diluted sugar solutions will be treated.

Chapter 4 deals with the properties of the catalyst. Diffusion and adsorption of sugars in ion exchangers were studied extensively because they play an important role in the kinetic results. When the diffusion is not slow relatively to the reaction it is very difficult to interprete the data. In that case it is indispensable to know the extent of adsorption in order to calculate the kinetic parameters from measured reaction velocities.

In chapter 5 literature data from the homogeneous and the heterogeneous isomerization will be discussed. Subsequently a kinetic model for the heterogeneous isomerization is introduced and a number of kinetic relations are derived. To interprete the experimental results a mathematical model is derived.

CHAPTER 2

Analysis

2.1. INTRODUCTION

For the study of the kinetics of a reaction, an accurate analysis of the reaction products is a prerequisite.

During the isomerization in an anion exchanger, the reactant and the reaction products will be distributed over the solution inside the catalyst and the free solution. The distribution over these phases can be described with adsorption constants. In chapter 3 we will return to this subject.

For the isomerization of glucose we can distinguish:

- the main isomerization products glucose*, fructose and mannose;
- several C_6-C_1 aldehydes and ketoses due to parallel and consecutive reactions, such as psicose (245,254), sorbose (255,256), glyceraldehyde and glycolaldehyde;
- sugar acids such as saccharinic acids, glycolic acid and formic acid.

In contrast with the circumstances in the experiments of Rendleman and Hodge (81) we can say that under our conditions the C_3-C_6 sugars are mainly in the free solution. On the other hand the sugar acids that are formed remain for almost 100% in the catalyst. To measure the quantity of the sugar acids we have to remove them from the catalyst e.g. with an excess of potassium chloride. As the chloride ion adsorbs very strongly, it will drive out the other products. Experimentally it is shown that a 3- to 4-fold of chloride is sufficient to remove more than 95% of the sugar acids.

Starting from lactose the following products will be formed:

- the main isomerization products of lactose, lactulose (O-β-D-galactopyranosyl-(1→4)-D-fructose and epilactose (O-β-D-galactopyranosyl-(1→4)-D-mannose);

* All products mentioned belong to the D-series.

- galactose in relatively high concentrations by glycosyl splitting of the disaccharides;
- other C_6-C_1 aldehydes and ketoses due to side- and consecutive reactions such as tagatose and talose from isomerization of galactose;
- sugar acids as saccharinic acids, glycolic acid and formic acid.

Thus, the composition of reaction samples can be quite complicated. However, depending upon the information required, a complete quantitative analysis is not necessary in each experiment. For most kinetic experiments starting with hexose, only the glucose, fructose and mannose concentrations are determined. For the lactose experiments generally the lactose, lactulose and galactose concentrations are measured only.

For the analysis of the reaction products we use 3 analytical techniques:

- ion exchange chromatography;
- colorimetric analysis of ketoses;
- isotachophoresis.

2.2. ION EXCHANGE CHROMATOGRAPHY

The analysis of the isomerization products by ion exchange chromatography has been described in several papers (85-94). For both the glucose and lactose isomerization reaction, analytical systems are developed.

2.2.1. EXPERIMENTAL

A scheme of the analytical system with a description is given in Figure 2.1. The eluant is kept at a temperature of 370 K to keep it degassed, and pumped to a precolumn with an Orlita membrane pump (type DMP/AE-10-4.4). This column, with a length of 130 mm and a diameter of 4 mm, is filled with a relatively inexpensive ion exchanger (Aminex AGZ-X8 from Bio-Rad). This column decreases the pressure pulsations across the analytical column and removes impurities in the eluant. The sample is injected by a self-made valve and a pneumatic actuator. The sample loop in injection valve 5 is filled with 10 nm^3

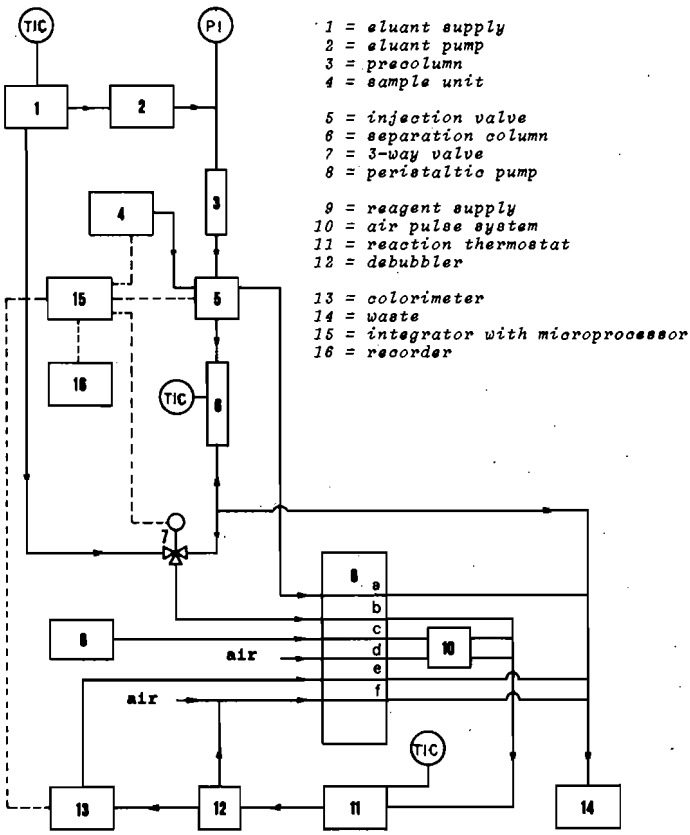

Figure 2.1. Block scheme of the liquid chromatograph. The flows of the peristaltic pump 8 are: a = 12 nm^3/s, b = 11 nm^3/s, c = 44 nm^3/s, d = 8 nm^3/s, e = 25 nm^3/s and f = 88 nm^3/s.

of sample by suction from the sample unit with a Technicon peristaltic pump 8 (type PPI). The thermostated separation column is slurry packed after suspending the ion exchange resin in 1 M NaCl. The dead volume on the top of the column is reduced to a minimum by using an adjustable spindle. The column is filled with Aminex A 25 from Bio-Rad with a particle diameter of 17.5 $\pm$ 2 µm. After the separation column almost 100% of the eluate is pumped to the reaction thermostat. For initial experiments the concentration of the starting material is relatively very high. To prevent an overload of the detection system, a three-way valve is mounted. When the eluant with too high a

concentration pulse leaves the separation column, the 3-way valve is switched to such a position that the pulse is drained to waste. The 3-way valve, the injection valve and the sample unit with the sample bottles are directed by a micro processor in the electronic integrator (L.D.C. type 304-50). This makes it possible to analyse continually without supervision. The detection takes place by reaction of the eluated components with orcinol reagent (70 v/v % H_2SO_4 with 1 g/dm^3 3,5-dihydroxytoluene). The reagent is segmented by air with a special air pulse system, mounted at the peristaltic pump. This makes it possible to inject air bubbles with the same frequency as the pump pulsation. Coherence of the pulsation of the pump and the pulsation by injection of air gives a strong decrease of the noise level. Just before the detector (Technicon single channel colorimeter) the reaction stream is debubbled by withdrawing only a part of the liquid through the cell of the colorimeter. To prevent pressure fluctuations in the cell an atmospheric outlet is created for the waste flow. The signals of the colorimeter are recorded and the peak areas are determined by the integrator.

2.2.2. ANALYSIS OF THE ISOMERIZATION PRODUCTS FROM GLUCOSE

This analysis is a modification of the method described by Verhaar and Dirkx (90). The analytical conditions are given in Table 2.1. The peak areas are converted to the corresponding concentrations is done by the relation:

$$C = c_1 A^{c_2} \qquad (2.1)$$

with C = concentration of a component in a sample;
A = peak area from the integrator;
c_1, c_2 = constants which can be calculated from the peak areas of calibration samples.

This equation makes it possible to correct for small deviations of the relation of Lambert-Beer ($c_2 \neq 1.0$).

Figure 2.2 gives a chromatogram of a reaction sample of the isomerization of glucose.

eluant composition	: .19 M H_3BO_3 .01 M $Na_2B_4O_7$ .025 M NaCl
eluant flow	: 11 nm^3/s
ion exchange resin	: Aminex A-25
column dimensions	: 215 x 4 mm
column temperature	: 348 K
chemical detection	: orcinol reagent
reagent flow	: 44 nm^3/s
reaction temperature	: 368 K
reaction time	: 800 s
detection	: colorimetric, 420 nm

Table 2.1. Conditions applied for the analysis of the glucose isomerization samples.

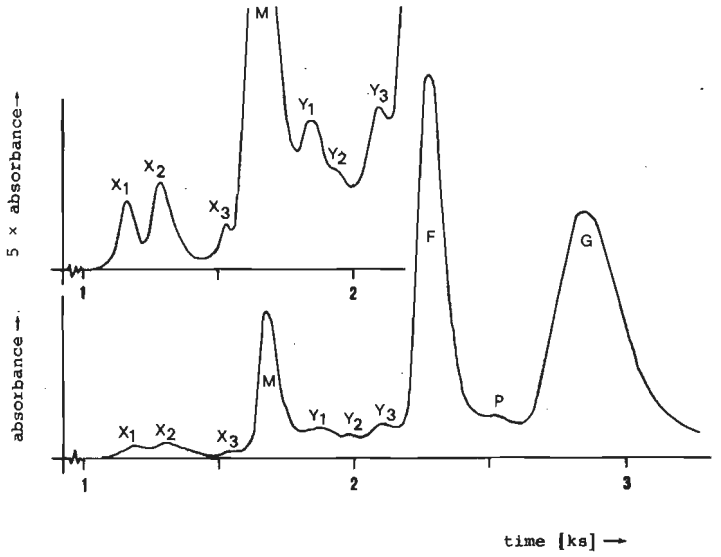

Figure 2.2. Chromatogram of a sample of an isomerization mixture obtained starting from fructose: M = mannose (1.1 mol m^{-3}), F = fructose (7.3 mol m^{-3}), P = psicose and G = glucose (6.4 mol m^{-3}). The upper curve is amplified 5 times as compared with the lower one.

The side-products X_1, X_2, X_3 and Y_1, Y_2 and Y_3 are present during heterogeneous as well as during homogeneous isomerization. The gross-retention times (t_r) relative to glucose are given in Table 2.2.

product	t_r
"injection"	.00
X_1	.38
X_2	.43
X_3	.57
M	.59
Y_1	.65
Y_2	.69
Y_3	.75
F	.80
P	.87
G	1.00

Table 2.2. Relative retention times of side products and isomerization products of glucose, fructose and mannose.

calibration sample	t_r
"injection"	.00
glycolaldehyde	.40
glyceraldehyde	.57
mannose	.59
arabinose	.65
ribose	.65
erithrose	.79
fructose	.80
psicose	.87
glucose	1.00
sorbose	1.20

Table 2.3. Relative retention times of calibration samples

For identification some calibration samples were injected. In Table 2.3 the results are given. Glycolaldehyde has a retention time between the products X_1 and X_2. Glyceraldehyde synchronizes with product X_3. Arabinose and ribose synchronize with product Y_1, while erythrose will be eluted together with fructose. Psicose[1)] gives a peak between glucose and fructose and sorbose will be eluated after the glucose peak.

1) Obtained from Dr. K. Vellenga of the Department of Technical Chemistry of the University of Groningen.

A more detailed identification of the products has not been carried out. The chromatogram of Figure 2.2 shows a reaction sample of fructose isomerized with low selectivity. Generally X_3, Y_2, psicose and sorbose are low and cannot be distinguished.

2.2.3. *ANALYSIS OF THE ISOMERIZATION PRODUCTS OF LACTOSE*

The determination of lactose, lactulose, epilactose, galactose and tagatose is similar to that given by Verhaar et al. (93). In Table 2.4 the analytical conditions are given.

eluant composition	: .400 M H_3BO_3
	.005 M $Na_2B_4O_7$
eluant flow	: 11 nm^3/s
ion exchange resin	: Aminex A-25
column dimensions	: 60 x 4 mm
column temperature	: 348 K
chemical detection	: orcinol reagent
reagent flow	: 44 nm^3/s
reaction temperature	: 368 K
reaction time	: 800 s
detection	: colorimetric, 420 nm

Table 2.4. Conditions applied for the analysis of the lactose isomerization samples.

An example of a chromatogram of a reaction mixture obtained starting from lactose is given in Figure 2.3. The signal of the last part of the chromatogram is amplified by a factor 10. Peak 5 was ascribed to talose. To confirm this an experiment was carried out starting with galactose. In figure 2.4 a chromatogram is given. Isomerization of galactose gives tagatose and in a smaller amount talose. This isomerization is similar to the conversion of glucose to fructose and a little mannose. Peak 7 (with 5 x extinction) has the appearance of a double peak. It was not identified. In analogy with the psicose

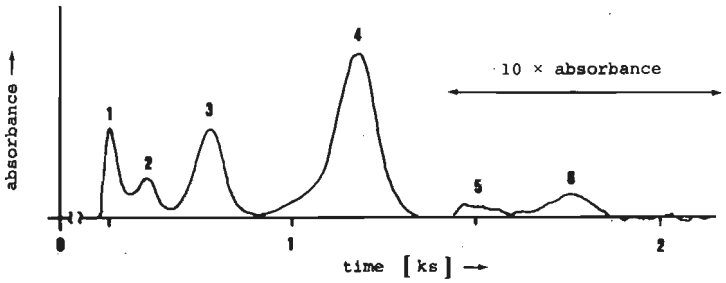

Figure 2.3. Chromatogram of a sample from a lactose isomerization experiment: peak 1 = remainder of the drained lactose peak, 2 = epilactose, 3 = galactose, 4 = lactulose and 6 = tagatose.

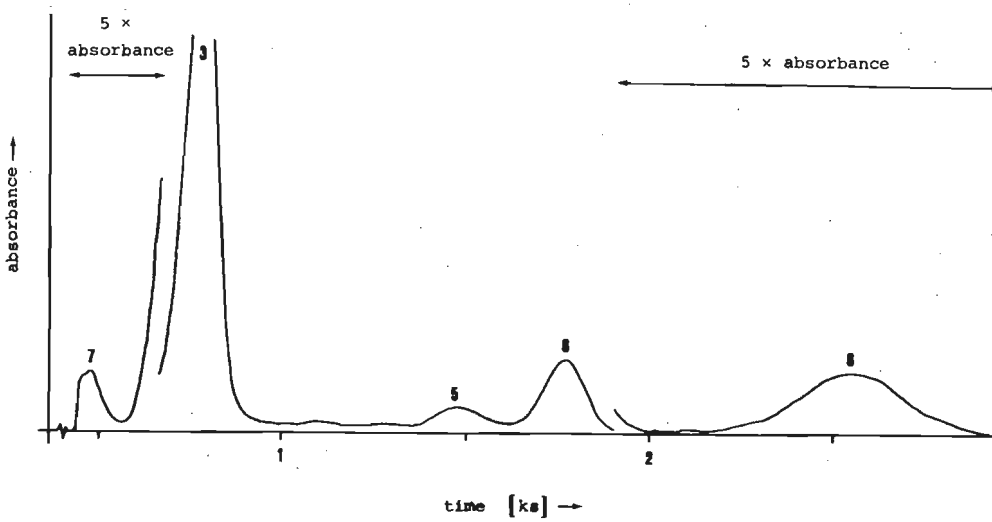

Figure 2.4. Chromatogram of a sample of an isomerization of galactose: peak 3 = galactose, 5 = talose, 6 = tagatose, 7 = unidentified and 8 = sorbose.

formation from fructose some sorbose can be expected (peak 8). This was checked by injecting a sample of the galactose isomerization mixture in the ion exchange chromatograph under the same conditions as for the analysis of glucose isomerization (see section 2.2.2).

In Figure 2.5 the chromatogram, combined with a calibration chromatogram is given.

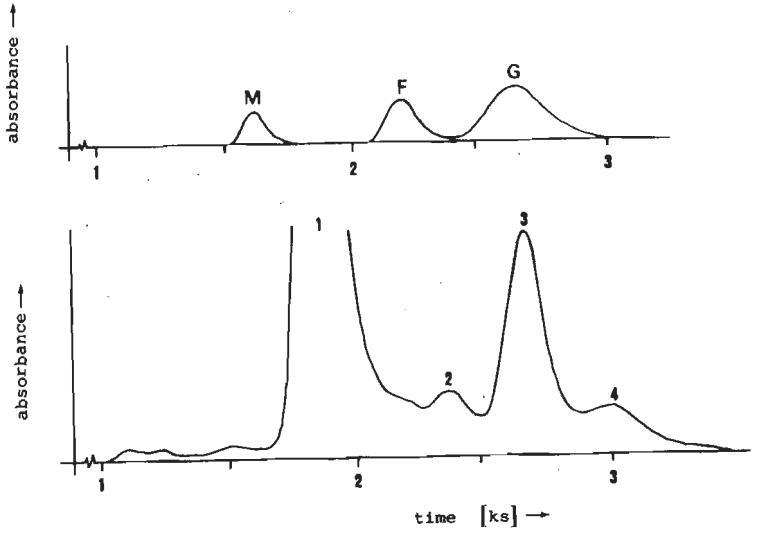

Figure 2.5. Chromatogram of a sample of an isomerization of galactose, analysed on a chromatograph under the conditions given for the analysis of glucose isomerization mixtures (Table 2.1): 1 = galactose, 2 = talose, 3 = tagatose, 4 = sorbose. The upper chromatogram is for a calibration sample with M = mannose, F = fructose and G = glucose.

The relative retention of peak 4 (1.20) is in full agreement with the value for sorbose (see section 2.2.2).

2.3. COLORIMETRIC ANALYSIS OF KETOSES

This analytical system makes it possible to determine ketoses quantitatively in the presence of a more than 5000 fold excess of aldose. It is based on the formation of coloured products by dehydratation of a ketose under the influence of hydrochloric acid. The concentration of the coloured products can be measured accurately with a colorimeter. Carbohydrates others than ketoses have only a minor influence on the results. Kennedy and Chaplin (94) showed that at a

wavelength of 415 nm the coloured products of glucose give an absorption which is only 0.05% of the absorption of fructose, while for mannose this value is 3.4%. This makes it possible to use this system for the analysis of the samples from the isomerization of glucose to fructose, of galactose to tagatose and of lactose to lactulose.

2.3.1. EXPERIMENTAL

A scheme of the analytical system is given in Figure 2.6.

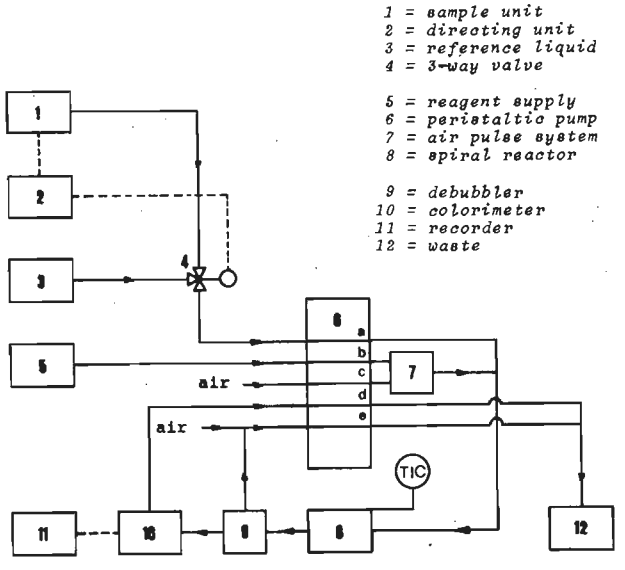

Figure 2.6. Block scheme of the ketose analysis. Flows of the peristaltic pump are: a = 12 nm^3/s, b = 56 nm^3/s, c = 12 nm^3/s, d = 10 nm^3/s and e = 88 nm^3/s.

For the determination according to this method a sample is drawn from sample unit 1 with a peristaltic pump (Chemlab type CPP 15). Air bubble segmented concentrated hydrochloric acid (chemically pure) is added, and the mixture is passed through a helical reactor. After atmospheric debubbling the colour is measured by a colorimeter (Chemlab Continuous Flow Colorimeter) and registred. To keep a stable base line it appeared necessary to keep the colorimeter thermostated at 300 K. Between two reaction samples the 3-way valve is excicated and

a reference sample introduced. It is preferable that the reference liquid is the same as the initial reaction mixture. This becomes important when concentrated samples with a high viscosity are used.

2.3.2. RESULTS

The analytical conditions for the fructose detection are given in Table 2.5.

sample flow	: 12 nm^3/s
reagent	: concentrated HCl
reagent flow	: 56 nm^3/s
reaction temperature	: 353 K
reaction time	: 16 s
wavelength	: 415 nm
cuvette length	: 10 nm
time for analysis	: 250 s

Table 2.5. Conditions for the ketose analysis.

When the total sugar concentration is lower than 50 mol m^{-3} we can use pure fructose solutions for the calibration. The lower detection limit is 0.1 mol m^{-3}. It is not possible to decrease this limit by increasing the reaction temperature because above 355 K the reagent starts to form bubbles in the reactor. Figure 2.7 shows an example of an analytical result. When the total sugar concentration is higher than 0.2 M, the calibration samples have to be a mixture of ketose and aldose with a total concentration equal to the total concentration of the unknown samples. When this is done not only the influence of the viscosity of the sample is eliminated but also the signal of the aldose is taken into account. To relate the concentrations to the signals an empirical relation of the following form has been used

$$\ln c_1 \cdot H = c_2 \cdot C^{c_3}$$

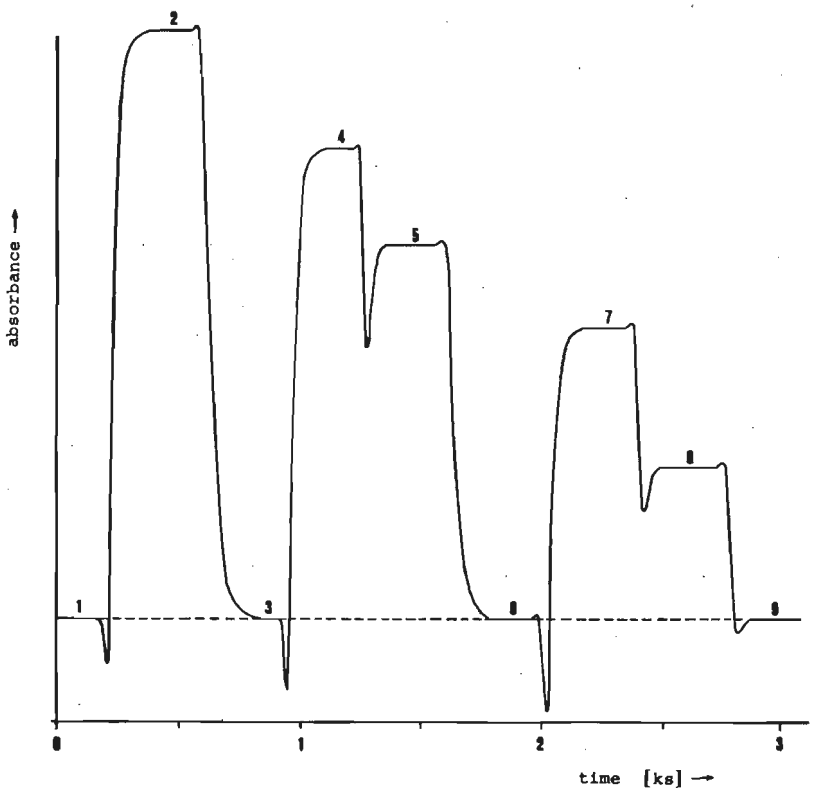

Figure 2.7. Extinction of calibration samples. The samples 1, 3, 6 and 9 contain the reference liquid, while the samples 2, 4, 5, 7 and 8 contain calibrations samples with a known ketose concentration.

with H = signal height with respect to the base line;
C = concentration of the ketose;
c_1, c_2, c_3 = constants which can be calculated from the signals of calibration samples.

In Figure 2.8 an example of a calibration curve is given.

For the detection of lactulose in a lactose solution the same analytical conditions have been used. Some calibration samples were obtained from pure lactulose, lactose and galactose (Figure 2.9).

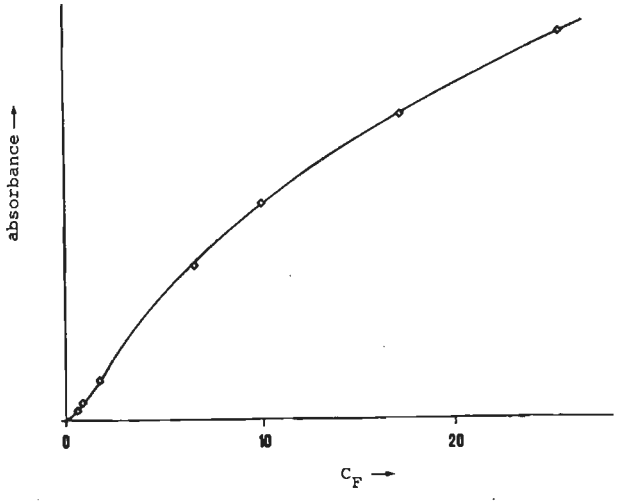

Figure 2.8. Calibration curve for the analysis of ketoses.

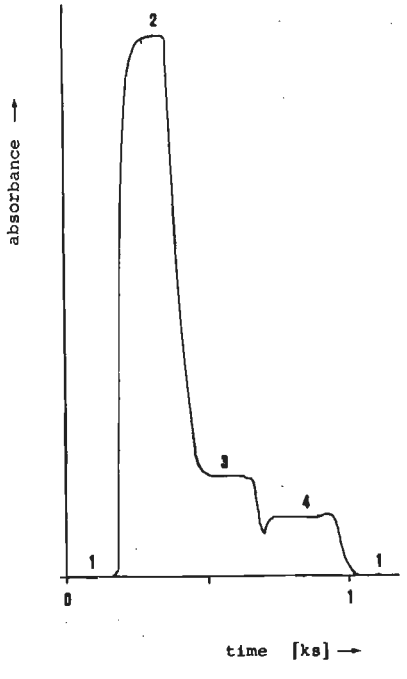

The signal per concentration unit, is for lactose 1.7 and for galactose .9 when the signal for lactulose is 100.

From these results we can conclude that for both isomerization reactions the ketose concentration can be determined accurately and quickly. The method has to be applied with circumspection because at higher conversions or under low selective circumstances the signal due to other ketoses as side products cannot be neglected any more.

Figure 2.9.
Calibration samples containing:
1 = water
2 = lactulose (10 mol m^{-3})
3 = lactose (100 mol m^{-3})
4 = galactose (100 mol m^{-3})

2.4. *ISOTACHOPHORESIS*

For the separation of ionic products washed from the ion exchanger, isotachophoresis is a most useful analytical system. The principle and the theoretical background of isotachophoresis have been described by Everaerts et al. (95-97).

Two sets of analytical conditions were used to analyse the degradation products. A good separation of C_5-C_6 aldonic acids can be realized at a relatively high pH of the terminator, while a separation of iso- and metasaccharinic acid requires a relatively low pH. In Table 2.6 and 2.7 the analytical conditions are given.

leading electrolyte	: .01 N Cl^- (pH = 6.02)
terminator	: .005 M morfoline ethane sulfonate (pH = 6.10)
counter ion	: histidine
capillary	: teflon: 200 x .5 mm
current strength	: 30 µa

Table 2.6. Conditions for the isotachophoresis of the C_5-C_6 aldonic acids.

leading electrolyte	: .01 N Cl^- (pH = 3.25)
terminator	: .01 M capronate (pH = 6.0)
counter ion	: β-alanine
current strength	: 30 µa

Table 2.7. Conditions for the isotachophoresis of iso- and metasaccharinic acid.

For the identification of the isotachopherogram metasaccharinic acid was prepared as described by Whistler (98) and isosaccharinic acid was obtained from Philips Duphar. For the identification of

2,4-dihydroxybutyric acid and 3-deoxypentonic acid an homogeneous glucose degradation experiment was carried out under the same conditions as described by Minderhout (99) and de Wit (100). The results are given in Table 2.8.

Products	Composition in mol %		
	de Wit	our results	
	1)		1)
formic acid	-	3	-
glycolic acid	3	3	3
acetic acid	-	6	-
lactic acid	69	60	66
glycerolic acid	1	1	1
2-methyl glyceric acid	1	1	1
2,4-dihydroxybutyric acid	9	8	9
3-deoxypentonic acid	1	3	3
saccharinic acids	14	15	17

Table 2.8. Comparison of the analysis of a glucose degradation experiment with results of de Wit (165).
1) formic acid and acetic acid are not taken into account to facilitate comparison.

As we found that 2-hydroxybutyric acid and 2,4-dihydroxybutyric acid show up at exactly the same place in the isotachopherogram, we assume that also 3,4-dihydroxybutyric acid may have the same transport rate. During isomerization of sugars 2,4-dihydroxybutyric acid as well as 3,4-dihydroxybutyric acid can be formed. In Figure 2.10 isotachopherograms of both analytical conditions are given.

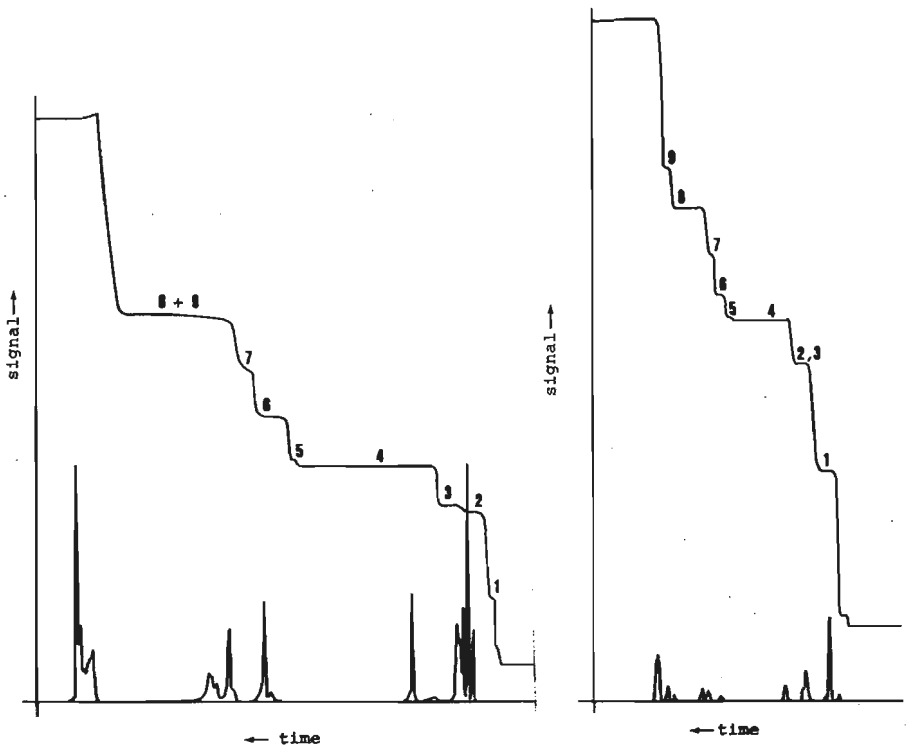

Figure 2.10. Isotachopherogram of a sample from the isomerization of glucose. The analytical conditions of the left isotachopherogram are given in Table 2.6, while the right one agrees with Table 2.7.

CHAPTER 3

Ionization and solvation of carbohydrates

3.1. INTRODUCTION

Carbohydrates are *ionized* in alkaline aqueous solutions. This reaction causes mutarotation and, via carbanion formation (enolate ion), isomerization and degradation take place.

Mutarotation is the transition between the α- and the β-hemiacetal isomers and the cyclic furanose and pyranose structures (104-106). Nowadays it is generally accepted that mutarotation takes place by ring-opening, forming a pseudo-cyclic intermediate (107-109). Also the solvent is supposed to play an important role (110,111). Gram et al. (112) and Kjaer et al. (170) found that the mutarotation is second order in the concentration of water. Kjaer et al. found that at low water concentrations this order even can rise to 3.7. This influence was also mentioned by other investigators (113-116). Recently de Wit et al. (117) stated that the complete rupture of the ring C-O bond, coupled with a substantial reorganization of the water mantle upon rotation will determine the energy barrier for mutarotation.

Mono- and reducible oligosaccharides are weak acids. The ionization of the anomeric OH-group is an essential step in the isomerization and epimerization reactions. As *ionization* is much faster than mutarotation (118,162), we can distinguish between the ionization constants of α- and β-forms. Los and Simpson (130) found for ΔpK_G (= $pK_{G,\alpha} - pK_{G,\beta}$ for the pyranose forms) a value of .29, while de Wit et al. (117) found that $\Delta pK_G = .19$. When only one pK_a-value is given in the literature, it must be considered to be an overall ionization constant. These constants have been determined for many carbohydrates at various temperatures (120-139). Different techniques were used including potentiometric, polarimetric, conductometric, thermometric, NMR and UV titrations. In Table 3.1 a survey is given of the pK_a-values at 298 K of five carbohydrates which are of interest for the

present study. All concentrations are expressed in mol m^{-3}. The concentrations in pH and pK_S, however, are expressed in kmol m^{-3}. This makes it possible to compare pK and pH values with literature data.

Author	pK_a				
	glucose	fructose	mannose	lactose	lactulose
Madsen (125)	12.23	11.99			
Hirch et al.(126)	12.107	11.693		11.98	
Urban et al.(127)	12.09	11.68			
Souchay et al. (128)	12.96				
Kilde et al.(129)	12.34				
Los et al. (130)	12.49[a)] 12.20[b)]				
Ramaiah et al. (131)	12.87	12.67			
Guillot et al. (132)	12.35	12.21	12.13		
Bunton et al. (133)	12.34 12.38				
Izatt et al.(134)	12.46	12.27	12.08		
de Wilt et al. (135)	12.51	12.31			
Christensen et al. (136)	12.28 12.72[c)]	12.03 12.53[c)]	12.08		
Degani (137)	12.35				
de Wit et al. (117)	12.78[a,d)] 12.60[b,d)] 13.9 [d,e)]	14.2[d,e)]	14.0[d,e)]	13.6[d,e)]	13.9[d,e)]

Table 3.1. Ionization constants of several sugars in a diluted aquous solution at 298 K. [a)] *= α-anomer;* [b)] *= β-anomer;* [c)] *= at 283 K;* [d)] *= at 276-278 K;* [e)] *= with a sugar concentration of 1100 mol* m^{-3}.

From this table we can conclude:

$$pK_{G,298\ K} = 12.4 \pm .25$$

$$pK_{F,298\ K} = 12.1 \pm .3$$

$$pK_{M,298\ K} = 12.1 \pm .1$$

When we leave out the results of de Wit et al., we see that fructose is more acidic than glucose ($\Delta pK_a = .27 \pm .10$). Izatt et al. (134) ascribed the lack of agreement between the various studies to the differences of the ionic strength of the solutions used. Thamsen (138) found at 273 K a slight increase of pK_a with increasing ionic strength. Degani (137) however was unable to find any influence.

Concentration glucose	$pK_{G,T}$				
	potentiometric			NMR	UV
	Michaelis and Rona (139)	Thamsen (138)		de Wit et al. (117)	de Wit et al. (83)
	290-292 K	291 K	273 K	277 K	283 K
.01				12.7	
.05		12.46	12.97		
.10	12.38	12.44	12.93		
.125					13.5
.20	12.28	12.40	12.88		
.50	12.26				13.8
1.0	12.05				
1.1				13.9	

Table 3.2. Literature data of $pK_{G,T}$ as a function of the concentration of glucose.

Only three authors describe a dependence of the pK_a on the hexose concentration. Michaelis and Rona (139) as well as Thamsen (138) found out that pK_a is decreasing with increasing glucose concentration, while de Wit et al. (117) found the opposite, as is shown in Table 3.2. In section 3.3.2 we will discuss this matter further.

Alsó, in an alkaline ion exchanger proton abstraction will take place before isomerization. Inside such a catalyst the concentration of the reaction components is relatively high. In view of the discrepancy of the literature data it was considered to determine the degree of ionization at high hexose concentrations.

3.2. EXPERIMENTAL

The ionization measurements were carried out by potentiometric titration. All chemicals used were pro analyse. The water used was distilled twice and CO_2-free. In a thermostated reactor of 150 cm^3, provided with a magnetic stirrer (Figure 3.1), the pH was measured with a glass electrode (Radiometer, type GK 2401 B) in combination with a pH controller (Radiometer, type TTT 1c).

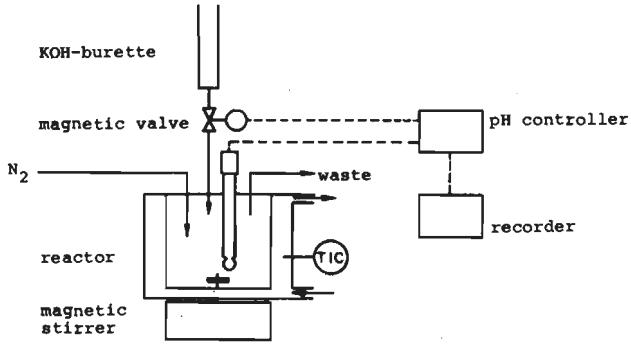

Figure 3.1. Reactor for potentiometric titrations.

Corrections were applied for the temperature and the concentration of the alkali. The electrode was calibrated with buffer solutions (Merck's Titrisol). The titration was controlled by titrating pure water with CO_2-free 1 N KOH solution. When more than 5 cm^3 KOH

solution was added, the calculated concentration OH^- differed less than 5%. The isomerization is neglected.

The experiments were carried out by titrating a known glucose solution (about 50 cm^3) under nitrogen to three different pH-values. All experiments are carried out at a temperature of 298 K.

3.3. RESULTS

The experimental results given in column (1)-(5) of Table 3.3 show the final composition of the glucose solution after adding the appropriate amount of alkali.

3.4. INTERPRETATION OF THE EXPERIMENTAL DATA

In solution, the chemical potential of each component is (140):

$$\mu_i = \mu_i^* + R \cdot T \cdot \ln (y_i \cdot C_i) \qquad (3.1)$$

with μ_i = chemical potential of a component in solution;
μ_i^* = reference value of the chemical potential;
R = gas constant;
T = temperature;
y_i = activity coefficient of component i;
C_i = concentration of component i.

For the solvent we define:

$$\mu_{H_2O} = \mu_{H_2O}^* + R \cdot T \cdot \ln (y_{H_2O} \cdot C'_{H_2O}) \qquad (3.2)$$

$\mu_{H_2O}^*$ = chemical potential of pure water, by consequence the concentration of water is expressed as a fraction:

$$C'_{H_2O} = C_{H_2O} / C_{H_2O,pure} \qquad (3.3)$$

Exp. nr.	$C_G \cdot 10^{-3}$ mol m^{-3}	$C_G \cdot 10^{-3}$ mol m^{-3}	pH	$C_{K^+(1)} \cdot 10^{-3}$ mol m^{-3}	$C_{OH^-(1)} \cdot 10^{-3}$ mol m^{-3}	$C_{G^-(1)} \cdot 10^{-3}$ mol m^{-3}	$K_{G(1)} \cdot 10^{9}$ mol m^{-3}	$pK_{G(1)}$	$\overline{pK_{G(1)}}$
(1)	(2)	(3)	(4)	(5)	(6)	(7)	(8)	(9)	(10)
1	.0635 .0611 .0563	.0602	10.05 11.00 11.50	.559 4.301 11.936	.112 1.000 3.162	.447 3.301 8.774	.632 .571 .584	12.200 12.243 12.234	12.226
2	.0635 .0610 .0561	.0602	10.97 11.00 11.50	.571 4.462 12.142	.117 1.000 3.162	.454 3.462 8.980	.612 .602 .603	12.213 12.221 12.220	12.218
3	.171 .156 .148	.158	10.04 11.00 11.20	1.234 9.986 14.331	.110 1.000 1.58	1.124 8.986 12.746	.604 .611 .595	12.219 12.214 12.226	12.220
4	.171 .156 .148	.158	10.03 11.00 11.20	1.221 9.782 14.231	.107 1.000 1.585	1.114 8.782 12.646	.612 .597 .590	12.213 12.224 12.210	12.222
5	.371 .352 .329	.351	10.00 10.50 10.80	2.828 7.757 13.772	.100 .316 .631	2.728 7.441 13.141	.741 .683 .659	12.130 12.166 12.181	12.159
6	.371 .353 .329	.351	10.01 10.50 10.80	2.737 7.584 13.830	.102 .316 .631	2.635 7.268 13.199	.699 .665 .662	12.156 12.177 12.179	12.171
7	.690 .673 .609	.657	9.81 10.11 10.50	3.945 7.573 16.442	.065 .129 .316	3.880 7.444 16.126	.876 .868 .860	12.057 12.061 12.065	12.061
8	.711 .701 .626	.679	9.90 10.01 10.50	5.037 6.314 16.361	.079 .102 .306	4.958 6.212 16.045	.884 .874 .932	12.054 12.059 12.080	12.064
9	1.194 1.106 1.007	1.102	9.53 10.00 10.30	4.479 11.448 19.366	.034 .100 .199	4.445 11.348 19.167	1.103 1.037 .972	11.958 11.984 12.012	11.985
10	1.144 1.108 1.047	1.100	9.53 10.00 10.20	4.403 11.281 16.175	.034 .100 .168	4.369 11.181 16.017	1.131 1.019 .980	11.946 11.992 12.009	11.982
11	1.526 1.496 1.384	1.469	9.30 9.50 9.90	4.040 5.966 12.986	.020 .032 .079	4.020 5.934 12.907	1.324 1.259 1.185	11.878 11.900 11.926	11.901
12	1.524 1.493 1.384	1.467	9.33 9.50 9.90	4.207 6.162 12.998	.021 .032 .079	4.186 6.130 12.919	1.288 1.304 1.186	11.890 11.885 11.926	11.900

Table 3.3. Experimental results and calculations of $K_{G(1)}$; C_{GH} is not in the table because $C_{GH} \sim C_G$.

As the experiments were carried out under constant atmospheric pressure, μ_i^* is only a function of the temperature. For non-ideal solutions $y_i \neq 1$.

When a solution is in equilibrium the chemical potential of the solution, G, is at a minimum and by consequence ΔG will be zero; hence:

$$\Sigma\, \nu_i \cdot \mu_{i\ eq} = \Sigma\{\nu_i \cdot \mu_i^*\} + R \cdot T \cdot \Sigma\{\nu_i \cdot \ln (y_i \cdot C_i)\}_{eq} = 0 \qquad (3.4)$$

$$\Delta G^* = \Sigma\{\nu_i \cdot \mu_i^*\} = - R \cdot T \cdot \Sigma\{\nu_i \cdot \ln (y_i \cdot C_i)\}_{eq} \qquad (3.5)$$

$$\Delta G^E = - R \cdot T \cdot \Sigma\{\nu_i \cdot \ln y_i\} \qquad (3.6)$$

with ΔG^* = the difference of free energy of the pure components;
ΔG^E = the excess free energy.

As μ_i^* is only a function of the temperature, ΔG^* will be also only a function of the temperature. The equilibrium constant is defined as:

$$\ln K_i = \Sigma\{\nu_i \cdot \ln (y_i \cdot C_i)\} = - \frac{\Delta G^*}{R \cdot T} \qquad (3.7)$$

Because pressure remains constant, the equilibrium constant should be only a function of the temperature.

Applied to a glucose solution and including hydration of all species:

$$GH \cdot h_{GH}\ H_2O + q\ H_2O \overset{K_G}{\rightleftharpoons} G^- \cdot h_{G^-}\ H_2O + H^+ \cdot h_{H^+}\ H_2O \qquad (3.8)$$

$$p\ H_2O \overset{K_{H_2O}}{\rightleftharpoons} H^+ \cdot h_{H^+}\ H_2O + OH^- \cdot h_{OH^-}\ H_2O \qquad (3.9)$$

with h = hydration number

$$q = h_{G^-} + h_{H^+} - h_{GH} \qquad (3.10)$$

$$p = h_{H^+} + h_{OH^-} + 1 \qquad (3.11)$$

$$K_G = \frac{y_{G^-} \cdot C_{G^-} \cdot y_{H^+} \cdot C_{H^+}}{y_{GH} \cdot C_{GH} \cdot y_{H_2O}{}^q \cdot C'_{H_2O}{}^q} \qquad (3.12)$$

$$K_{H_2O} = \frac{y_{H^+} \cdot C_{H^+} \cdot y_{OH^-} \cdot C_{OH^-}}{y_{H_2O}{}^p \cdot C'_{H_2O}{}^p} \qquad (3.13)$$

In the following sections the equilibrium constant will be calculated on the basis of three different assumptions:

1. ideal solution, no hydration;
2. non-ideal solution, no hydration;
3. non-ideal solution, hydration.

They will be discussed in next sections.

3.4.1. IDEAL SOLUTION, NO HYDRATION

In ideal solution the glucose and water dissociation constants (equation 3.12 and 3.13) are simplified to:

$$K_{G(1)} = \frac{C_{G^-} \cdot C_{H^+}}{C_{GH}} \qquad (3.14)$$

$$K_{H_2O(1)} = C_{H^+} \cdot C_{OH^-} \qquad (3.15)$$

During titration the total glucose concentration decreases somewhat. The following relations hold:

$$C_{H^+(1)} = 10^{3 - pH} \quad \text{mol m}^{-3} \qquad (3.16)$$

$$C_{OH^-}(1) = K_{H_2O(1)} / C_{H^+}(1) \quad (pK_{H_2O,298} = 13.9965) \qquad (3.17)$$

$$C_{G^-}(1) = C_{K^+}(1) + C_{H^+}(1) - C_{OH^-}(1) \quad \text{(electro-neutrality)} \qquad (3.18)$$

$$C_{GH(1)} = C_{G(1)} - C_{G^-}(1) \quad \text{(glucose balance)} \qquad (3.19)$$

In Table 3.3 column (6) and (7) the results of the calculations of C_{OH^-} and C_{G^-} are shown. Furthermore, the values of $K_{G(1)}$ and $pK_{G(1)}$ according to equation 3.13 are presented in column (8)-(10). As was mentioned in section 3.1 three authors (117,138,139,165) have found a relation between K_G and the glucose concentration. In Figure 3.2 literature data together with our results are given. For the sake of clearness only the data of column (10), Table 3.3, are given.

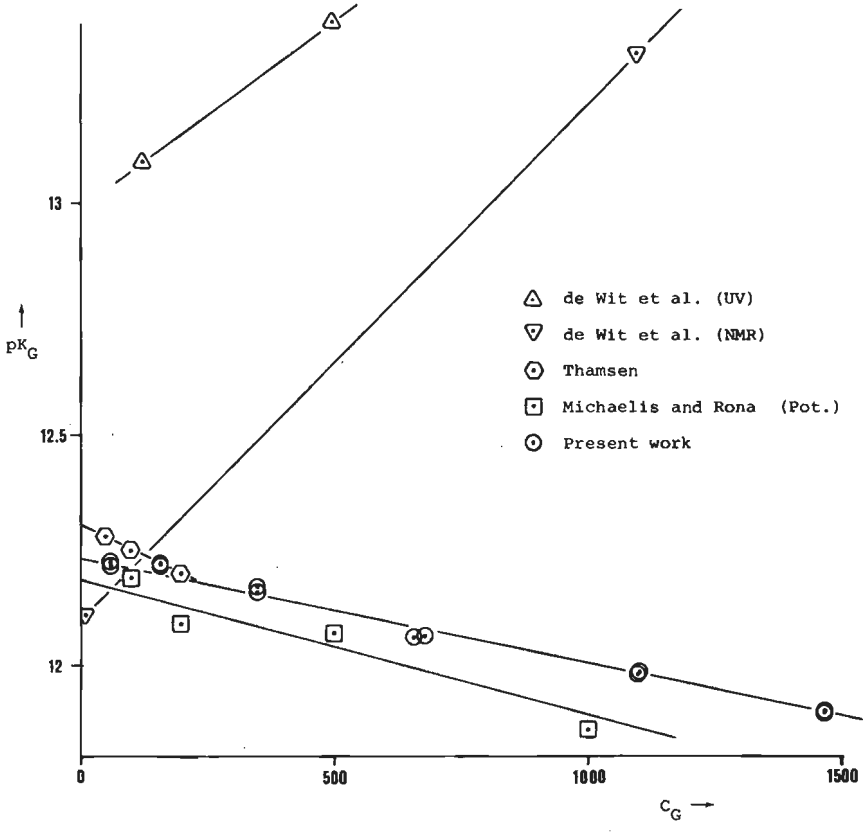

Figure 3.2. pK_G as a function of the glucose concentration at 298 K. The temperature dependence of the data of Thamsen is used to recalculate them to the reference temperature 298 K.

At low concentrations all results agree with the other literature data of Table 3.1. The concentration dependence of all potentiometric titrations (Thamsen, Michaelis and Rona and ours) agrees with each other, while the NMR- and UV-titration result shows an opposite dependence. Just like Thamsen we find a slight decrease of $pK_{G(1)}$ with increasing ionic strength. It is clear that this approach does not lead to a concentration independent equilibrium constant.

3.4.2. NON-IDEAL SOLUTION WITHOUT HYDRATION

Equations (3.12) and (3.13) are now simplified to:

$$K_{G(2)} = \frac{y_{G^-} \cdot C_{G^-} \cdot y_{H^+} \cdot C_{H^+}}{y_{GH} \cdot C_{GH}} \qquad (3.20)$$

$$K_{H_2O(2)} = \frac{y_{H^+} \cdot C_{H^+} \cdot y_{OH^-} \cdot C_{OH^-}}{y_{H_2O} \cdot C'_{H_2O}} \qquad (3.21)$$

$$\text{with } a_{H_2O} = y_{H_2O} \cdot C'_{H_2O} \qquad (3.22)$$

It is very difficult to calculate the thermodynamic activity of water in a multi-component system (163). For our experimental circumstances (Table 3.3) the glucose concentration C_{GH} is much higher than the ionic concentrations, viz.:

$$C_{GH} > 5.5\ (C_{G^-} + C_{OH^-}) \qquad (3.23)$$

For this reason the activity of water was provisionally assumed to be equal to a_{H_2O} in a pure glucose solution. The latter can be calculated from the measurements of Bonner and Breazeale (161). These authors gave the activity coefficient of glucose γ_{GH} and the osmotic coefficient ϕ_{GH} as a function of the glucose molality m_{GH} in a neutral solution. In formula:

$$\gamma_{GH} = 1 + .022 \cdot m_{GH}^{1.25} \qquad (0 \leq m_{GH} \leq 2) \qquad (3.24)$$

$$\phi_{GH} = 1 + .012 \cdot m_{GH}^{1.25} \qquad (0 \leq m_{GH} \leq 2) \qquad (3.25)$$

The activity of water can be calculated from (142):

$$\ln a_{H_2O} = - m_{GH} \cdot M_{H_2O} \cdot \phi_{GH} \cdot 10^{-3} \qquad (0 \leq m_{GH} \leq 2) \qquad (3.26)$$

with M_{H_2O} = mol weight of water.

The activity coefficient γ_{G^-} and γ_{OH^-} have been calculated with the Debye-Hückel expression, as corrected by Robinson and Stokes (142) for solvation and the activity of the solvent.

$$^{10}\log \gamma_i = \frac{- A_T \cdot I^{\frac{1}{2}}}{1 + B_T \cdot d_i \cdot I^{\frac{1}{2}}} - {}^{10}\log (1 - .018 \cdot h_i \cdot m_i) + h_i \cdot {}^{10}\log a_{H_2O} \qquad (3.27)$$

$$I = m_{K^+} + m_{H^+} = m_{G^-} + m_{OH^-} \qquad (3.28)$$

with $A_{298\ K}$ = .5115 $kg^{\frac{1}{2}}\ mol^{-\frac{1}{2}}$ (Debye-Hückel constant);
$B_{298\ K}$ = $3.291 \cdot 10^9\ kg^{\frac{1}{2}}\ mol^{-\frac{1}{2}}\ m^{-1}$ (Debye-Hückel constant);
d_{G^-} = diameter $G^- \sim 8 \cdot 10^{-10}$ m;
d_{OH^-} = diameter $OH^- \sim 2 \cdot 10^{-10}$ m;
h_i = solvation number; mol H_2O per mol i;
I = ionic strength in mol kg^{-1}.

The activity of water is calculated from γ_{GH}, γ_{G^-} and γ_{OH^-} with the Gibbs-Duhem equation (140). It appeared that a_{H_2O} calculated with relation 3.26 is a good approximation.

The thermodynamic quantities are between the following limits:

$$1.000 < \gamma_{GH} < 1.045 \qquad (3.29)$$
$$.882 < \gamma_{G^-} < 1.000 \qquad (3.30)$$
$$.853 < \gamma_{OH^-} < 1.000 \qquad (3.31)$$
$$.967 < a_{H_2O} < 1.000 \qquad (3.32)$$

To calculate the ionization constant a molality-molarity conversion has to be applied:

$$m_i = \frac{C_i}{\rho - M_{GH}\cdot C_{GH} - M_{G^-}\cdot C_{G^-} - M_{OH^-}\cdot C_{OH^-}} \qquad (3.33)$$

and for the density of the solution:

$$\rho = 1000 + 0.067\cdot C_G \qquad (3.34)$$

In Figure 3.5 the equilibrium constant $pK_{G(2)}$ is given as a function of the glucose concentration. We see that the linear concentration dependence of $pK_{G(2)}$ with regard of $pK_{G(1)}$ has almost not changed.

It is apparently not possible to eliminate the concentration dependency by using the best known thermodynamic quantities from the literature.

3.4.3. NON-IDEAL SOLUTION WITH HYDRATION

The literature data on the hydration of molecular glucose are given in Table 3.4. We see that at 298 K most authors report an hydration number of about 3.5.

For the hydration number of G^- no literature data are available.

From the entropy change during ionization conclusions have been drawn about the hydration of GH and G^- (153,165,166). For that reason we will pay attention to this matter. The entropy change during ionization in water is a result of:

- The change of the number of particles. From the point of view of statistical thermodynamics an increase of the number of particles causes an entropy increase of the system. When the hydration of the species formed, differs from that of the non dissociated compound, hydration will have an influence on the total entropy change;
- The increased ionic strength. Ions give an increase of the electrostatic field in the solution. The solvent water is strongly polar so that the water molecules will be hindered in their rotation (167, 168). This effect causes an entropy decrease upon ionization;

Investigator	h_{GH}			experimental method
	267 K	278 K	298 K	
Shiio (143)			3.5	ultrasonic interferometer
Yasunaga et al. (144)			3.5	ultrasonic interferometer
Tait et al. (145)		2.3	1.8	dielectric relaxation
		2.2		^{17}O NMR relaxation
Franks et al. (146)		6		dielectric relaxation
		5		^{17}O NMR relaxation
			3.5	compressibility
Harvey et al. (147)	>10			^{17}O NMR relaxation
Suggett (148)			3.7	dielectric relaxation
		2.7		freezing process
Miyahara (149)			2.0	activity method

Table 3.4. Hydration of glucose, literature data.

- The intramolecular hydrogen-bonding. An increase of intramolecular H-bonding will lead to a decrease of the entropy of the glucose molecule (153,330).

For glucose in solution an entropy change upon ionization of - 110 J mol^{-1} K^{-1} is calculated (119,128,134,136). Allen and Wright (166) ascribed this negative entropy effect to a decrease of the number of particles by an increase of the hydration of glucose during ionization. If one excludes the ordening effect of the electrostatical field, the entropy change upon ionization should be positive, when no change in hydration takes place. Christensen and Izatt (164) give a survey of the entropy change upon ionization of 103 acids. All of them exhibited a negative entropy effect.

In our opinion the entropy change upon ionization cannot be explained only by assuming an increase of the hydration of glucose. The electrostatic field, combined with intra-molecular hydrogen bonding, must have a dominating effect.

The stoichiometric coefficient p, as defined in equation 3.9 and 3.11, is generally given as 2 in literature (269,308,324-327). For the hydration of H^+ and OH^- mostly 1 and 0 are supposed (269,308).

Inside the ion exchanger the concentration of SH, S^- and OH^- can be very high. According to Schwabe (163) it is impossible to determine activity coefficients at high electrolyte concentrations. As we want to describe the ionization inside the resin, we looked for a more simple method. Therefore we replace the literature information on the activity coefficients of the various components in our system by the simple assumption that the excess free energy ΔG^E (equation 3.5) equals zero and that further effects must be ascribed to hydration. For the water relative concentration ($C'_{H_2O,free}$) hydration water is not taken into account. This approach was also used by other investigations (155-160). Equations 3.12 and 3.13 then are transformed to:

$$K_{G(3)} = \frac{C_{G^-\cdot aq} \cdot C_{H_3O^+}}{C_{GH\cdot aq} \cdot C'^{q}_{H_2O,free}} \tag{3.35}$$

$$K_{H_2O(3)} = \frac{C_{H_3O^+} \cdot C_{OH^-}}{C'^{2}_{H_2O,free}} \tag{3.36}$$

with

$$C'_{H_2O,free} = 1 - \frac{6.28 \cdot C_G + h_{GH} \cdot C_{GH} + h_{G^-} \cdot C_{G^-}}{55508} \tag{3.37}$$

In (3.37) we used the total relative water concentration:

$$C'_{H_2O,total} = 1 - \frac{6.28 \cdot C_G}{55508} \qquad (0 < C_G < 2000) \tag{3.38}$$

as calculated directly from literature data (154).

To obtain a concentration independent $K_{G(3)}$ an optimization criterion δ_{ion} is defined (318):

$$\delta_{ion} = \sum_{i}^{36} \left\{ \frac{K_{G(3)} - \overline{K_{G(3)}}}{\overline{K_{G(3)}}} \right\}^2 \qquad (3.39)$$

Minimizing δ_{ion} gives the best description of the experimental data with the used model. In Figure 3.3 δ_{ion} is given as function of the hydration of GH for several values of q (see equations 3.8 and 3.10).

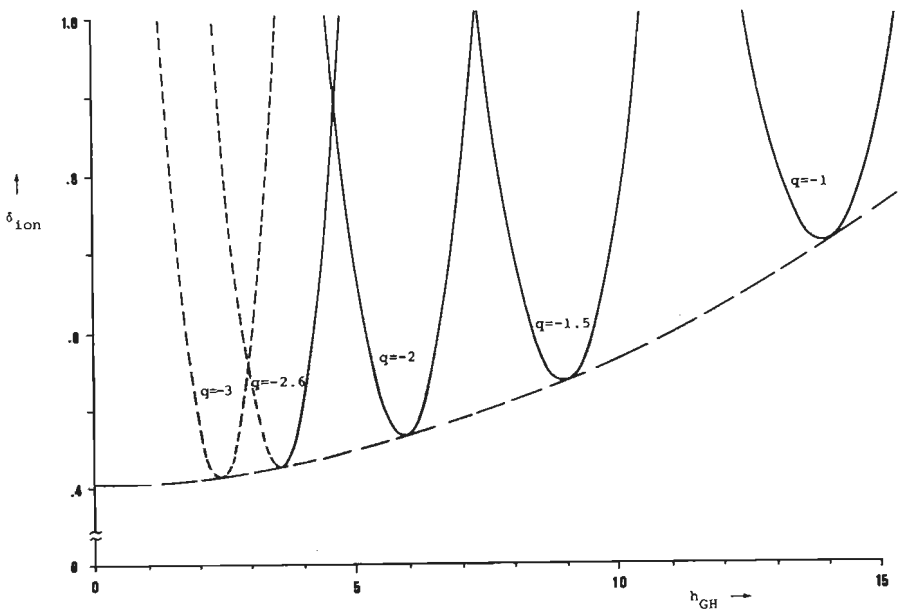

Figure 3.3. Optimization of the ionization constant with respect to the hydration of GH for different values of q. The dotted lines (---) represent negative hydration numbers of $\bar{G}$.

In Table 3.5. some points of the local minima are given.

q	h_{GH}	h_{G^-}	$K_{G(3)} \cdot 10^9$	$pK_{G(3)}$	$\delta_{ion,min}$
-0.5	22.5	21.0	.624	12.205	.1530
-1.0	13.9	11.9	.605	12.218	.0711
-1.5	9.0	6.5	.594	12.226	.0536
-2.0	6.0	3.0	.588	12.231	.0468
-2.2	5.0	1.8	.586	12.232	.0451
-2.4	4.3	0.9	.585	12.233	.0439
-2.6	3.6	0.0	.584	12.234	.0430
-2.8	2.9	-0.8	.584	12.234	.0421
-3.0	2.4	-1.6	.583	12.234	.0415

Table 3.5. Local minima of δ_{ion} as a function of h_{GH} at several values of q.

It is clear that, judging from $\delta_{ion,min}$, with decreasing q the description of the ionization improves. The hydration of G^-, however, cannot be negative so that the best result is:

$$q = -2.6 \quad (h_{GH} = 3.6 \text{ and } h_{G^-} = 0) \tag{3.40}$$

Since the optimization is subjected to statistical errors, it is safe to conclude from these results:

$$-2.6 < q < -2.0 \tag{3.41}$$

and by consequence:

$$3.6 < h_{GH} < 6 \tag{3.42}$$

$$0 < h_{G^-} < 3 \tag{3.43}$$

In Figure 3.4 the hydration of GH is given as a function of h_{G^-}.

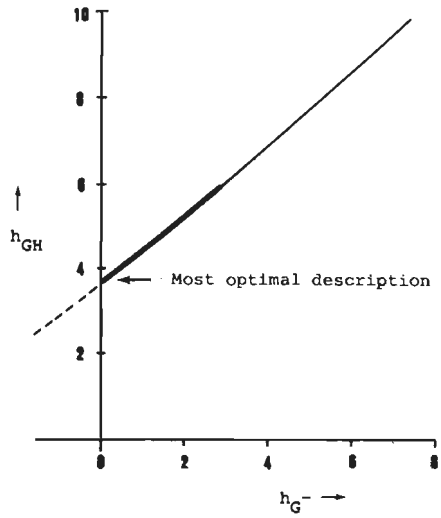

Figure 3.4. Hydration of GH as a function of h_{G^-} corresponding with the optimal description, corresponding with the dotted (- - - - - - - -) line in Figure 3.3.

In terms of hydration numbers the result is given by:

$$h_{GH} = 3.6 + .8 \cdot h_{G^-} \qquad 0 \leq h_{G^-} \leq 3 \qquad (3.44)$$

Combination of this relation with the result from the literature for the hydration of GH at 298 K of about 3.5 (143,144,146,148) gives an hydration number of G^- of about zero:

$$h_{GH} \sim 3.5$$

$$h_{G^-} \sim 0$$

This combination agrees also with the most optimal description of the experimental data (Figure 3.4). Although this combination of hydration numbers gives the best description and the value of h_{GH} agrees with the available literature data, we have to interprete these data

as the best possible estimates of the hydration within the assumptions made.

In Figure 3.5 the calculated $pK_{G(3)}$ is given, together with the linear relations of $pK_{G(1)}$ and $pK_{G(2)}$.

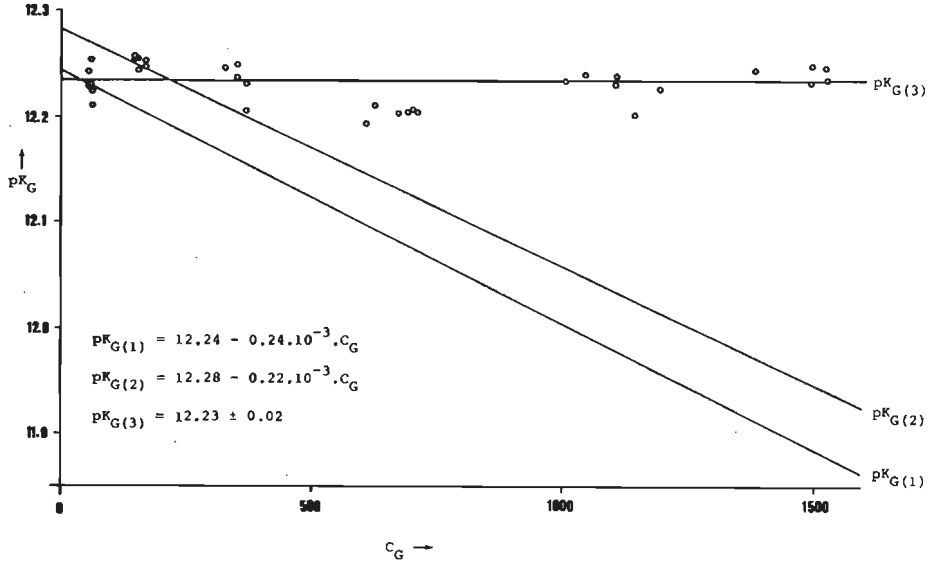

Figure 3.5. pK_G as a function of the glucose concentrations. The points belong to $pK_{G(3)}$.

3.5. INFLUENCE OF THE TEMPERATURE ON HYDRATION AND IONIZATION

In section 3.4.3 it was mentioned that hydration is decreasing with increasing temperature. Shiio (143) described the "adsorption" of water per hydroxyl group with a Langmuir adsorption equation:

$$\ln \frac{h_{GH}/n_{GH}}{1 - h_{GH}/n_{GH}} = \frac{\Delta H}{R \cdot T} + c_1 \qquad (3.45)$$

with n_{GH} = number of hydroxyl groups (for glucose $n_{GH} = 5$);
c_i = constant.

He found for glucose a heat of hydration of -55 kJ mol^{-1}. According to this model the hydration of glucose cannot exceed the number of hydroxyl groups. At low temperature however, Harvey et al. (147) found a hydration number of at least 10. For this reason we recalculated the experimental data of Shiio with a linear and with a Freundlich adsorption mode. The temperature dependence for both models can be described with:

$$\ln h_{GH} = - \frac{\Delta H}{R \cdot T} + c_2 \qquad (3.46)$$

In Table 3.6 the results are given.

Temperature	Experimental data of Shiio	Calculated data according:			
		Langmuir adsorption		Linear/Freundlich	
T	$h_{GH,exp}$	h_{GH}	δ_{hyd}	h_{GH}	δ_{hyd}
293	4.2	4.05	1.28	4.12	.40
298	3.5	3.72	3.93	3.60	.80
308	2.8	2.92	1.74	2.79	.02
318	2.2	2.07	3.47 / 10.42 +	2.19	.01 / 1.23 +
ΔH [kJ mol^{-}]		- 55		- 20	

Table 3.6. Hydration of glucose as a function of the temperature, with data of Shiio.

In column (3) and (5) the hydration numbers calculated with equation 3.45 and 3.46, respectively, using best estimates for ΔH and c_i are given. δ_{hyd} is defined according:

$$\delta_{hyd} = \frac{(h_{GH} - h_{GH,exp})^2}{h_{GH,exp}} \times 1000 \qquad (3.47)$$

It is clear that the linear/Freundlich adsorption models give a better fit for the description of the hydration of glucose. The corresponding heat of "adsorption" is then calculated to be -20 kJ mol^{-1}.

When we apply this temperature dependence to our experimental results, we find hydration numbers as given in Table 3.7.

T	267 K	278 K	298 K	303 K	313 K	323 K	333 K
h_{GH}	9.2	6.4	3.6	3.2	2.4	1.9	1.5

Table 3.7. Hydration of GH as a function of the temperature.

The low temperature hydration number $h_{GH,267\ K}$ is about the same as found by Harvey et al. (147).

The temperature dependency of the ionization constant is measured by de Wilt (135):

$$E_{ion,G} = -16.8\ kJ\ mol^{-1} \qquad (3.48)$$

3.6. DISCUSSION

In section 3.4.3 we found that during the ionization of glucose the hydration disappears. This can be understood from the difference in conformation between the ionic and the molecular form of glucose.

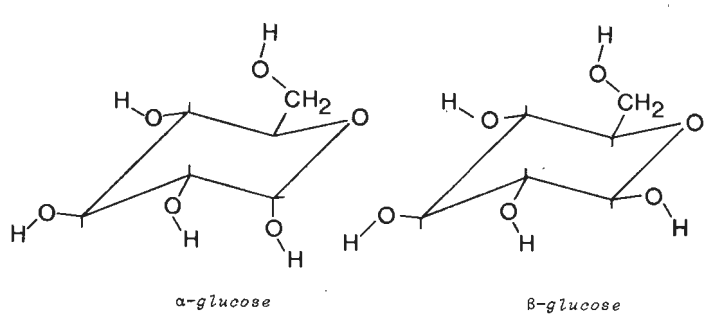

Figure 3.6. Conformation of α- and β-glucose molecule.

In the glucose molecule there are little if any intramolecular hydrogen bonds (153). In Figure 3.6 the conformation and α- and β-glucopyranose. Proton abstraction from the hemiacetal hydroxyl anomeric group gives a negative charge on the O_1-atom. Delocalization of this negative charge of oxygen of C_2-C_6 by intramolecular H-bonding was suggested by Rendleman (153). The conformation of glucose can then be considered as shown in Figure 3.7 for the α-glucose anion.

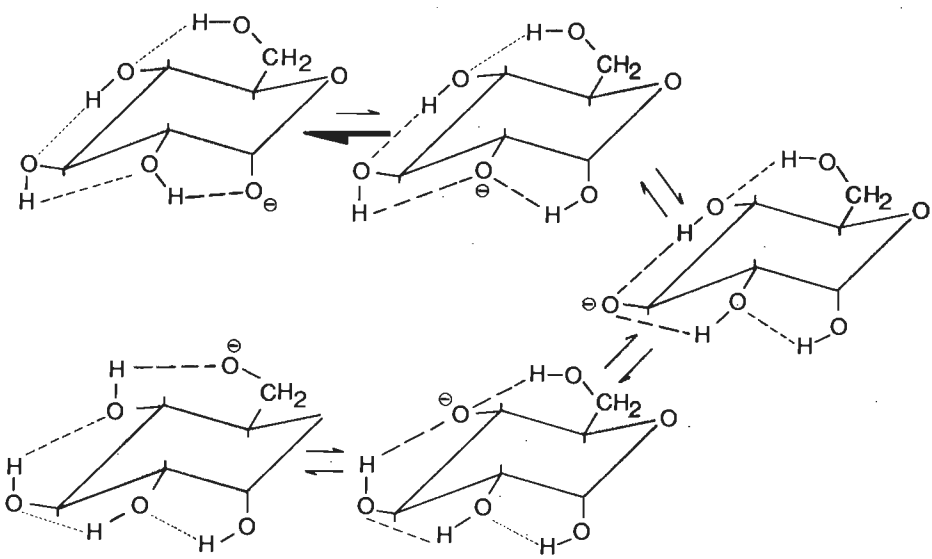

Figure 3.7. Intramolecular H-bonding in the α-glucose ion.

All ions shown in Figure 3.7 would exist in equilibrium with each other, with the C_1-anion predominating. Due to the intramolecular H-bonding the free rotation of the hydroxyl groups decreases. The hydroxyl groups then will be oriented preferently into certain directions for optimal H-bonding. This effect contributes to the entropy decrease of the glucose molecule upon ionization. The difference in entropy decrease between α- and β-glucose during ionization measured by Los and Simpson (119), can be ascribed to a difference of the strength of an axial-equatorial and an equatorial-equatorial hydrogen bonding (see Figure 3.8). In an axial-equatorial sequence of OH-groups, as is present in α-glucose with C_1OH/C_2OH, the system can

easily adapt the geometry for efficient H-bonding. The reverse is true for an equatorial-equatorial sequence of OH-groups (247).

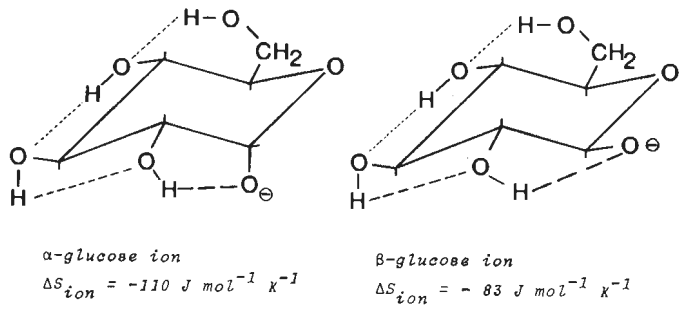

Figure 3.8. Intramolecular H-bonding in the α- and β-glucose ion.

The hydration of sugars can be considered as an hydration of the hydroxyl groups (143,146). It takes place by H-bonding between hydroxyl groups of a sugar and hydrate water molecules, as well as hydrate water molecules mutually. After ionization of glucose the hydroxyl groups are oriented and stabilized by intramolecular H-bonding. Consequently no glucose hydroxyl groups are then available any more for bonding towards solvent water molecules.

More detailed research will be necessary to evaluate the propounded hydration model.

In conclusion, the final formulae for the ionization constant of glucose will be represented here as a function of the hydration number of glucose:

$$K_{G(3)} = \frac{C_{G^-} \cdot C_{H_3O^+}}{C_{GH} \cdot C_{H_2O,free}^{(1-h_{GH})}} \qquad (3.49)$$

$$\frac{K_{G(3)}}{K_{H_2O(3)}} = \frac{C_{G^-} \cdot C'^{(1+h_{GH})}_{H_2O,free}}{C_{GH} \cdot C_{OH^-}} \qquad (3.50)$$

$$h_{GH} = 3.6 \cdot e^{\frac{20000}{R}\left(\frac{1}{T} - \frac{1}{298}\right)} \tag{3.51}$$

$$K_{G(3)} = .583 \cdot e^{\frac{-16800}{R}\left(\frac{1}{T} - \frac{1}{298}\right)} \tag{3.52}$$

CHAPTER 4

Properties of anion exchangers used as a catalyst

4.1. INTRODUCTION

Ion exchange resins can be used as a catalyst for almost all reactions, catalyzed by acids or bases. Kunin (171) gives a survey of the application and the catalytic activity of resins. The alkaline isomerization of glucose and lactose can be considered as one of the applications.

The carrier for the active groups in ion exchange resins is generally obtained by homogeneous copolymerization of styrene and 1.4-divinylbenzene. This carrier is homogeneous of structure and is known as gel-type. When the polymerization has been carried out in the presence of an inert solvent/non solvent (pertaining to polymer) system, macroreticular carriers are formed. The macroporosity is determined by the solvent/nonsolvent ratio. In Figure 4.1 both types of resin, used in our study, are indicated.

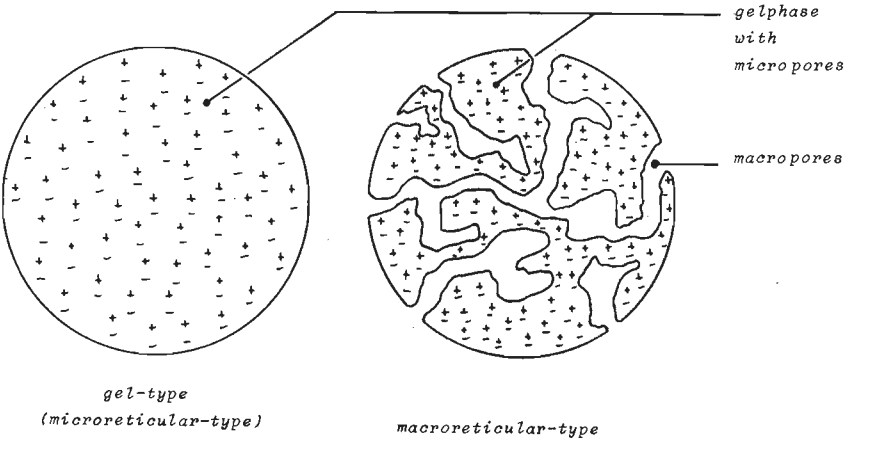

Figure 4.1. Gel- and macroreticular-type of resins.

The physical properties such as porosity, pore volume, pore radius and specific surface can be influenced by adding special additives (172,173,185) during the copolymerization. When the copolymer is treated with dichloromethyl ether in the presence of a Friedel-Crafts catalyst ($ZnCl_2$, $AlCl_3$, $SnCl_4$) and subsequently with a tertiary amine, a strongly basic type I anion exchanger is obtained (Figure 4.2.).

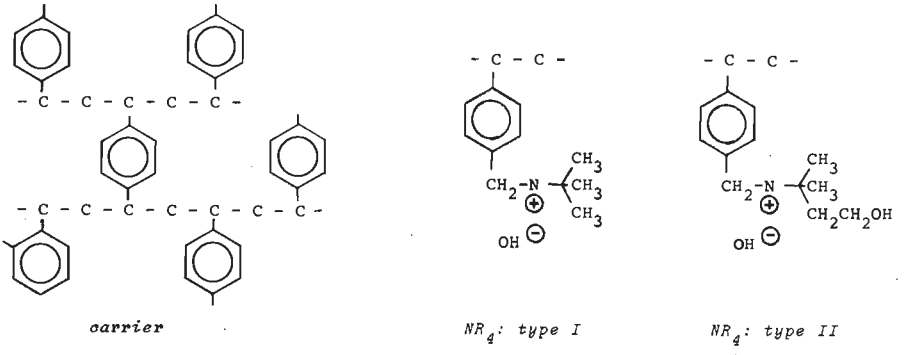

Figure 4.2. Presentation of strongly basic ion exchanger.

When a methyl group is replaced by an ethanol group, a so called type II resin is obtained. Weaker anionic resins have tertiary, secundary or primary amines as active groups.

The quaternary ammonium groups, initially with OH^- counter ions, are the active sites for the ionization and subsequent isomerization of hexoses. For the gel-type resin Amberlite IRA 401 the average NR_4^+-NR_4^+ distance ($\overline{d}_{site}$) is about 1 nm (181). For macroreticular resins $\overline{d}_{site}$ within the gel phase is difficult to determine because the polymer fraction of the particle is dependent of the used method. For this reason $\overline{d}_{site}$, as calculated in section 4.3.3, must be considered as an overall NR_4^+-NR_4^+ distance within the whole particle.

The physical properties of a catalyst can influence the catalytic activity and selectivity for a given reaction. For the isomerization of glucose, the fructose formed must be removed from the resin. The concentration gradient, necessary for diffusion, is a function of physical properties like porosity, pore volume and particle size. When due to these physical properties this diffusion is very slow, the concentration of fructose in the catalyst becomes relatively high.

As we mentioned in section 1.3.2 the rate of alkaline degradation of fructose is much higher than that for glucose, consequently a low rate of diffusion will lower the selectivity of the isomerization under all circumstances. For this reason much attention is paid to the physical properties in section 4.3, whereas the diffusion of sugars in ion exchangers will be discussed in section 4.4.

The adsorption relative to the capacity (degree of coverage) as a function of the concentration in the solution, of the temperature and of the type of catalyst, will be discussed extensively in section 4.5.

4.2. CHEMICAL PROPERTIES

4.2.1. ACTIVATION

Commercial available anion exchangers in the Cl^--form must be activated with alkali to bring them in the required hydroxyl form:

$$R\text{-}NR_3^+Cl^- + NaOH \rightleftharpoons R\text{-}NR_3^+OH^- + NaCl \qquad (4.1)$$

The activation procedure comprises the following steps:
- the ion exchanger is brought into a thermostated tubular reactor at a temperature of about 310 K;
- washed with at least 3 bed volumes of distilled water for at least 2 ks;
- activated with a 25-fold excess (relative to the amount of active groups in the resin) of 1 N NaOH solution during about 60 ks;
- and, finally, washed with at least 20 bed volumes of distilled water during at least 10 ks.

During the activation the gel-type exchangers will swell about 25% so that the reactor can be filled for about 70% only. The activated ion exchanger must be stored under N_2 to prevent CO_2-adsorption from the air.

During the use of the catalyst, the resin becomes deactivated. Such a deactivated resin can be reactivated by the same procedure. When the resin is strongly deactivated, a pretreatment with a solution of 2 M NaCl and 1 N NaOH can be applied. When the resin is so strongly contaminated that this pretreatment is not sufficient, a

pretreatment with hydrochloric acid will give better results. Some loss of active groups during reactivation with hydrochloric acid cannot be prevented (171,175). According to Tilsley (182) the macroreticular resins have better regenerative qualities. Christofides and Smits (183) worked out 4 different regeneration procedures.

4.2.2. CAPACITY DETERMINATION

To measure the amount of active groups (the capacity) of an ion exchange resin, the ion exchange resin is brought in a measuring cilinder with an excess of water and vibrated for 2 ks. During this vibration the particles are compacted towards their densest packing. The water above the bed was sucked off before the weight of the wet compacted resin (W_{wc}) as well as the volume (V_{wc}) was determined. Because Cl^- adsorbs much stronger than OH^- (171), a 3-fold excess of KCl is sufficient to drive out practically all the hydroxyl ions from the exchanger to the solution. With an automatic titration unit*) the obtained solution outside the resin can be titrated with HCl. In Figure 4.3 a titration curve of any fresh catalyst is given. The titrated Cl^- at the breakpoint (total capacity Cap_t) divided by the weight of the wet compacted resin (W_{wc}) is called *the specific capacity* (Cap') in mol kg^{-1}. In Table 4.2, section 4.3.3 the specific capacity of the used resins are tabulated.

The capacity of dried ion exchangers was also measured by elemental analysis. The C and H amount could be measured precisely while the N-determination is less accurate. Nevertheless, by repeating the analysis many times, we could establish that in Amberlite IRA 401 only 50% of the phenyl groups contains quaternary ammonium groups. For *each* new batch of activated ion exchanger the specific capacity must be determined because there are fluctuations in the properties of the commercial resins (5-10%). Furthermore it has to be ascertained that the ion exchanger is CO_2-free. When CO_2 adsorbs, we have:

*) The automatic titration unit from Radiometer as we have used consists of glass electrode type GK 2401 B, pH-controller type PHM, autoburette type ABU 11, titrator type TTT 60 and recorder type REA 160 with titrigraph module.

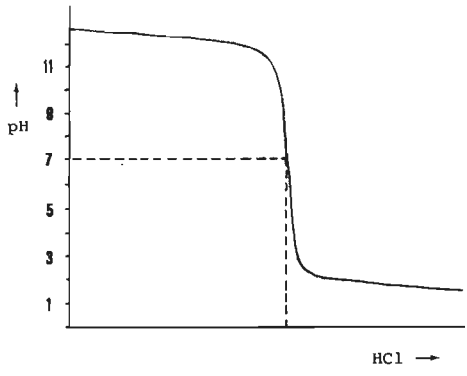

Figure 4.3. Shape of titration curve of a fresh resin in water.

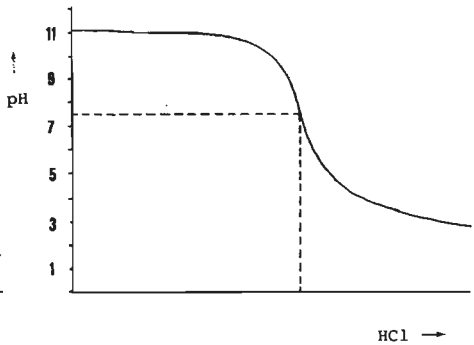

Figure 4.4. Typical titration curve of a deactivated resin in a sugar solution.

$$R\text{-}NR_3^+OH^- + CO_2 \rightleftharpoons R\text{-}NR_3^+HCO_3^- \qquad (4.2)$$

$$R\text{-}NR_3^+HCO_3^- + NR_4^+OH^- \rightleftharpoons (R\text{-}NR_3^+)_2CO_3^{2-} + H_2O \qquad (4.2')$$

and in the titration curve we then can distinguish 3 inflection points. When the specific capacity is known for a certain batch, the total capacity Cap_t can be calculated directly from the weight of the wet compacted resin:

$$Cap_t = Cap' \cdot W_{wc} \qquad (4.3)$$

When a component (i) adsorbs, the coverage (θ) is defined as the ratio of the adsorbed component (Ads_i in mol), relative to the total capacity:

$$\theta_i = \frac{Ads_i}{Cap_t} \qquad [mol\ eq^{-1}] \qquad (4.4)$$

To measure the rest activity of a deactivated resin (Ac_r in eq eq^{-1}) the total solution can be titrated in the reactor after adding a 3-fold excess of NaCl. Due to the presence of sugars the inflection

point is at about pH 7.5 instead of 7.0 (Figure 4.4). Experimentally it is proven that for the specific capacity as well as for the rest activity determination, a 3-fold excess of NaCl is sufficient.

4.2.3. STABILITY

4.2.3.1. MECHANICAL STABILITY

The mechanical stability of resins is a function of the porosity, the percentage of crosslinking, the additives, and, to a minor extent, other production conditions.

The stability of the ion exchanger increases with an increasing percentage of crosslinking but the porosity will generally decrease. In most cases macroreticular resins have a lower mechanical stability than gel-type resins. A high porosity with a reasonable mechanical strength is attained by using a high percentage of divinylbenzene, combined with monomeric modifications as terpinol (171,172,175).

The mechanical stability of gel-type ion exchangers is not different among themselves and is better than of macroreticular resins. From the macroreticular resins Amberlite IRA 938 has a very poor mechanical stability, relative to the others.

4.2.3.2. CHEMICAL STABILITY

The chemical stability of ion exchangers is dependent on the type of resin, the counter ion and the temperature.

Weakly basic ion exchangers are less stable than strongly basic resins (171). Of the strongly basic resins type II (of Figure 4.2) is less stable than type I (176).

An ion exchanger is much more stable in the chloride form than in the hydroxyl form (171,175).

At high temperatures the resin will loose activity (177-179). Two types of degradation reactions can be distinguished (175) for type I resins:

- the splitting off of trimethylamine from the ion exchanger:

$$R\text{-}CH_2\text{-}N(CH_3)^+OH^- \rightleftharpoons R\text{-}CH_2\text{-}CH_2OH + N(CH_3)_3 \qquad (4.4')$$

- the Hofmann degradation reaction:

$$N(CH_3)_3^+OH^- \rightleftharpoons CH_3OH + R \qquad (4.5)$$

In this way the strongly basic function is degenerated to a weak one. Both types of degradation occur in a ratio of about 1:1. In the case of type II resins elimination of the ethanol group, as acetaldehyde, may occur yielding $R\text{-}CH_2\text{-}N(CH_3)_2$.

4.2.4. SUMMARY CHEMICAL PROPERTIES

The chemical properties of ion exchangers, discussed in this section, are important when using these resins as catalysts.

A standardized activation of the ion exchanger is necessary to obtain a reproducable catalytic activity. To measure this activity a standardized capacity determination is developed. The mechanical as well as the physical properties are imperative to long time operations in commercial plants.

4.3. PHYSICAL PROPERTIES

4.3.1. PARTICLE SIZE

In section 4.1 we have seen already that diffusion may influence the selectivity. For this reason the particle diameter may have an influence on the selectivity. The particle size distribution was measured with a microscope. In Figure 4.5 the particle size distribution of Amberlite IRA 401 in the chloride form is given. The average particle diameter, defined as

$$\bar{d}_p = \sqrt[3]{\frac{\Sigma\ n_i \cdot d_p^{\,3}}{\Sigma\ n_i}} \qquad (4.6)$$

is the most appropriate quantity in theories in relating particle size with pore diffusion.

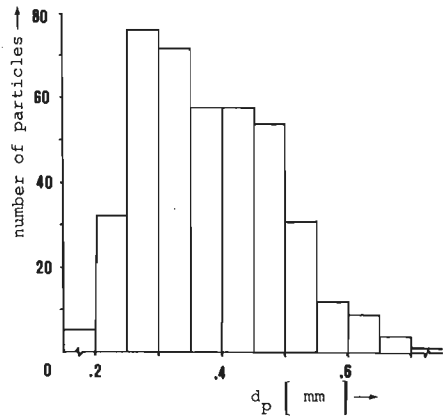

Figure 4.5. Particle size distribution of IRA 401.

In Table 4.1 the average particle diameters of some resins are presented. They do not exhibit large deviations. An increase of the average diameter of 8% (171) occurs during the conversion of the chloride form to the hydroxyl form.

Resin (OH^--form)	$\overline{d}_p$ mm
Amberlite IRA 401	.47
Amberlite IRA 900	.52
Amberlite IRA 904	.50
Amberlite IRA 938	.40

Table 4.1. Particle diameter of several resins.

4.3.2. POROSITY

With regard to the pore radius, anion exchangers can be divided into different groups. Oehme and Martinola (174) gave a survey of the various pore ranges and compared them with filtering materials (Figure 4.6).

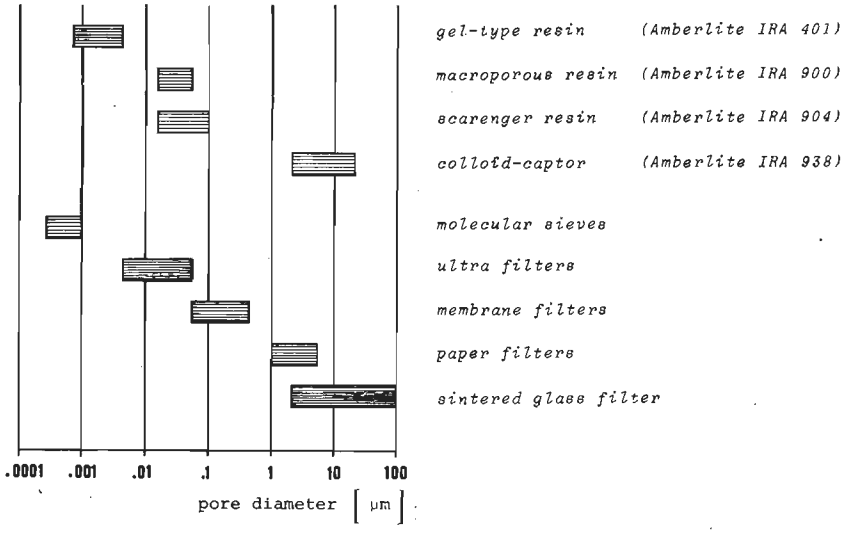

Figure 4.6. Pore diameter of some materials.

The porosity is studied with a mercury penetration porosimeter model 905-1 (180)*).

The lower limit of this method is about 5 nm, so that it was not possible to measure the porosity of gel-type resins.

In Figure 4.7 the porosity curve of Amberlite IRA 904, as measured by Hg-porosimetry, is shown. The line with circles (—o—), determined from right to left during the measurement, gives us the specific pore volume related to theory weight, available for mercury penetration. The average pore diameter of IRA 904 is .061 µm. In Figure 4.8 some pictures of this resin are given, made with a scanning electron microscope, type Stereoscan MK II.

*) We gratefully acknowledge the assistance of N. van Westen of the Delft University of Technology for performing the actual determinations.

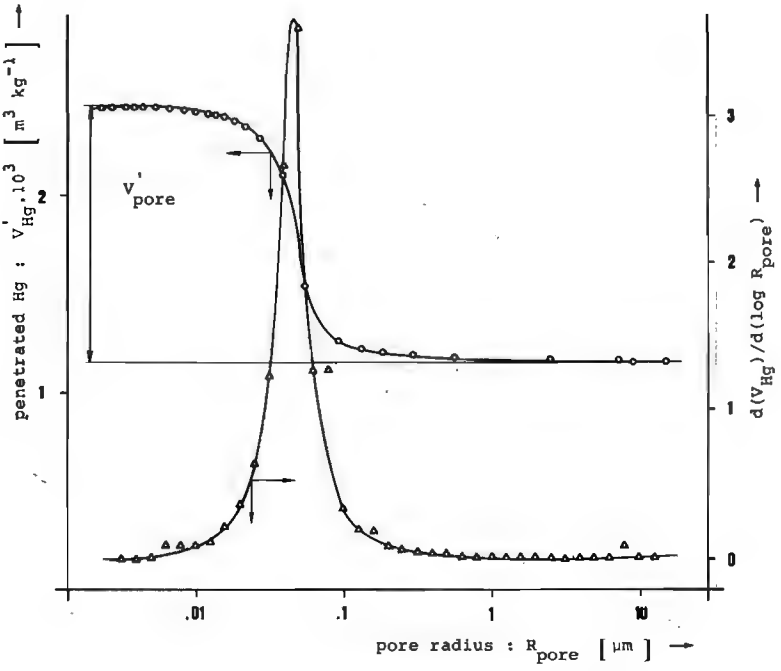

Figure 4.7. Porosity of Amberlite IRA 904: V'_{Hg} (—o—) and $d(V'_{Hg})/d(\log R_{pore})$ (—Δ—) as a function of the pore radius.

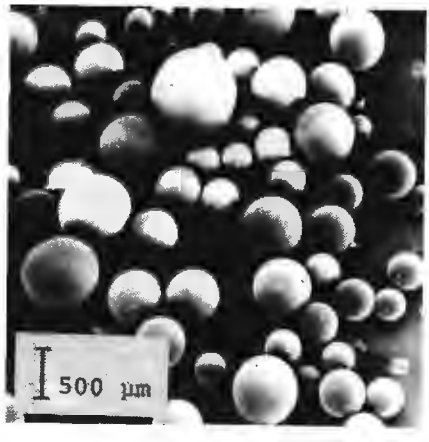

Fig. (a): survey

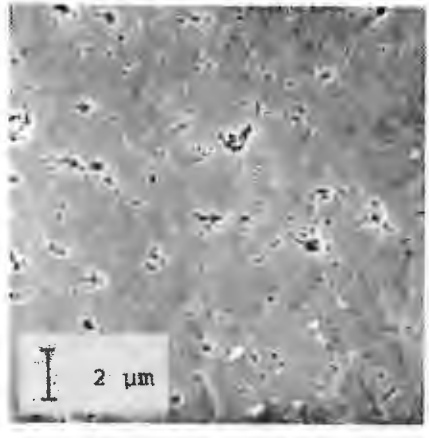

Fig. (b): visible pores

Figure 4.8. Pictures of Amberlite IRA 904. Figure (b) shows the pores in the macroreticular resin.

The porosity curve of Amberlite IRA 938 (Figure 4.9) shows at least 2 types of pores, one with radii about .17 μm and another around 8 μm.

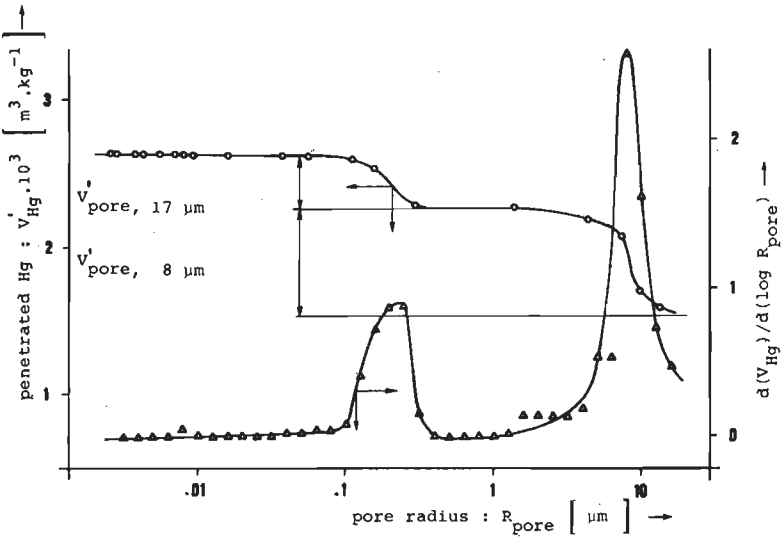

Figure 4.9. Porosity of Amberlite IRA 938.

There are very few pores with radii between .17 μm and 3 μm, so that at least two distinguishable kinds of pores must be present. In Figure 4.10 (a) and 4.10 (b) a picture of a narrow sieve fraction of IRA 938 is shown. In these pictures we can distinguish 2 types of particles present in a ratio of about 3:2, one type with large and one type with small pores. In the particle with large macro pores sometimes fusion of the sub-particles is noticed (Figure 4.10 (d)). In the Figures 4.10 (c) to (f) the pores can be studied in more detail. The electron microscope pictures confirm the mercury penetration measurement.

Fig. (a): survey

Fig. (b): 3 particles

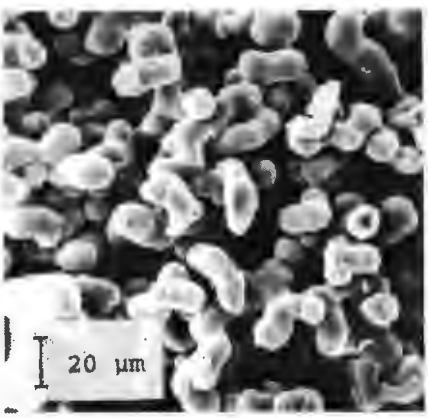

Fig. (c): large pores

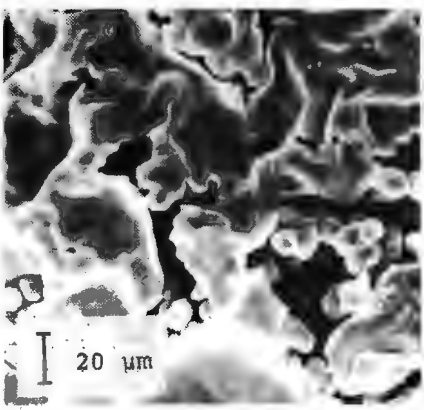

Fig. (d): large pores with fusion

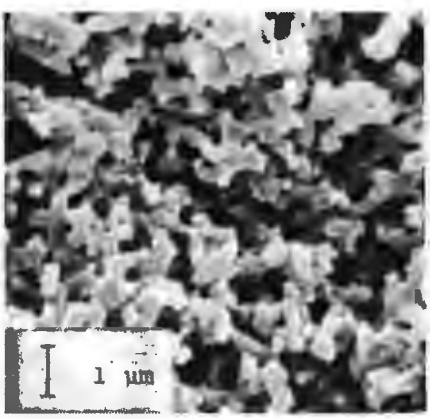

Fig. (e): small pores

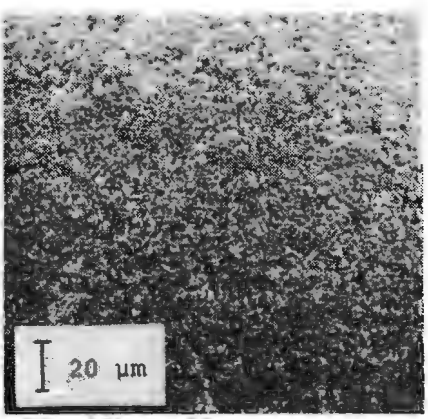

Fig. (f): small pores

Figure 4.10. Pictures of Amberlite IRA 938.

4.3.3. PORE VOLUME

To relate differences in catalytic selectivity to differences in concentrations in the catalyst pores, the *total* pore volume and the adsorption has to be known. The total pore volume was measured at a temperature of 293 K for several ion exchangers in the hydroxyl form. As the temperature dependence is very small, it can be considered to be independent of the temperature between 295 K and 323 K.

The following procedure was applied:
An amount of activated resin with a known W_{wc}, and Cap' is filtered for one minute on a suction filter, weighed (W_f) and then dried under vacuum at 400 K until its weight does not change anymore (100 ks): W_{pol}. We suppose that all the water has been evaporated. The density of the dry polymer (ρ_{pol}) is about 1100 kg m^{-3} and of the water in the resin (ρ_{H_2O}) it is about 1000 kg m^{-3}. For the exchanger in the hydroxyl form we can calculate:
- the weight fraction of the polymer, relative to the particle:

$$x'_{pol} = \frac{W_{pol}}{W_f} \tag{4.7}$$

- the volume fraction of the polymer, relative to the particle:

$$x''_{pol} = \frac{\rho_{H_2O} \cdot x'_{pol}}{\rho_{pol} \cdot \left(1 - x'_{pol}\right) + \rho_{H_2O} \cdot x'_{pol}} \tag{4.8}$$

- the pore volume, relative to the capacity:

$$PV = \frac{W_f - W_{pol}}{Cap' \cdot \rho_{H_2O} \cdot W_{wc}} \qquad \left[m^3\ eq^{-1}\right] \tag{4.9}$$

- the concentration of active groups relative to the pore volume:

$$C_{NR_4} = \frac{1}{PV} \qquad [\text{eq m}^{-3}] \qquad (4.10)$$

- the average distance between the active sites:

$$\bar{d}_{site} = \sqrt[3]{\frac{PV}{\left(1 - x''_{pol}\right) \cdot 6.02\ 10^{23}}} \cdot 10^9 \qquad [\text{nm}] \qquad (4.11)$$

In Table 4.2 column (1)-(7) the most important results for a series of ion exchange resins are given.

type	resin	Cap' $\frac{eq}{kg}$	x'_{pol} $\frac{kg}{kg}$	x''_{pol} $\frac{m^3}{m^3}$	$\bar{d}_{site}$ nm	$PV_{\theta=0} \cdot 10^3$ $\frac{m^3}{eq}$	$\frac{dPV}{d\theta_G} \cdot 10^3$ $\frac{m^3}{eq}$	$V'_{tot} \cdot 10^3$ $\frac{m^3}{eq}$
(1)	(2)	(3)	(4)	(5)	(6)	(7)	(8)	(9)
SB-I-G	Imac S-5-50	.86	.40	.38	1.07	.49	.038	1.5
SB-I-G	IRA 401	.83	.38	.36	1.09	.52	.070	1.6
SB-I-G	Lew M 504	.93	.31	.29	1.07	.53	.033	2.2
SB-I-MP	Lew MP 500	.78	.29	.27	1.13	.65	.078	2.4
SB-I-MP	IRA 900	.76	.29	.27	1.15	.66	-	2.4
SB-I-MP	IRA 904	.44	.35	.33	1.36	1.05	.127	1.9
SB-I-MP	IRA 938	.38	.19	.18	1.39	1.32	.025	4.3
SB-II-G	IRA 410	1.30	.50	.48	.94	.29	.023	1.0
SB-II-G	Imac S-5-42	1.06	.42	.40	.99	.38	-	1.4
SB-II-MP	Lew CA 9223	1.04	.38	.36	.99	.38	.177	1.6

Table 4.2. Experimental physical properties of some ion exchangers in the hydroxyl form. SB = strongly basic, I = type I, II = type II, G = gel-type, MP = macroreticular.

The differences among the various types of resins are evident. Various resins of the same type do not differ strikingly. The scavenger IRA 904 and the colloid captor IRA 938, however, have particular high porosities. From the point of low diffusion resistance these two exchangers are preferable.

When glucose adsorbs on a resin, this resin is converted from the hydroxyl form into the glucose form and a change of the pore volume is expected. With an adsorption experiment (section 4.5) the coverage of the resin with e.g. glucose relative to the capacity can be measured (θ_G). As not all the adsorbed glucose has to be dissociated, θ_G can be greater than one. The pore volume of this resin can be determined in analogy with the procedures for a fresh resin. In Figure 4.11 the final results are given.

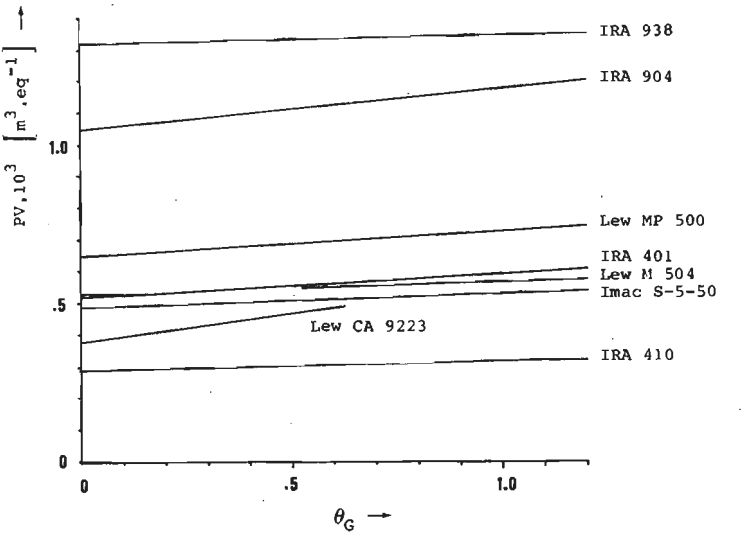

Figure 4.11. Pore volume as a function of the degree of coverage θ.

All the ion exchange resins swell when glucose adsorbs. The degree of swelling depends on the physical properties of the polymer skeleton (184). It can be defined by:

$$PV = \frac{dPV}{d\theta} \cdot \theta + PV_{\theta=0} \qquad (4.12)$$

In Table 4.2, column (7) and (8), the experimental results are tabulated for some resins. More information about the ion exchangers applied is given in appendix 2.

In column (9) the total specific pore volume relative to the dry weight (V'_{tot}) is given:

$$V'_{tot} = \frac{1 - x'_{pol}}{\rho_{H_2O} \cdot x'_{pol}} \qquad [m^3\ kg^{-1}] \qquad (4.13)$$

The total pore volume is supposed to be equal to the water content of the resin.

The high porosity of IRA 904 is not expressed in V'_{tot} because of its low water content and high polymer fraction relative to IRA 938 (column (4) and (5) of Table 4.2). The pore volume of macroreticular and type I resins is greater than that of gel and type II ion exchange resins.

In section 4.3.2 the porosity of the resins IRA 904 and IRA 938 as measured with a mercury penetration porosimeter is discussed. From Figure 4.7 and 4.8 the specific pore volume of the macropores (> 5 nm) can be read off directly. The difference with the total specific pore volume is roughly an indication for the amount of micropores (< 5 nm). In Table 4.3 the results are given.

Both resins have about the same fraction of macropores but differ markedly in the quantity of the micropores. The gel-phase of IRA 938 is much more porous than the gel-phase of IRA 904, which is caused by a higher degree of crosslinking of IRA 938.

Resin	V'_{tot} (all pores) $m^3\ kg^{-1}$	V'_{Hg} (macropores) $m^3\ kg^{-1}$	$V'_{tot} - V'_{Hg}$ (micropores) $m^3\ kg^{-1}$
IRA 904	1.9	1.3	.6
IRA 938	4.3	1.1	3.2

Table 4.3. Specific pore volumes of IRA 904 and IRA 938.

4.3.4. SUMMARY PHYSICAL PROPERTIES

The physical properties of ion exchangers are required to explain observed differences in catalytic activity and selectivity.

The particle size as well as the porosity may influence the diffusion of the reaction components inside the resin particle and by that the selectivity of the reaction. The pore volume, combined with adsorption data, yields the concentrations within the ion exchanger. This makes it possible to relate catalytic effects directly to conditions inside the catalyst.

For these reasons the measured physical properties will be used in chapter 5 of this thesis.

4.4. ADSORPTION

Adsorption of sugars on ion exchangers has been studied by a few authors only (192,193,202,254). Fujji et al. (192,193) measured the adsorption of sucrose, glucose and fructose on Amberlite IRA 900 and IRA 401. Their adsorption experiments with sucrose, carried out with $2 < C_{G_{sol}} < 60$ mol m^{-3}, could be described with a Freundlich relation. Sucrose, glucose and fructose adsorbed in this order increasingly on IRA 900, while the adsorption of sucrose on IRA 401 is somewhat less than on IRA 900. Addition of KCl decreased the adsorption of sucrose linearly while the Cl^- adsorbed completely on the resin. Besides the preliminary measurements of London et al. (202) and Turton and Pascu

(254) only the adsorption of glucose and fructose on a resin in the aluminate-form has been reported by Shaw and Tsao (78,79) very briefly.

Michaeli and Katchalsky (199) studied the adsorption of Na^+ on a cation resin by measuring the pH in the solution:

$$H^+_{ie} + Na^+_{sol} \rightleftharpoons H^+_{sol} + Na^+_{ie} \qquad (4.14)$$

The adsorption of sugars however cannot be measured with such a simple method.

For our kinetic study we need the adsorption of the different types of sugar on various types of ion exchangers as a function of the temperature and the concentration of the outside sugar solution.

The adsorbed sugar (S_{ie}) is partly dissociated. The dissociated sugar (S^-_{ie}) is more or less fixed on the active sites which causes a limited mobility. The mobility of molecular sugar, however, is not reduced by ionic forces.

4.4.1. ADSORPTION MODELS

In section 4.2.1 the activation of the resin was discussed. This operation can be considered as the exchange of the strongly adsorbing Cl^- with the more weakly adsorbing OH^- (204):

$$OH^-_{sol} + Cl^-_{ie} \rightleftharpoons OH^-_{ie} + Cl^-_{sol} \qquad (4.15)$$

Sugar anions adsorb roughly about equally strong as OH^-.

$$S^-_{sol} + OH^-_{ie} \overset{K_{ES}}{\rightleftharpoons} S^-_{ie} + OH^-_{sol} \qquad (4.16)$$

with

$$C_{OH^-_{ie}} = C_{OH^-_{ie},t=0} - C_{G^-_{ie}} \qquad (4.16')$$

As the hydration of the different ions is supposed to be only a function of the temperature, no solvation water has to be taken into account to define the exchange equilibrium constant:

$$K_{ES} = \frac{y_{S^-_{ie}} \cdot C_{S^-_{ie}}}{y_{S^-_{sol}} \cdot C_{S^-_{sol}}} \cdot \frac{y_{OH^-_{sol}} \cdot C_{OH^-_{sol}}}{y_{OH^-_{ie}} \cdot C_{OH^-_{ie}}} \tag{4.17}$$

In the solution outside the resin the total ionic concentration is very low (pH $\sim$ 7). According to the Debye-Hückel expression (relation 3.27), combined with a molality-molarity conversion, we can conclude:

$$y_{S^-_{sol}} \sim y_{OH^-_{sol}} \sim 1.00 \tag{4.18}$$

Inside the ion exchanger the total ionic concentration for gel-type resins is about 4000 mol m^{-3}, and is about equal to the concentration of the active groups. The ionic strength I (relation 3.26) is strongly dependent on the coverage. For glucose e.g. I increases from 4.0 to 7.5 mol kg^{-1} when θ_G (= θ_{GH} + θ_{G^-}) increases from 0 to 2. With relation 3.27 these values give the activity coefficients at 298 K as shown in Table 4.4.

	$y_{G^-_{ie}}$	$y_{OH^-_{ie}}$	$y_{G^-_{ie}} / y_{OH^-_{ie}}$
θ_G = 0; I $\sim$ 4.0	.69	.36	1.9
θ_G = 2; I $\sim$ 7.5	.68	.32	2.1
average	.68	.34	2.0

Table 4.4. Calculated activity coefficients in a gel-type anion exchanger according to equation 3.27.

The ratio $y_{G^-_{ie}} / y_{OH^-_{ie}}$ varies hardly with the concentration so that the average of 2.0 is used for all concentrations. Due to lack of further data we also assume that for all concentrations may be written:

$$\frac{y_{G^-_{ie}} \cdot y_{OH^-_{sol}}}{y_{G^-_{sol}} \cdot y_{OH^-_{ie}}} = 2.0 \qquad (4.19)$$

So that

$$0.5\ K_{EG} = \frac{C_{G^-_{ie}}}{C_{G^-_{sol}}} \cdot \frac{C_{OH^-_{sol}}}{C_{OH^-_{ie}}} \qquad (4.20)$$

The ionization in the solution as well as in the resin can be described with equation 3.50:

$$\frac{K_{G(3)}}{K_{H_2O(3)}} = \frac{C_{G^-_{sol}} \cdot C'^{\,(1+h_{GH})}_{H_2O_{sol}}}{C_{GH_{sol}} \cdot C_{OH^-_{sol}}} = \frac{C_{G^-_{ie}} \cdot C'^{\,(1+h_{GH})}_{H_2O_{ie}}}{C_{GH_{ie}} \cdot C_{OH^-_{ie}}} \qquad (4.21)$$

When equation 4.21 is substituted in equation 4.20 we find:

$$0.5\ K_{EG} = \frac{C_{GH_{ie}}}{C_{GH_{sol}}} \cdot \left\{ \frac{C'_{H_2O_{sol}}}{C'_{H_2O_{ie}}} \right\}^{(1+h_{GH})} \qquad (4.22)$$

$$\frac{0.5\ K_{EG} \cdot K_{H_2O(3)}}{K_{G(3)}} = K'_{EG} = \frac{C'^{\,(1+h_{GH})}_{H_2O_{sol}} \cdot C_{G^-_{ie}}}{C_{GH_{sol}} \cdot C_{OH^-_{ie}}} \qquad (4.23)$$

As the ion exchange particles have no net overall charge, the electroneutrality equation inside the exchanger must be obeyed:

$$C_{NR_4^+} + C_{H_3O^+_{ie}} = C_{OH^-_{ie}} + C_{G^-_{ie}} \qquad (4.24)$$

$$\text{with } C_{H_3O^+_{ie}} << C_{NR_4^+} \qquad (4.25)$$

The coverage for component i is defined as:

$$\theta_i = \frac{C_{i_{ie}}}{C_{NR_4^+}} \tag{4.26}$$

Substituting (4.26) in (4.23) gives us for sugar S:

$$K'_{ES} = \frac{C'^{(1+h_{SH})}_{H_2O_{sol}}}{C_{SH_{sol}}} \cdot \frac{\theta_{S^-}}{1 - \theta_{S^-}} \tag{4.27}$$

Some other adsorption models are:

Linear adsorption, with:

$$K_{LiS} = \frac{1}{C_{S_{sol}}} \cdot \theta_{S^-} \tag{4.28}$$

Langmuir adsorption (186), with:

$$K_{AS} = \frac{1}{C_{S_{sol}}} \cdot \frac{\theta_{S^-}}{1 - \theta_{S^-}} \tag{4.29}$$

Freundlich adsorption (189-191), with:

$$K_{FrS} = \frac{1}{C_{S_{sol}}^{\alpha}} \cdot \theta_{S^-} \tag{4.30}$$

Sips adsorption (194-198), with:

$$K_{SiS} = \frac{1}{C_{S_{sol}}^{\alpha}} \cdot \frac{\theta_{S^-}}{1 - \theta_{S^-}} \tag{4.31}$$

The Sips model is the most universal. The other models are just special cases of the Sips model.

In section 4.4.3 these models will be discussed in more detail to describe the experimental data of the adsorption of sugars on ion exchangers.

4.4.2. EXPERIMENTAL

The adsorption experiments were carried out under N_2 in a thermostated stirred reactor of 200 cm^3. A sugar solution is brought into the reactor and recirculated via the measuring and reference cell of a thermostated refraction meter (Waters, R4). When the system is stable, the reference cell is shortcircuited and an amount of ion exchanger is added. Adsorption causes a decrease of the concentration of the solution. The solution is titrated with a more concentrated sugar solution to maintain the original concentration. In Figure 4.12 a block diagram is given.

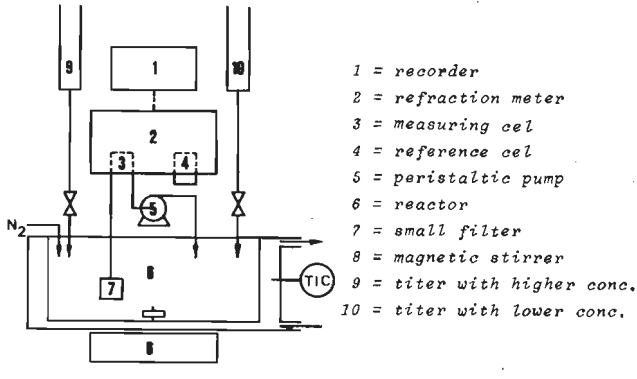

Figure 4.12. Block diagram for adsorption experiments.

To prevent chemical reactions, the experiment starts at 273 K. When adsorption equilibrium is reached, the temperature is raised with increments of 5 K. At these higher temperatures sugar desorbs from the resin. The solution must then be titrated with a more diluted solution.

A series of adsorption experiments have been carried out covering a concentration range from 0.2 to 2000 mol m^{-3}, temperatures between 273 and 313 K and the sugars glucose, fructose, mannose, lactose and lactulose. The exchangers IRA 401, IRA 900, IRA 904, IRA 938 and Lewatit M 504 have been studied in this way.

4.4.3. RESULTS AND DISCUSSION

The degree of coverage of a sugar (θ_S) can be calculated from the adsorption experiments, and from that the pore volume and $C_{NR_4^+}$ (equation 4.9 and 4.10). The total sugar concentration inside the resin is:

$$C_{S_{ie}} = C_{SH_{ie}} + C_{S^-_{ie}} = (\theta_{SH} + \theta_{S^-})\, C_{NR_4^+} = \theta_S \cdot C_{NR_4^+} \qquad (4.32)$$

In chapter 3 the ionization of glucose has been discussed. To calculate the ionization for other sugars in the ion exchanger, the following assumptions are made:

- for the hydration phenomenon:

$$h_{F^-} = h_{M^-} = h_{G^-} = 0$$

$$h_{La^-} = h_{Lu^-} = h_{FH} = h_{MH} = h_{GH}$$

$$h_{LaH} = h_{LuH} = 2\, h_{GH}$$

- The ionization constants of the other sugars are estimated from literature data (Table 3.1). The activation energies of K_G and K_F, measured by de Wilt (135), are used to estimate the influence of the temperature on the ionization:

$$pK_{G,298} = 12.23 \text{ with } E_{ion,G} = -17 \text{ kJ mol}^{-1}$$

$$pK_{F,298} = 11.96 \text{ with } E_{ion,F} = -22 \text{ kJ mol}^{-1}$$

$$pK_{M,298} = 11.97 \text{ with } E_{ion,M} = -20 \text{ kJ mol}^{-1}$$

$$pK_{La,298} = 12.36 \text{ with } E_{ion,La} = -17 \text{ kJ mol}^{-1}$$

$$pK_{Lu,298} = 12.09 \text{ with } E_{ion,Lu} = -22 \text{ kJ mol}^{-1}$$

As the resin particles are electrically neutral, the electro-neutrality equation holds:

$$C_{NR_4^+} + C_{H_3O^+_{ie}} = C_{S^-_{ie}} + C_{OH^-_{ie}} \tag{4.33}$$

with

$$C_{S^-_{ie}} = C_{S_{ie}} - C_{SH_{ie}} \quad \text{and} \quad C_{H_3O^+_{ie}} << C_{NR_4^+} \tag{4.34}$$

It is now possible to calculate $C_{SH_{ie}}$, $C_{S^-_{ie}}$ and $C_{H_2O_{ie}}$, and from these values with equation 4.31 θ_{SH}, θ_{S^-} and θ_{OH^-} (= 1 - θ_{S^-}). The actual evaluation of the adsorption data requires several numerical iteration operations.

In the following sections the influence of the concentration, the temperature, the type of resin, and the type of sugar will be discussed.

4.4.3.1. INFLUENCE OF THE CONCENTRATION ON THE ADSORPTION

In Figure 4.12 the calculated θ_G, θ_{G^-}, θ_{GH} and θ_{OH^-} for the adsorption of glucose on IRA 401 at 278 $\pm$ 5 K is given. A concentration axis is added in this figure based on a pore volume of .59 10^{-3} m^3 eq^{-1}. To obtain a high accuracy, 56 experiments have been carried out for this condition.

In this figure we see that the adsorption is increasing with the outer concentration. When the ionic and molecular adsorption are considered separately, two regions can be distinguished:

region 1: $0 < C_{G_{sol}} < 150$ mol m^{-3}: $\theta_{G^-} \sim \theta_G < .85$; $\theta_{GH} << \theta_{G^-}$

Here, almost all the adsorbed glucose is dissociated and the molecular glucose in the exchanger can thus be neglected.

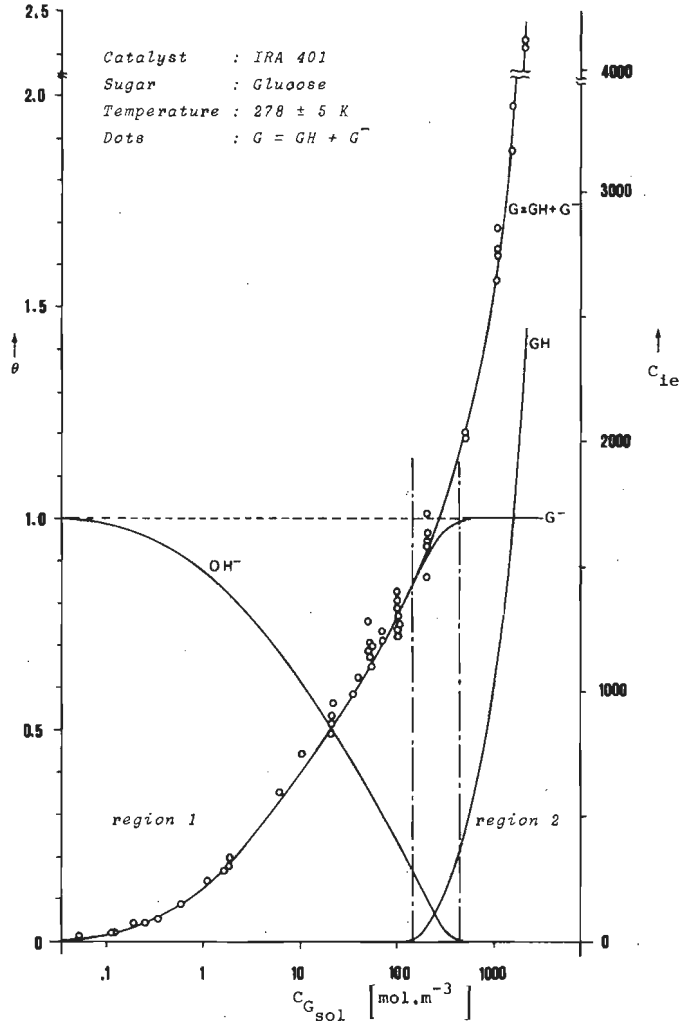

Figure 4.13. Adsorption of glucose on IRA 401 at 278 K.

region 2: $C_{G_{sol}} > 450$ mol m^{-3}; $\theta_{G^-} \sim 1.0$; $\theta_{GH} \sim \theta_G - 1.0$.
The coverage θ_{G^-} is constant and thus independent of the glucose concentration in the bulk.

When the adsorption is considered as a simple exchange of ions, it has to be described with K'_{ES} (relation 4.27).

In Figure 4.14 K'_{ES} is given as a function of the bulk glucose concentration $C_{G_{sol}}$.

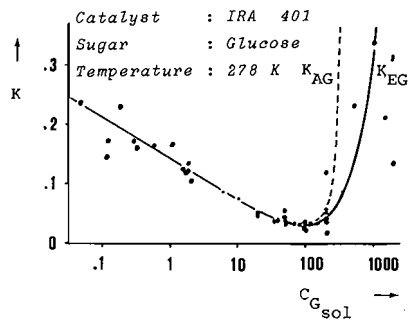

Figure 4.14. K_{AG} and K'_{EG} as a function of $C_{G_{sol}}$.

It is clear that it is not possible to describe the adsorption over a wide range with a simple exchange coefficient K'_{ES}.

Although the Langmuir adsorption model is mentioned in literature to describe adsorption on resins (187,188.79), for the adsorption of glucose the model is not valid (broken line in Figure 4.14). In section 4.1 and Table 4.2 we saw that the average NR_4^+-NR_4^+ distance is about 1 nm. When a glucose ion (molecular diameter about .8 nm) adsorbs on a NR_4^+-site, it might hamper adsorption of G^- on neighbouring sites.

Fujji et al. (192,193) described the adsorption of sugars with a Freundlich relation. In Figure 4.15 the degree of coverage θ and the concentration in the solution are both plotted on a logarithmic scale, with the purpose to find a straight line in this figure. It shows that the linear relation, following from the Freundlich isotherm as found by Fujji, is not present; it can only be obtained for a narrow concentration range.

For the total range of concentrations the relation of Sips gives superior results. This isotherm (equation 4.31) can be rewritten as:

$$\log \frac{\theta}{1-\theta} = \alpha \log C_{S_{sol}} + \log K_{SiS} \qquad (4.35)$$

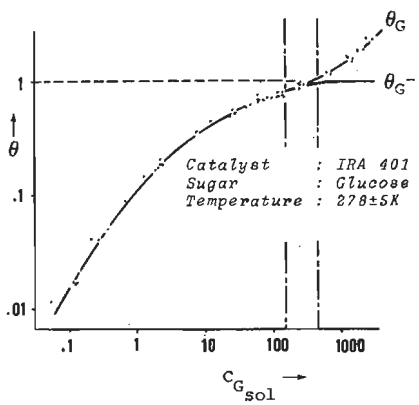

Figure 4.15. Adsorption of glucose on IRA 401 at 278 K according to the relation of Freundlich.

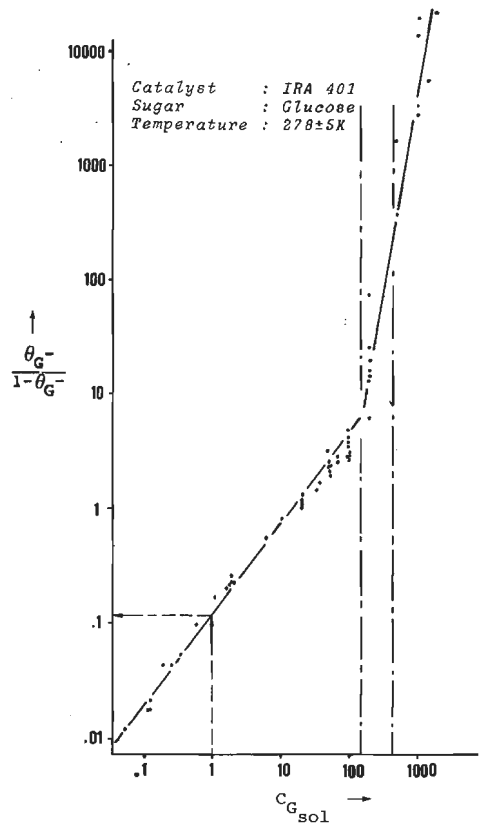

Figure 4.16. Adsorption of glucose on IRA 401 at 278 K according to the relation of Sips.

and this relation gives a straight line when $\theta_G^-/(1 - \theta_G^-)$ and $C_{G_{sol}}$ are both plotted logarithmically (Figure 4.16). In region 1 as well as in region 2 the adsorption can be described with the Sips isotherm. The linear relation in region 2 is only of academic interest, as the coverage is about 1.0. From Figure 4.16 we read: $K_{SiS,298} = .144$ and $\alpha = .67$. The value $(1 - \alpha)$ is a measure of the interference of adsorbed sugar anion with neighbouring sites.

The same type of relation is found for 5 types of sugars and 5 types of ion exchangers investigated.

For the isomerization not only the coverage of the resin but also the relative water concentration $C'_{H_2O,free}$ and the residual C_{OH^-} are of importance. In Figure 4.17 the external as well as the internal water concentration is given as a function of the external glucose concentration (relation 3.34).

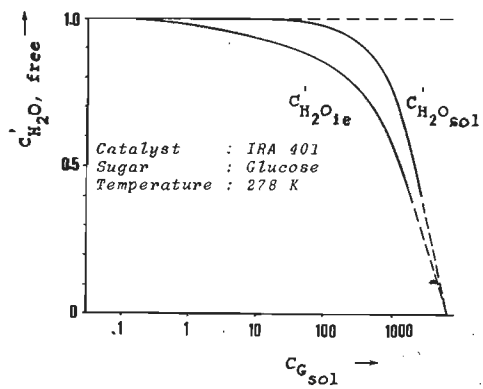

Figure 4.17. $C'_{H_2O,free}$ *inside and outside the resin.*

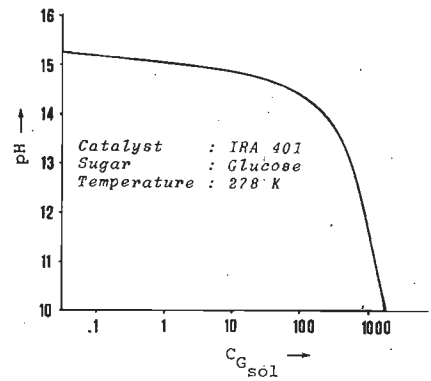

Figure 4.18. pH as a function of $C_{G_{sol}}$.

The lower water concentration inside the resin shows the sugar concentrating effect of the resins.

In Figure 4.18 the pH in the ion exchanger, as calculated from the different relations, is given as a function of the external sugar concentration. At high concentrations this internal pH decreases strongly. In chapter 5 we will return to this.

4.4.3.2. INFLUENCE OF THE TEMPERATURE OF THE ADSORPTION

The adsorption experiments have been carried out at temperatures from 273 K till 313 K with intervals of 5 K. As the temperature influence is relatively small, the experiments are lumped into 3 groups:

$T_1 = 278 \pm 5$ K
$T_2 = 293 \pm 5$ K
$T_3 = 308 \pm 5$ K

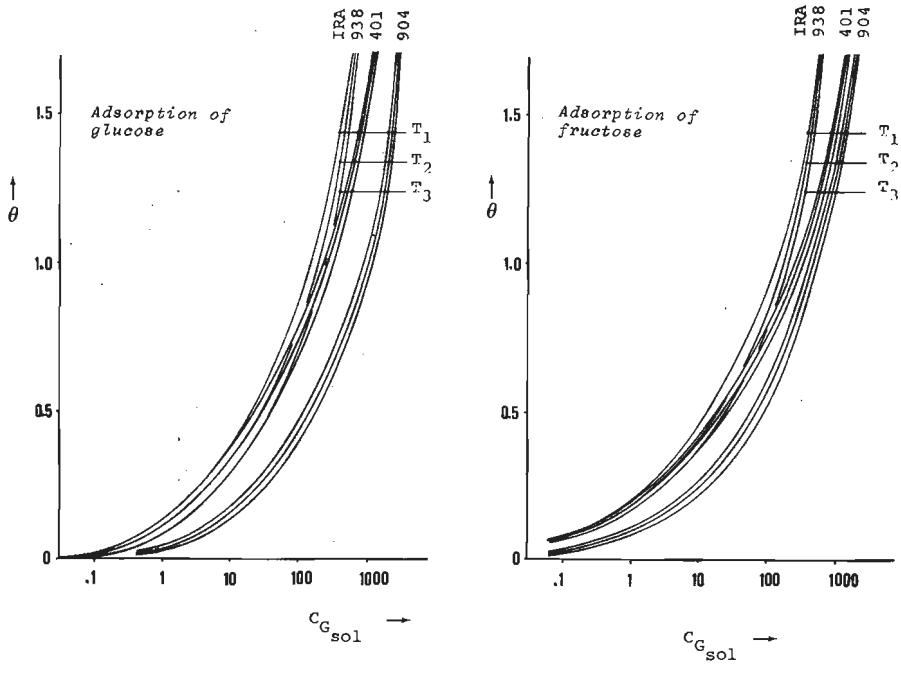

Figure 4.19. Adsorption of glucose. Figure 4.20. Adsorption of fructose.

In the Figures 4.19-4.22 the degree of coverage is given for respectively glucose, fructose, mannose and the disaccharides lactose and lactulose. Each figure shows the adsorption on the resins IRA 938, IRA 401 and IRA 904 at the temperatures T_1, T_2 and T_3.

From these data the adsorption constant K_{SiS} and the exponent α in the Sips relation can be calculated as shown for glucose on IRA 401 at 278 K in the previous section.

According to Sips (195) the average heat of adsorption can be calculated with:

$$\ln K_{SiS} = \frac{\overline{Q}_{ads} \cdot \alpha}{R \cdot T} - \alpha \cdot \ln a \qquad (4.36)$$

The final results are given in Table 4.5.

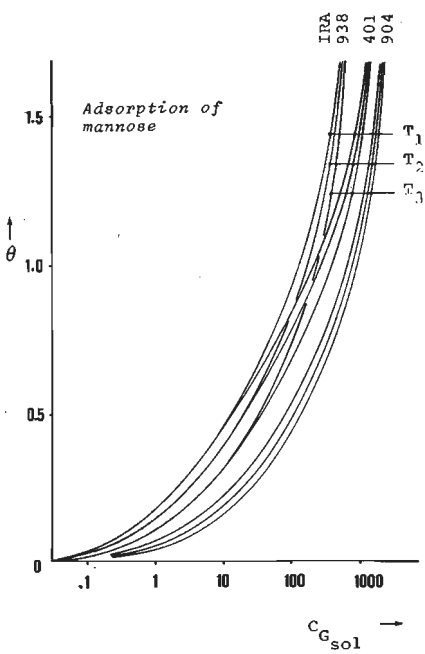

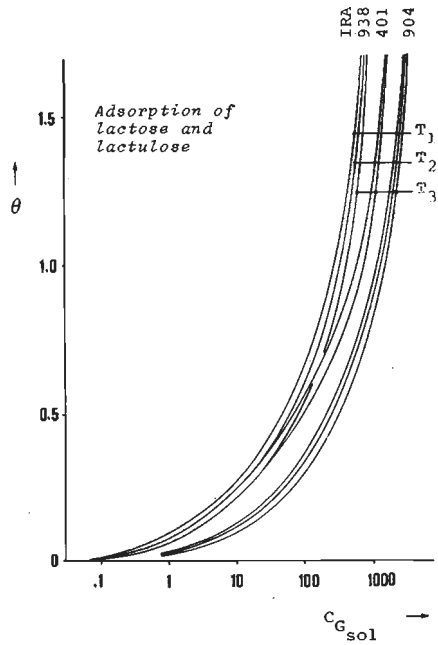

Figure 4.21. Adsorption of mannose. *Figure 4.22. Adsorption of lactose and lactulose.*

resin	sugar	K_{SiS}			$\overline{Q}_{ads}$	α			$\overline{\alpha}$
		278 K	293 K	308 K	kJ/mol	278 K	293 K	308 K	
IRA 401	glucose	.122	.098	.080	14.7	.67	.64	.62	.64
	fructose	.223	.175	.156	15.7	.52	.53	.53	.53
	mannose	.165	.122	.094	19.5	.70	.68	.63	.67
IRA 904	glucose	.043	.039	.037	6.0	.57	.56	.54	.56
	fructose	.047	.043	.039	6.2	.66	.65	.64	.65
	mannose	.048	.044	.042	5.1	.62	.61	.59	.61
	La, Lu	.034	.031	.029	6.4	.52	.53	.53	.53

Table 4.5. Adsorption constants according to the relation of Sips.

The exponent α tends to decrease slightly with increasing temperature. This means that the influence of an adsorbed sugar anion on surrounding sites increases with temperature, as would be expected. The marked higher degree of adsorption for fructose as compared to the other sugars on IRA 401, is reflected in an higher degree of interference as follows from the lower α. No relation between the α of different sugars *nor* between the different exchangers can be distinguished. In Table 4.5 and Figure 4.23 the differences in K_{SiS} (and $\overline{Q}_{ads}$) are shown.

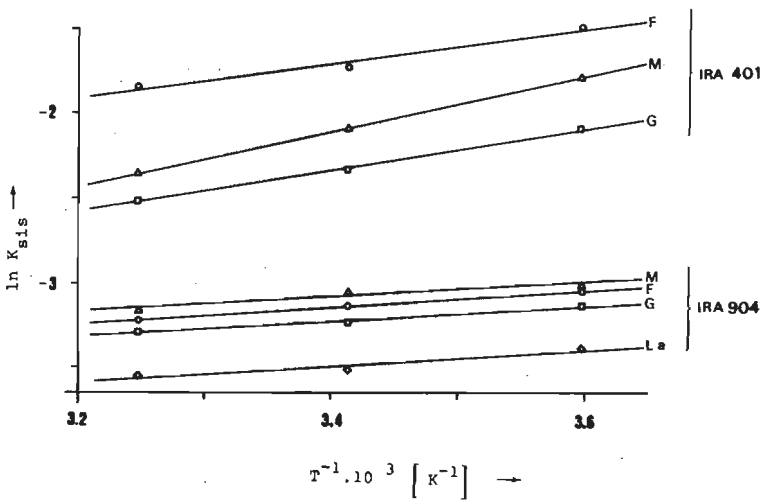

Figure 4.23. Temperature dependence of K_{SiS}.

4.4.3.3. INFLUENCE OF THE TYPE OF SUGAR AND RESIN ON THE ADSORPTION

Table 4.5 and Figure 4.23 show that on IRA 401 mannose adsorbs weaker than fructose, while on IRA 904 almost no difference is measured. Besides the heat of adsorption of mannose for IRA 401 is greater than that of glucose and fructose, while for IRA 904 it is smaller. We cannot exclude that the different behaviour of mannose relative to the other sugars is a consequence of impurities present (Fluka nr. 63580).

For both ion exchangers fructose anion adsorbs stronger than glucose anion. This is confirmed by a competition adsorption experiment in which ion exchanger is added to a solution containing equal quantities of glucose and fructose. After adsorption less fructose than glucose was found in the solution while in the exchanger there was more fructose than glucose.

Between the disaccharides lactose and lactulose no significant difference was found, but, as expected, the bigger disaccharides adsorb not as good as the monosaccharides. The adsorption decreases with increasing diameter of the adsorbing molecule, relative to the porosity of the gel-phase of the resin.

The total adsorption of sugars on the macroreticular resin IRA 904 is lower than on the gel-type resin IRA 401, while IRA 938 has only a higher molecular adsorption (see Figures 4.19-4.23). These differences can be ascribed to differences of the porosity of the gel-phase of the macroreticular resins. In section 4.3.3 we concluded already that the gel-phase of IRA 904 is less porous than in IRA 938. A decreasing porosity relative to the diameter of the adsorbing molecule, decreases the adsorption too. This is in agreement with Svetlow and Demenkova (200) who found a decrease of the adsorption with decreasing porosity of gel-type resins and Martinola and Siegers (201) who stated that the adsorption in the gel-phase of macroreticular resins is relatively low. The adsorption behaviour of IRA 938 gives the impression that the gelphase of IRA 938 is the same as the gel-phase of IRA 401. The higher molecular adsorption is apparently realized in the macropores.

The heat of adsorption on IRA 401 is significantly higher than on IRA 904. One would conclude that not only more but also stronger adsorption bonds are formed on IRA 401.

Also the adsorption on the gel-type resin Lewatit M 504 and the macroreticular resin IRA 900 was studied and appeared to be the same as for IRA 401. As the physical properties correspond with those of IRA 401 (Table 4.2) we may expect that the other type I resins, which have all comparable properties, will also show similar characteristics as IRA 401.

4.4.4. SUMMARY ADSORPTION

In this section the ionic as well as the adsorption of sugars in ion exchangers is studied.

The ionic adsorption can be described carefully with the relation of Sips for a coverage $0 < \theta_{S^-} < 0.85$. This coverage will be used to calculate rate constants k_{IJ} in s^{-1} from kinetic experiments.

The total adsorption is important to calculate the internal concentrations. Comparing of the rate constants with the internal concentrations makes it possible to relate catalytic effects.

4.5. DIFFUSION

Diffusion can play an important role in the kinetics of the isomerization reaction. As the activation energy for diffusion is lower than for isomerization, the influence of diffusion will be greater at a higher temperature.

The isomerization of glucose within the gel-type resin Amberlite IRA 401 gives at temperatures higher than 323 K reaction rate constants deviating from the Arrhenius straight line obtained for temperatures below 323 K (chapter 5). The lower overall activation energy indicates a diffusion limitation. Bulk diffusion is negligible, which has been verified with 2 experiments with stirring rates of 3 and 10 r.p.s. respectively gave the same rate of reaction.

In the literature two different models for the diffusion in resins have been distinguished.

- Boyd et al. (205) and Reichenberg (206) suppose that the undissociated *molecule* diffuses into and through the ion exchanger until an active site has been reached and adsorption takes place. For a sugar:

$$SH_{sol} \rightleftharpoons SH_{ie} \qquad (4.36')$$

$$SH_{ie} + R\text{-}NR_3^+OH^- \rightleftharpoons R\text{-}NR_3^+S^- + H_2O_{ie} \qquad (4.37)$$

The counterions are considered to be more or less static and bound on the active sites. No interaction of the diffusive particles with

the exchanger material is supposed and no backflow of expelled water is taken into account. A method is given to calculate $\mathbb{D}_{GH,ie}$ from diffusion experiments.

- Helfferich and Plesset (209-211), Marinsky (212) and Turner et al. (213) consider the distribution of the counter ions to be dynamic. These ions are mobile and can be interchanged by another counter ion. When molecular sugar adsorbs, ionization takes place immediately at the surface of the particle and the dissociated *ion* diffuses into the inside of the particle. To maintain electro-neutrality, OH^-_{ie} is transported in the opposite direction with the same flux. The diffusion of S^-_{ie} is directly related to the diffusion of OH^-_{ie}. Helfferich gives a method to calculate from experimental results $\mathbb{D}_{S^-_{ie}}$ when $\mathbb{D}_{OH^-_{ie}}$ is known.

Both models are rough approximations.

4.5.1. LITERATURE SURVEY

In section 4.4 it was mentioned that the glucose anion concentrations inside the ion exchangers are relatively high. Gladden and Dale (208) found that at high concentration the diffusion coefficient decreases, while its activation energy increases. In Table 4.6 some of his data are given.

C_G [mol m^{-3}]	0	580	1170	2620	4330
$\mathbb{D}_G.10^9$ [m^2 s^{-1}]	.675	.580	.486	.302	.133
E_{diff} [kJ mol^{-1}]	17.6	-	-	24.7	32.7

Table 4.6. Concentration dependency of the rate and the activation energy of diffusion of glucose in solution.

These data will be applied for developing an overall equation for diffusion (section 4.5.3). For that purpose we converted these data to the following expressions.

$$\mathbb{D}_G^{298} = \mathbb{D}_{G=0}^{298} \cdot e^{-5.7\ x_G} \qquad (4.38)$$

with

$$\mathbb{D}^{298}_{G=0} = .675.10^{9}\ m^2\ s^{-1}$$

$$E_{diff} = E_{diff,G=0}\ (1 + 6.4\ x_G) \tag{4.39}$$

with

$$E_{diff,G=0} = 17.6\ kJ\ mol^{-1}$$

$$x_G = \frac{M_{H_2O} \cdot C_G}{\rho - (M_G - M_{H_2O}) \cdot C_G} \tag{4.40}$$

In section 4.5.3 some diffusion coefficients of glucose are calculated from experimental results according to the description of Boyd. $\mathbb{D}_{S^-_{ie}}$ according to Helfferich could not be calculated because $\mathbb{D}_{OH^-_{ie}}$ was unknown.

In the literature *4 types of relations* for the diffusion coefficient in an ion exchanger can be found. Of these the relations of Zimmerman (214) and of Katoaka et al. (215) will not be discussed because they have little practical value.

Mackie and Meares (216) give for the diffusion coefficient in the resin:

$$\mathbb{D}_{S_{ie}} = \mathbb{D}_S \left\{ \frac{1 - x''_{pol}}{1 + x''_{pol}} \right\}^2 \tag{4.41}$$

with x''_{pol} is the polymeric fraction, as discussed in section 4.3.3, Table 4.2. In their model an ion exchanger is considered to be a concentrated polyelectrolyte solution.

Yasuda et al. (217) have developed the relation:

$$\mathbb{D}_{S_{ie}} = \mathbb{D}_S \cdot e^{-Ya_S \frac{x''_{pol}}{1 - x''_{pol}}} \tag{4.42}$$

with Ya_S = constant of Yasuda.
The constant of Yasuda depends on the type of material, diffusing into the exchanger. This derivation is based on Cohen's free volume theory (221,222) and Doolittle (219,220) has shown that for a comparable constant (for viscosity) a relation exists that, translated into terms of Yasuda's constant, reads:

$$Ya_S = Ya_{S=0} \cdot \frac{E_{diff}}{E_{diff,S=0}} \tag{4.43}$$

On the basis of Doolittle's study it can further be assumed that Ya_S is independent of the type of exchanger and the temperature. Fernandex-Prini and Philipp (218) extended the model of Yasuda:

$$\mathbb{D}_{S_{ie}} = Q \cdot \mathbb{D}_S \cdot e^{-Ya_S \frac{x''_{pol}}{1 - x''_{pol}}} \tag{4.44}$$

where Q is a correction factor for electrostatic interaction of ions with the ion exchanger.

We have been unable to find literature data for the diffusion of sugars in basic ion exchange resins. Lagos and Kitchener (223) measured $\mathbb{D}_{G_{ie}}$ and Wong et al. (224) measured $\mathbb{D}_{F_{ie}}$ in acidic cation resin. The model of Yasuda gave the best description of their experimental data with

$$Ya_{G=0} = Ya_{F=0} = 1.0 \text{ (at low } C_{S_{ie}}) \tag{4.45}$$

$$Q \sim 1.0 \text{ (electrostatic interaction is negligible)} \tag{4.46}$$

For the diffusion of glucose or fructose in anion exchangers the constant of Yasuda must have the same value because it is independent of the resin. The influence of the electrostatic interaction (Q) however is not known in the anion exchangers.

We will return to the literature data when the experimental results will be discussed (section 4.5.3).

4.5.2. EXPERIMENTAL

The diffusion experiments have been carried out under N_2 in a thermostated (298 K) stirred reactor of 200 cm^3. A glucose solution (100 cm^3, 1 M) is pumped through the measuring and the reference cell of a thermostated refraction meter (Waters, R4). When the baseline is stable, the reference cell is short-circuited and about 1 meq of filtered exchanger in the hydroxyl form is brought into the reactor. Diffusion of glucose into the exchanger causes a decrease of the concentration in the solution, which results in a change of the refraction index. In Figure 2.24 a block diagram is given.

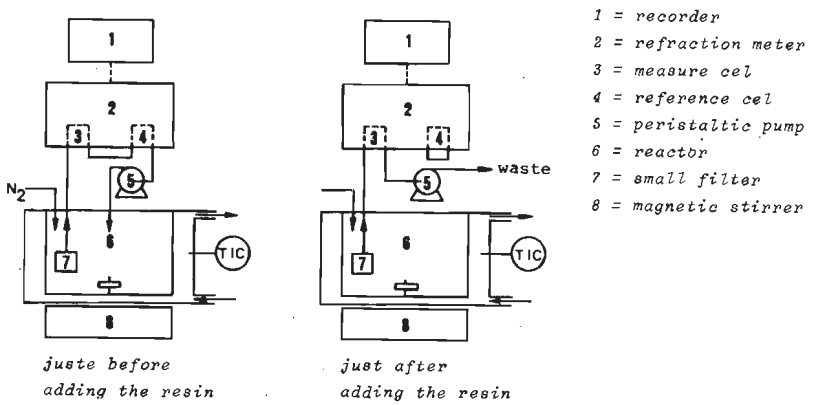

Figure 4.24. Block diagram for diffusion experiments.

With the aid of a calibration curve for the refractive index, the change of the glucose concentration is measured with the time, yielding the rate of glucose adsorption.

4.5.3. RESULTS AND DISCUSSION

From the concentration decrease in the solution the degree of coverage of the exchanger (θ_t) can be calculated.

The diffusion coefficient in the exchanger $\mathbb{D}_{G_{ie}}$ can then be calculated according to the method of Boyd et al. (205) and Reichenberg (206):

For $\theta_{G,t}/\theta_{G,t\to\infty} < .85$:

$$\mathbb{D}_{G_{ie}} = \frac{d_p^2}{4\pi^2} \frac{d}{dt} \left\{ 2\pi - \frac{\pi^2 \cdot \theta_{G,t}/\theta_{G,t\to\infty}}{3} - 2\pi \sqrt{1 - \frac{\pi \cdot \theta_{G,t}/\theta_{G,t\to\infty}}{3}} \right\} \tag{4.47}$$

For $\theta_{G,t}/\theta_{G,t\to\infty} > .85$:

$$\mathbb{D}_{G_{ie}} = \frac{d_p^2}{4\pi^2} \frac{d}{dt} \left[- \ln \left\{ \frac{\pi^2}{6} \left(1 - \theta_{G,t}/\theta_{G,t\to\infty} \right) \right\} \right] \tag{4.48}$$

with $\theta_{G,t}$ = coverage of the resin with glucose at a time t;
$\theta_{G,t\to\infty}$ = coverage of the resin with glucose at equilibrium;
d_p = particle diameter, being a function of the coverage (see section 4.3.2 and 4.3.3).

Due to the rather low reproducibility the experiments have been carried out in 4-fold (IRA 401) and in 3-fold (IRA 938). From the degree of coverage of the exchanger and its pore volume the internal concentrations during the experiment can be calculated. The diffusion coefficients calculated from the experimental data are plotted as a function of the internal concentration in Figure 4.25 (gel-type resin IRA 401) and 4.26 (macroreticular-type IRA 938). Here these data are compared with the diffusion coefficients in pure solutions calculated according to Gladden and Dole (equation 4.38) and in resins according to Yasuda et al. (equation 4.42) and Mackie and Meares (equation 4.41).

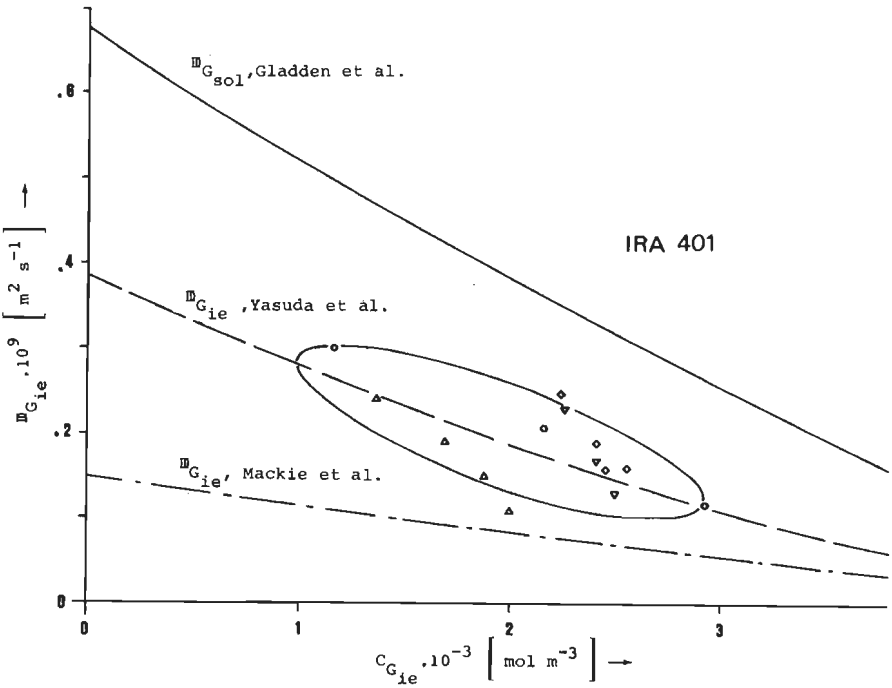

Figure 4.25. Diffusion coefficient of glucose in IRA 401 ($\mathbb{D}_{G_{ie}}$) as a function of the internal concentration ($C_{G_{ie}}$). The different types of points correspond with different experiments.

In spite of the spread in our experimental data it is plausible that also the diffusion of sugars in different types on anion exchangers can be approximated with the diffusion coefficient, based on the relation of Yasuda:

$$\mathbb{D}_{G_{ie}}^{298} = m_G^{298} \cdot e^{-Ya_G \frac{x''_{pol}}{1 - x''_{pol}}} \qquad (4.49)$$

with

$$\mathbb{D}_G^{298} = \mathbb{D}_{G=0}^{298} \cdot e^{-5.7\, x_{G_{ie}}} \qquad (4.50)$$

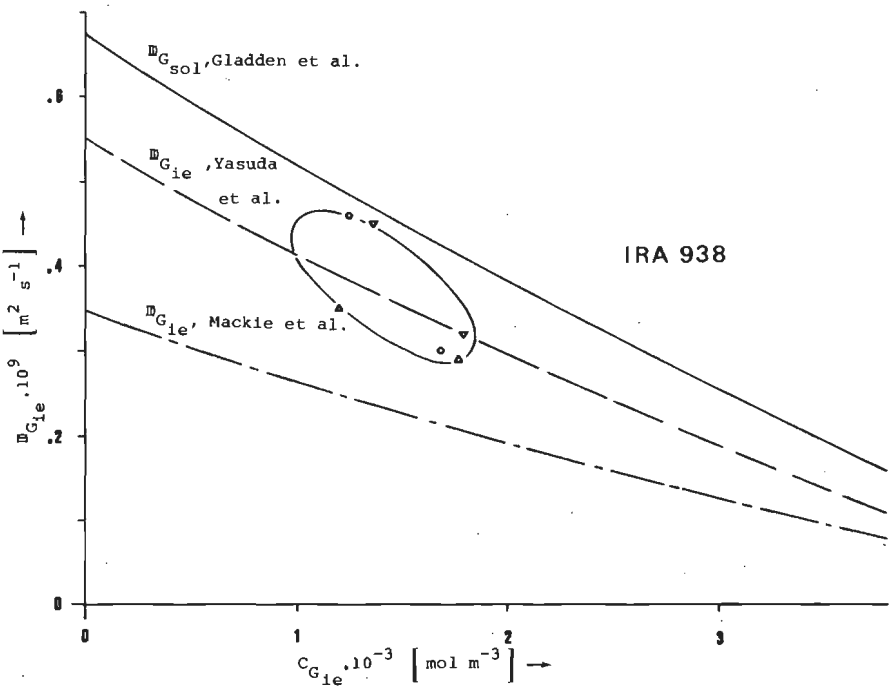

Figure 4.26. Diffusion coefficient of glucose in IRA 938 ($\mathbb{D}_{G_{ie}}$) as a function of the internal concentration ($C_{G_{ie}}$).

$$\mathbb{D}^{298}_{G=0} = .675 \cdot 10^{-9} \text{ m}^2 \text{ s}^{-1} \tag{4.51}$$

$$Ya_G = Ya_{G=0} \cdot \frac{E_{diff,ie}}{E_{diff,G=0}} \tag{4.52}$$

$$Ya_{G=0} = 1.0 \tag{4.53}$$

$$E_{diff,ie} = E_{diff,G=0} \left(1 + 6.4\, x_{G_{ie}}\right) \tag{4.54}$$

Substituting 4.50-4.54 in 4.49 gives:

$$\mathbb{D}^{298}_{G_{ie}} = .675 \cdot 10^{-9}\, e^{-\left\{5.7\, x_{G_{ie}} + \left(1 + 6.4\, x_{G_{ie}}\right) \frac{x''_{pol}}{1 - x''_{pol}}\right\}} \tag{4.55}$$

4.5.4. SUMMARY DIFFUSION

In this section the diffusion of glucose in anion exchangers is described at a temperature of 298 K. A model based on the relation of Yasuda, is developed.

The application of the model can be enlarged by substituting the temperature dependency of diffusion:

$$\mathbb{D}^{T}_{S_{ie}} = \mathbb{D}^{298}_{S=0}\, e^{\frac{-Ya_{S=0}\cdot E_{diff,S=0}}{R}\left(\frac{1}{298}-\frac{1}{T}\right)\left|5.7\, x_{S_{ie}} + \left(1 + 6.4\, x_{S_{ie}}\right)\frac{x''_{pol}}{1 - x''_{pol}}\right|} \qquad (4.56)$$

This relation is valid for all types of sugars and resins as a function of the temperature (T) and the internal concentration ($x_{S_{ie}}$). The influence of the type of sugar is expressed in $\mathbb{D}^{298}_{S=0}$ and $E_{diff,S=0}$. The resin characteristics are represented in the polymeric fraction x''_{pol}. For hexoses the best value of $Ya_{S=0} = 1.0$.

In the next chapters the effect of diffusion on the kinetics of isomerization reactions will be discussed.

CHAPTER 5

Kinetics of glucose and lactose isomerization with ion exchangers

5.1. INTRODUCTION

In this chapter the kinetics of the heterogeneous alkaline isomerization will be discussed in relation to the homogeneous reactions. A literature survey of the homogeneous and heterogeneous isomerization is given first.

The kinetics of the homogeneous isomerization and degradation reactions, have been studied by MacLaurin and Green (225). Isbell et al. (108,226) and de Wit (165) measured the relative enolization rates of the various hexoses. We will return to their results in section 5.5. Other important papers are those published by Bamford et al. (227-229), Garrett and Young (230), Kooyman et al. (231), de Wit et al. (83) and others (232-245).

Since the report of Montgomery and Hudson in 1930 (258), several studies are published about the homogeneous isomerization of lactose (101,259-264) and other oligosaccharides (265-268).

The possibility to use anion exchangers as a catalyst for the glucose isomerization to yield fructose and mannose was first mentioned by Rebenfeld and Pascu (82). The isomerization is reported to be catalyzed by strongly basic (61,81,101,193,254-256 and 270-280) and by weakly basic resins (281,282). Katz et al. (278,279) developed a complete production unit using a macroreticular anion exchanger as a catalyst.

In a recent article Demainay and Baron (283) described the isomerization of lactose to lactulose over an anion exchanger quantitatively.

A kinetic study of the heterogeneous isomerization was not published until the article of Rendleman and Hodge (81) at the end of 1979. His reaction conditions differed widely from ours and gave no information for industrial applications.

Besides the isomerization products, also degradation products are formed. Samuelson and Stolpe (284) and de Wilt and Kuster (285) studied the homogeneous oxidative degradation of glucose. They found formic, glycolic, acetic, glyceric, erithronic and arabinonic acids as degradation products. De Wit (100,165,286) and other investigators (99,287-303) studied homogeneous degradation of monosaccharides under N_2-atmosphere. The most recent articles suppose a degradation via the 1,2-enolate ion. Besides fructose and mannose Koizumi et al. (293) found small amounts of arabinose, ribose and ribulose upon isomerization of glucose.

For the isomerization of glucose with an ion exchanger lactic acid and glycolic acid are formed (192,193,270). According to Hulme (305) for the glucose isomerization no lactic acid was found when the resin was in the carbonate form. This effect is roughly confirmed by our own results (see section 5.5.3 and 5.6.1).

The alkaline degradation of oligosaccharides has been described by several investigators (263,265,309-313). Löwendahl and Samuelson (313) observed for the degradation of cellobiose with $NaHCO_3$ instead of NaOH, a change in the product distribution of the sugar acids.

A kinetic model for the isomerization of carbohydrates will be discussed in section 5.2, and the experiments are described in section 5.3. In section 5.4 the processing of the experimental data and in section 5.5 and 5.6 the final results of the glucose and lactose isomerization are described.

5.2. *KINETIC MODEL*

Already in 1895 Lobry de Bruin and Alberda van Ekenstein (55) suggested that the conversion of glucose to fructose proceeds via an intermediate enolate. Recent work of Isbell et al. (226), Sallam (244) and de Wit et al. (83) confirmed the enolate ion hypothesis. Also the formation of degradation sugars and sugar acids proceeds via the enolate ion as well (294,314).

For the heterogeneous isomerization the same enolate ion mechanism is supposed for the reaction inside the ion exchanger. With the data of chapter 4 the total sugar concentration inside the resin is calculated. From the total capacity and the ionization degree (chapter 3)

the internal concentrations of GH, G^- and OH^- can be found. This makes it possible to describe the heterogeneous isomerization as a pseudo homogeneous reaction inside the pores of the catalyst. On the analogy of the homogeneous reaction (231), the isomerization is supposed to be first order in G^-.

The formed degradation *products* (De^-_{ie}) can be divided into reversibly adsorbing *sugars* (D^-_{ie}) and irreversibly adsorbing sugar *acids* (E^-_{ie}). To simplify the scheme the formation to the degradation sugars (D) is supposed to be irreversible and the consecutive reaction to degradation acids is neglected. As also mannose enters the reaction network, the latter can be presented by Figure 5.1.

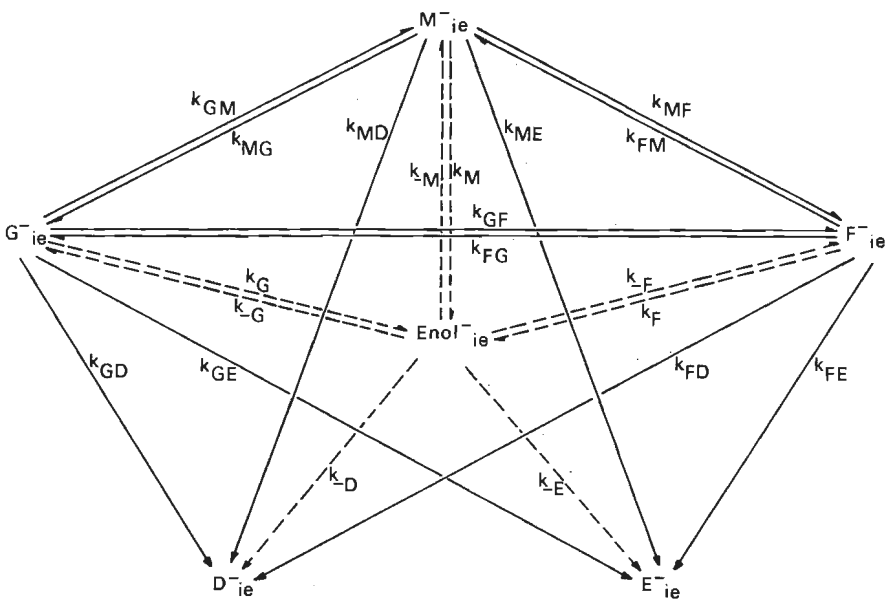

Figure 5.1. Overall (⇌) and enolate (⇢⇠) model of the interconversion of glucose (G^-), fructose (F^-), mannose (M^-) and the degradation products (D^- and E^-) inside an ion exchanger resin.

The solid lines represent the *overall model* and the broken lines the *enolate model*.

In section 5.2.1 the differential equations are derived for the concentration of the components in a batch reactor. Section 5.2.2 deals with the transformation of the reaction rate constants from one model to another.

5.2.1. OVERALL MODEL

From the adsorption and the pore volume relations (chapter 4), the internal concentration at the initial state of the experiment can be calculated directly from the experimental data, if we assume that the different species inside the resin are distributed homogeneously over the pore volume available. However, only the concentrations in the outer solution can be measured. For this reason the internal concentrations have to be expressed as a function of the concentrations in the solution. For glucose the differential equation is:

$$\frac{d}{dt}\left\{V_{sol}\left(C_{GH_{sol}} + C_{G^-_{sol}}\right) + V_{pore}\left(C_{GH_{ie}} + C_{G^-_{ie}}\right)\right\} =$$

$$k_{FG}\cdot V_{pore}\cdot C_{F^-_{ie}} + k_{MG}\cdot V_{pore}\cdot C_{M^-_{ie}} - \Sigma\, k_{GJ}\cdot V_{pore}\cdot C_{G^-_{ie}} \qquad (5.1)$$

with V_{sol} = volume of the solution outside the resin;
V_{pore} = total pore volume of the resin;
$\Sigma\, k_{GJ} = k_{GF} + k_{GM} + k_{GD} + k_{GE}$ (5.2)
J = G, F, M, D, E

Substituting relation 4.24, 4.25 and 4.26 in 4.29 gives the general equation:

$$C_{S^-_{ie}} = K_{AS}\cdot C_{OH^-_{ie}}\cdot C_{S_{sol}} \qquad (5.3)$$

We may simplify because:

$$C_{G^-_{sol}} << C_{GH_{sol}} \qquad (pH_{sol} \sim 7) \qquad (5.4)$$

$$C_{GH_{ie}} << C_{G^-_{ie}} \qquad (\text{for } \theta_{G^-} \leq .95) \qquad (5.5)$$

Substituting equation 5.3, 5.4 and 5.5 in 5.1 gives:

$$\frac{d}{dt} C_{G_{sol}} = \left(k_{FG} \cdot K_{AF} \cdot C_{OH^-_{ie}} \cdot C_{F_{sol}} + k_{MG} \cdot K_{AM} \cdot C_{OH^-_{ie}} \cdot C_{M_{sol}} - \Sigma k_{GJ} \cdot K_{AG} \cdot C_{OH^-_{ie}} \cdot C_{G_{sol}} - K_{AG} \cdot \frac{d}{dt} C_{OH^-_{ie}} \cdot C_{G_{sol}} \right) \Big/ \left(V_{sol} / V_{pore} + K_{AG} \cdot C_{OH^-_{ie}} \right) \quad (5.6)$$

The differential equations for the fructose and mannose concentrations are similar:

$$\frac{d}{dt} C_{F_{sol}} = \left(k_{GF} \cdot K_{AG} \cdot C_{OH^-_{ie}} \cdot C_{G_{sol}} + k_{MF} \cdot K_{AM} \cdot C_{OH^-_{ie}} \cdot C_{M_{sol}} - \Sigma k_{FJ} \cdot K_{AF} \cdot C_{OH^-_{ie}} \cdot C_{F_{sol}} - K_{AF} \cdot \frac{d}{dt} C_{OH^-_{ie}} \cdot C_{F_{sol}} \right) \Big/ \left(V_{sol} / V_{pore} + K_{AF} \cdot C_{OH^-_{ie}} \right) \quad (5.7)$$

$$\frac{d}{dt} C_{M_{sol}} = \left(k_{FM} \cdot K_{AF} \cdot C_{OH^-_{ie}} \cdot C_{F_{sol}} + k_{GM} \cdot K_{AG} \cdot C_{OH^-_{ie}} \cdot C_{G_{sol}} - \Sigma k_{MJ} \cdot K_{AM} \cdot C_{OH^-_{ie}} \cdot C_{M_{sol}} - K_{AM} \cdot \frac{d}{dt} C_{OH^-_{ie}} \cdot C_{M_{sol}} \right) \Big/ \left(V_{sol} / V_{pore} + K_{AM} \cdot C_{OH^-_{ie}} \right) \quad (5.8)$$

For the degradation products and for the free active sites $\left(OH^-_{ie}\right)$, we derive simply:

$$\frac{d}{dt} C_{D_{sol}} = \left(k_{GD} \cdot K_{AG} \cdot C_{OH^-} \cdot C_{G_{sol}} + k_{FD} \cdot K_{AF} \cdot C_{OH^-_{ie}} \cdot C_{F_{sol}} + k_{MD} \cdot K_{AM} \cdot C_{OH^-_{ie}} \cdot C_{M_{sol}} - K_{AD} \cdot \frac{d}{dt} C_{OH^-_{ie}} \cdot C_{D_{sol}} \right) \Big/ \left(V_{sol} / V_{pore} + K_{AD} \cdot C_{OH^-_{ie}} \right) \quad (5.9)$$

$$\frac{d}{dt} C_{E^-_{ie}} = \nu_G \cdot k_{GE} \cdot K_{AG} \cdot C_{OH^-_{ie}} \cdot C_{G_{sol}} + \nu_F \cdot k_{FE} \cdot K_{AF} \cdot C_{OH^-_{ie}} \cdot C_{F_{sol}} + \nu_M \cdot k_{ME} \cdot K_{AM} \cdot C_{OH^-_{ie}} \cdot C_{M_{sol}} \quad (5.10)$$

with ν_S = number of molecules sugar acids, formed from one molecule of the sugar S.

Because of electro-neutrality relation in the resin we obtain:

$$\frac{d}{dt} C_{OH^-_{ie}} = \left\{ -\frac{d}{dt} C_{E^-_{ie}} - C_{OH^-_{ie}} \left(K_{AG} \cdot \frac{d}{dt} C_{G_{sol}} + K_{AF} \cdot \frac{d}{dt} C_{F_{sol}} + K_{AM} \cdot \frac{d}{dt} C_{M_{sol}} + K_{AD} \cdot \frac{d}{dt} C_{D_{sol}} \right) \right\} \Big/ \left(1 + K_{AG} \cdot C_{G_{sol}} + K_{AF} \cdot C_{F_{sol}} + K_{AM} \cdot C_{M_{sol}} + K_{AD} \cdot C_{D_{sol}} \right) \quad (5.11)$$

The differential equations 5.6-5.11 with the appropriate initial conditions describe the concentration changes during a batch experiment.

5.2.2. ENOLATE MODEL

From Figure 5.1 we see that the overall model requires 12 reaction constants and the enolate model 8 constants. To simplify the relation between both models, the degradation products are taken together, i.e.:

$$k_{-De} = k_{-D} + k_{-E} \quad (5.12)$$

In Figure 5.2 the simplified scheme for the isomerization is given. The enolate concentration is described by:

$$\frac{d}{dt} C_{Enol^-} = {}_I\Sigma\, k_I \cdot C_I - {}_J\Sigma\, k_{-J} \cdot C_{Enol^-} \quad (5.13)$$

with I = G, F, M; $I \neq J$.

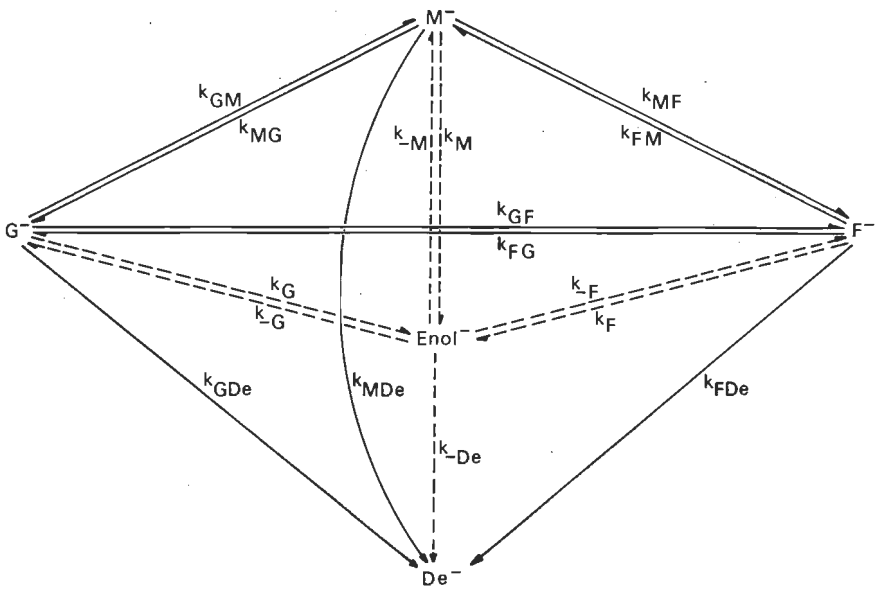

Figure 5.2. Kinetic model of the interconversion of glucose, fructose and mannose, together with the degradation products De.

As the absolute value of C^-_{Enol} is very small, the conversion to the enolate ion is assumed to be equal to the total conversion from the enolate ion:

$$ {}_J\Sigma\ k_{-J} \cdot C_{Enol^-} = {}_I\Sigma\ (k_I \cdot C_I) \qquad (5.14) $$

Because only the product of $\Sigma\ k_{-J}$ and C_{Enol^-} and not the separate values can be calculated, the reaction constants *from* the enolate model are defined in a relative manner:

$$ k'_{-J} = \frac{k_{-J}}{\Sigma\ k_{-J}} \qquad (5.15) $$

with

$$ \Sigma\ k'_{-J} = k'_{-G} + k'_{-F} + k'_{-M} + k'_{-De} = 1 \qquad (5.17) $$

In appendix 3 the transformation of the enolate model to the overall model and reverse is derived. Only the final results are given. For the two models the following relations are defined:

Overall model:		Enolate model:	
$K_{GF} \cdot K_{FM} \cdot K_{MG} = 1$	(5.16)	$\Sigma\, k'_{-J} = 1$	(5.17)
$X_I = k\hat{}_{II} \cdot \frac{k_{IDe}}{k\hat{}_{IDe}}$	(5.18)	$X_I = k_I \cdot k'_{-I}$	(5.19)
$Y_I = \frac{k\hat{}_{II}}{k\hat{}_{IDe}}$	(5.20)	$Y_I = \frac{k'_{-I}}{k'_{-De}}$	(5.21)
$Z_I = k_{IDe} \cdot \Sigma\, Y_I$	(5.22)	$Z_I = k_I \cdot (1 - k'_{-De})$	(5.23)

with $\hat{I} = G, F, M; \hat{I} \neq I$.

The auxiliary constant Z_I also can be defined as a function of isomerization constants only.

For glucose:

$$Z_G = k_{GF} + k_{GM} + \frac{k_{FG} \cdot k_{GM}}{k_{FM}} \tag{5.24}$$

With the aid of the auxiliary constants X_I, Y_I and Z_I, the relations between the reaction constants of the two models obtain a simple form.

Conversion from the enolate to the overall model:

$$k_{IJ} = k_I \cdot k'_{-J} \tag{5.25}$$

$$k_{IDe} = k_I \cdot k'_{-De} = Z_I \cdot \frac{k'_{-De}}{1 - k'_{-De}} \tag{5.26}$$

Conversion from the overall to the enolate model:

$$k_I = X_I + {}_J\Sigma\, k_{IJ} \tag{5.27}$$

$$k'_{-I} = \frac{Y_I}{\Sigma Y_I + 1} \tag{5.28}$$

$$k'_{-De} = \frac{1}{\Sigma Y_I + 1} \tag{5.29}$$

$$k'_{-De} = \frac{k_{IDe}}{k_{IDe} + Z_I} \tag{5.30}$$

More relations are given in appendix 3.

The overall model (Figure 5.2) is described with 9 reaction rate constants. With the relations 5.24 and 5.26 it is possible to express 2 degradation constants as a function of the third degradation constant and some isomerization constants. With relation 5.16 the number of independent variables in the overall model is reduced to 6. Within the enolate model relation 5.17 reduces the number of independent variables also to 6. So, the kinetic system is totally described with 5 isomerization constants and one degradation constant. The degradation reaction is characterised by the relative rate constant k'_{-De} or by the selectivity, defined in the enolate model as:

$$Sel_{en} = 1 - k'_{-De} \tag{5.31}$$

5.3. EXPERIMENTAL

The isomerization experiments are carried out under N_2 in a thermostated and stirred (7 r.p.s.) reactor of 1 dm^3 (Figure 5.3). The sugar solution is brought into the reactor while the ion exchanger is kept in a special vessel. When the catalyst is added to the solution, the experiment starts. With a special vacuum system catalyst-free samples are taken. In a separate vessel the pH is measured.

At the end of an experiment, the rest activity of the ion exchanger is determined in the reactor according to the method described in section 4.2.2.

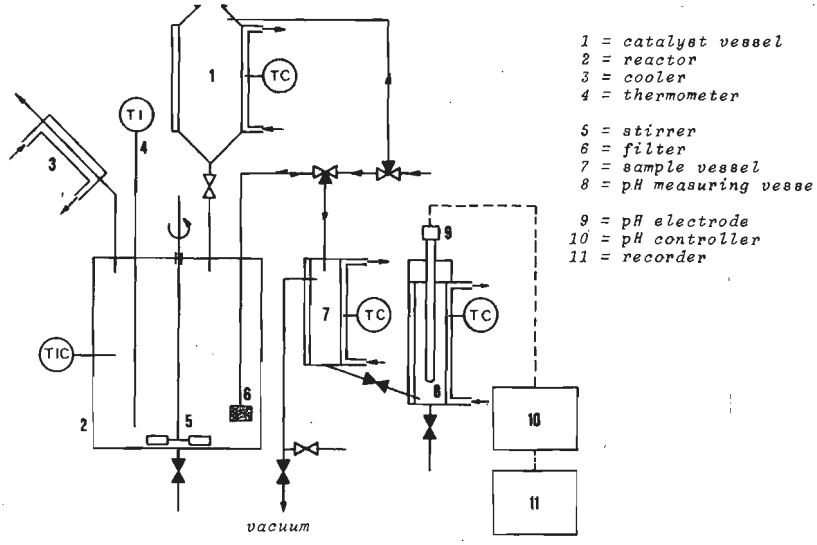

Figure 5.3. Reactor for kinetic experiments.

The sugars are analysed with ion exchange chromatography (section 2.2) and the sugar acids with isotachophoresis (section 2.4). When a small conversion of an aldose to a ketose has to be measured accurately, the special ketose analysis (section 2.3) is applied.

The experiments cover a concentration range from 20 to 3200 mol m^{-3} in the bulk solution and a temperature range from 295 K to 362 K. Experiments are carried out, starting from glucose, fructose, mannose, lactose, lactulose and galactose. In appendix 2 a list of the catalysts studied is given. The quantities of sugar and catalyst are given as a ratio (S/ie) of the total amount of sugar and sites, both expressed in mol and related to the same external volume in m^3.

The standard conditions for an experiment are:

- sugar : glucose;
- catalyst : IRA 401;
- temperature : 313 K;
- S/ie : 100/40.

In the further text only deviations from these standard conditions will be mentioned.

5.4. PROCESSING OF EXPERIMENTAL DATA

From the batch experiments we obtain the concentrations of the sugars as a function of the time: $C_{S_{sol}} = f(t)$. The accuracy of the analytical data is as follows:

- ion exchange chromatography: $C_S \pm 3\%$
- ketose detection: $C_{F,Lu} \pm 2\%$

In Figure 5.4 an example of the course of the $C_{S_{sol}} = f(t)$ plots is given for a fructose experiment. It may be noted that the concentration degradation sugars in solution $\left(C_{D_{sol}}\right)$ is about equal to the mannose concentration.

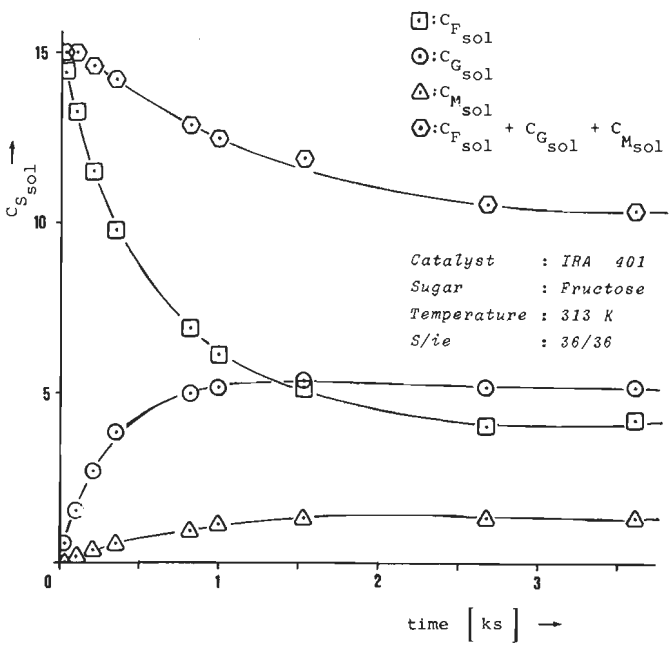

Figure 5.4. Concentration profiles from a batch experiment.

The concentration profile has been corrected in order to account for the increase of the concentration of the catalyst during the sampling. A small initial effect is present due to the fact that inside the catalyst a certain product concentration should be reached before equilibrium exists between the reaction rate and the diffusion rate.

Also impurities may cause initial effects. Both effects have been corrected by extrapolation of the stationary region to initial conditions.

There are two different procedures to calculate the selectivity from the experimental data. Both methods are based on a selectivity, independent of the reaction course and will be discussed in section 5.4.1 and 5.4.2.

5.4.1. SELECTIVITY CALCULATED FROM INITIAL DATA

The reaction rate constants can be calculated from the *initial slopes* of the concentration profiles. Starting from e.g. glucose, the substitution of the values of these slopes in the relations 5.6-5.8 (with e.g. in equation 5.6 $C_{F_{sol},t=0} = C_{M_{sol},t=0} = 0$ and $C_{OH^-_{ie}} \sim C_{OH^-_{ie},t=0}$) gives directly the constants Σk_{GJ}, k_{GF} and k_{GM}.

A more accurate way, used for our experiments, is to determine these kinetic constants by analytical extrapolation methods. To calculate e.g. k_{GF} the following approximations for $C_{G_{sol}}$, $C_{F_{sol}}$ and $C_{OH^-_{ie}}$ are substituted in equation 5.7 to obtain a differential equation in $C_{F_{sol}}$:

$$C_{M_{sol}} \sim \frac{\left(\frac{d}{dt} C_{M_{sol}}\right)_{t\to 0}}{\left(\frac{d}{dt} C_{F_{sol}}\right)_{t\to 0}} \cdot C_{F_{sol}} =$$

$$\frac{k_{GM}\left(V_{sol}/V_{pore} + K_{AF}\cdot C_{OH^-_{ie},t=0}\right)}{k_{GF}\left(V_{sol}/V_{pore} + K_{AM}\cdot C_{OH^-_{ie},t=0}\right)} \cdot C_{F_{sol}} \qquad (5.32)$$

$$C_{G_{sol}} \sim C_{G_{sol},t=0} - C_{F_{sol}} - C_{M_{sol}} \qquad (5.33)$$

$$C_{OH^-_{ie}} \sim C_{OH^-_{ie},t=0}$$

This allows a direct integration.
Elimination of k_{GF} gives:

$$k_{GF}(t) = P_{GF} \cdot C_{F_{sol}} \cdot \frac{e^{Q_{GF} \cdot t} - 1}{Q_{GF}}$$

$$= P_{GF} \cdot \frac{C_{F_{sol}}}{t} \cdot \left(1 + \frac{Q_{GF} \cdot t}{2!} + \frac{Q_{GF}^2 \cdot t^2}{3!} + \ldots\right)^{-1} \qquad (5.34)$$

with

$$P_{GF} = \frac{V_{sol}/V_{pore} + K_{AF} \cdot C_{OH^-_{ie},t=0}}{K_{AG} \cdot C_{G_{sol},t=0} \cdot C_{OH^-_{ie},t=0}} \qquad (5.35)$$

$$Q_{GF} = \frac{C_{OH^-_{ie},t=0}}{V_{sol}/V_{pore} + K_{AF} \cdot C_{OH^-_{ie},t=0}} \cdot$$

$$\left\{ \frac{k_{GM}\left(V_{sol}/V_{pore} + K_{AF} \cdot C_{OH^-_{ie},t=0}\right)}{k_{GF}\left(V_{sol}/V_{pore} + K_{AM} \cdot C_{OH^-_{ie},t=0}\right)} \cdot \right.$$

$$\left. \left(k_{MF} \cdot K_{AM} - k_{GF} \cdot K_{AG}\right) - k_{GF} \cdot K_{AG} - K_{AF} \sum k_{FJ} \right\} \qquad (5.36)$$

The constants P_{GF} can be calculated directly from the initial conditions. The auxiliary constant Q_{GF}, however, is a function of the various kinetic constants, including k_{GF}. When the kinetics are not yet known, certain assumptions for k_{IJ} have to be made so that Q_{GF} can be calculated as well. Substituting the experimental data (t, $C_{F_{sol}}$) then gives the reaction rate constant as a function of time (Figure 5.5). As relation 5.35 is independent of the approximation for $t \to 0$, extrapolation of $k_{GF}(t)$ to $t \to 0$ gives the most accurate value of k_{GF}.

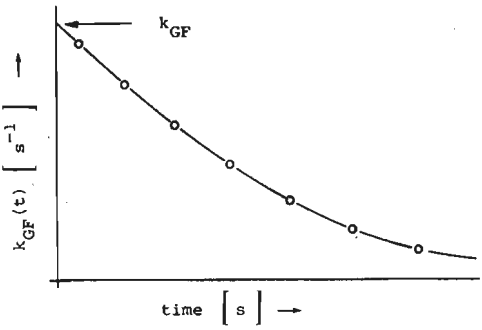

Figure 5.5. Method for calculating k_{IJ}.

With a somewhat modified derivation $\Sigma\ k_{GJ}$ can be calculated from the glucose concentration course:

$$\Sigma\ k_{GJ} = P_G \cdot \frac{\ln\left(C_{G_{opl},t=0} / C_{G_{opl}}\right)}{t} \tag{5.37}$$

with

$$P_G = \frac{V_{sol}/V_{pore} + K_{AG} \cdot C_{OH^-_{ie},t=0}}{K_{AG} \cdot C_{OH^-_{ie},t=0} \cdot C_{G_{sol},t=0}} \tag{5.38}$$

By extrapolation $\Sigma\ k_{GJ}$ can be determined similarly as is shown in Figure 5.5.

The degradation constant k_{GDe} is:

$$k_{GDe} = \Sigma\ k_{GJ} - \left(k_{GF} + k_{GM}\right) \tag{5.39}$$

With relation 5.30 and 5.24 k'_{-De} and the selectivity, defined as the fraction G, F and M formed from the enolate ion ($Sel_{en} = 1 - k'_{-De}$), can be calculated directly. From experiments, starting from fructose and mannose, the degradation constants k_{FDe} and k_{MDe} and also the selectivity can be calculated in a similar way.

This method of calculating the selectivity, however, has certain drawbacks:

- The reaction constant k_{GF} and k_{FM} are respectively 30 and 3 times higher than k_{GM}. Only when k_{GM} is calculated with a relation like 5.34, combined with accurate approximations for k_{IJ} in Q_{GM}, an adequate accuracy can be reached.
- As the concentrations are measured with an accuracy of 3%, the accuracy of the calculated k_{GF} will be of the same order. Because the absolute value of $C_{G_{sol}}$ is much higher than for $C_{F_{sol}}$ and $C_{M_{sol}}$, the absolute error in $C_{G_{sol}}$ is much higher and the determination of $\frac{d}{dt} C_{G_{sol}}$ is more inaccurate than $\frac{d}{dt} C_{F_{sol}}$ and $\frac{d}{dt} C_{M_{sol}}$.

The selectivity also can be defined as a function of the concentrations in the solution. This selectivity, the gross selectivity, is defined as:

$$Sel_{gr} = \frac{C_{F_{sol}} + C_{M_{sol}}}{C_{G_{sol},t=0} - C_{G_{sol}}} \tag{5.40}$$

The gross selectivity as a function of the conversion gives a good characterization of the catalyst. Extrapolation to initial conditions gives:

$$Sel_{gr,t\to 0} = \frac{k_{GF} + k_{GM}}{\Sigma\, k_{GJ}} \tag{5.41}$$

When k_{GF} and k_{GM} are determined from initial slopes or with an extrapolation method, the selectivity can be calculated again with relations 5.39, 5.30 and 5.24.

The accuracy is not increased essentially because it is based on the same experimental data.

5.4.2. SELECTIVITY CALCULATED FROM ONE SINGLE CONCENTRATION CURVE

When the 6 isomerization constants are calculated as described in the previous section and, if necessary, corrected conform to relation

5.16, only the degradation constant k'_{-De} remains unknown. Calculation of $k_{GF}(t)$ for different values of k'_{-De} gives the best degradation constant when $\frac{d}{dt} k_{GF}(t)$ will be zero (see Figure 5.6).

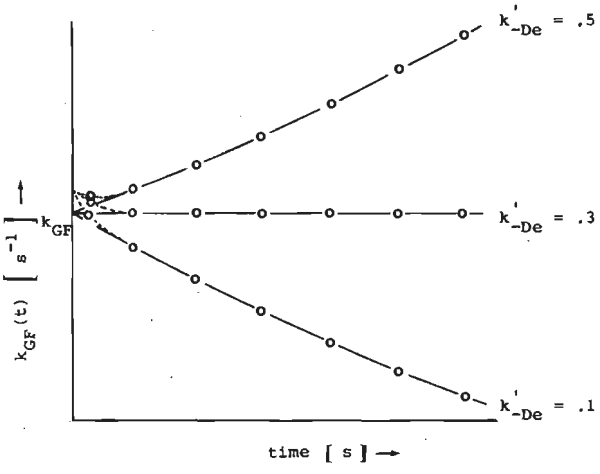

Figure 5.6. Method of determinating k'_{-De}.

As the approximation $C_{M_{sol}} = f\left(C_{F_{sol}}\right)$ gave too low a value for $C_{M_{sol}}$, this results in a slight overestimated k'_{-De}. So, the actual selectivity will be higher than Sel_{en}. Due to this systematic deviation, the selectivity from k'_{-De} only can be considered as an overall selectivity during the experiment. The changes in the catalytic behaviour of the ion exchanger is not taken into account. Nevertheless Sel_{en} is useful for comparison of the selectivity as a function of different parameters. A precondition, however, is that the selectivity is always calculated from the same conversion curve of k_{GF}. As the degradation of fructose is 3 times as fast as that of glucose and 10 times that of mannose, the change of k_{GF} from the fructose concentration curve gives the most accurate results.

At lower temperatures a starting effect can be present (broken line in Figure 5.5). The selectivity must be measured from the slope after the starting effect.

5.5. *RESULTS FOR THE ISOMERIZATION OF GLUCOSE*

In this section the influence of several parameters on the kinetics of the glucose isomerization using basic ion exchangers as a catalyst is discussed.

The reproducibility of the experiments appeared to be excellent. The homogeneous isomerization can be neglected totally when the pH in the outside solution does not exceed a value of 8.

5.5.1. *INFLUENCE OF THE TEMPERATURE*

As we also expect a concentration dependency, the influence of the temperature is measured at two different glucose concentrations for the gel-type resin Amberlite IRA 401. At concentrations of 80 mol m^{-3} and 3320 mol m^{-3}, the temperature influence on the isomerization constant k_{GF} is almost the same, as shown in Figure 5.7.

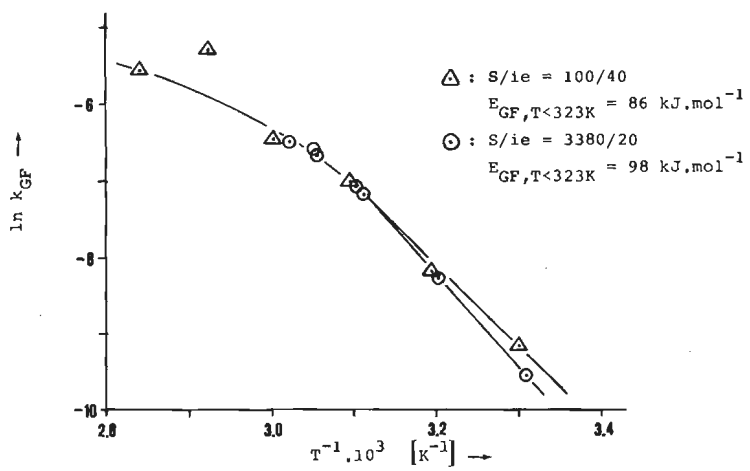

Figure 5.7. Arrhenius plot of k_{GF} for 2 different concentrations.

Only at the lower temperatures the activation energy differs slightly. For both concentrations a deviation from the Arrhenius straight lines sets in above 323 K due to diffusion influences. To ascertain that for T < 323 diffusion effects do not influence the kinetics, we varied the particle size ($\bar{d}_p$ = .3 mm and $\bar{d}_p$ = .55 mm) as well as the

Description	IRA 401				IRA 904	
	323 K	313 K	303 K	295 K	295 K	
	(1)	(2)	(3)	(4)	(5)	
$C_{S_{sol},t=0}$	78	77	75	75	82	
$C_{S_{ie},t=0}$	1080	1140	1200	1260	440	
$C_{H_2O_{ie},t=0}$	.88	.88	.87	.86	.95	
$pH_{ie,t=0}$	13.2	13.5	13.6	13.85	13.77	
						$E_{IRA\ 401}$
$k_{GF}.10^3$	.90	.28	.105	.0394	.0350	86
$k_{FG}.10^3$	.69	.215	.074	.0271	.0235	89
$k_{FM}.10^3$	.080	.032	.0077	.0029	.0030	94
$k_{MF}.10^3$	.34	.104	.022	.0070	.0085	109
$k_{MG}.10^3$	.104	.024	.0069	.0020	.0019	108
$k_{GM}.10^3$	.032	.0095	.0033	.0012	.0010	90
						$\Delta H_{IRA\ 401}$
K_{GF}	1.30	1.30	1.40	1.45	1.50	- 3
K_{FM}	.24	.30	.35	.41	.35	-15
K_{MG}	3.20	2.55	2.05	1.70	1.90	18
						$\Delta S_{IRA\ 401}$
ΔG_{GF}	- .70	- .65	- .85	- .90	- .95	- 7
ΔG_{FM}	3.80	3.00	2.65	2.10	2.50	-58
ΔG_{MG}	-3.10	-2.35	-1.80	-1.20	-1.55	65

Table 5.1. Effects of temperature and catalyst on the kinetics of the isomerization of glucose, fructose and mannose. The isomerization constants are expressed in s^{-1}, ΔH and ΔG are expressed in kJ mol^{-1} and ΔS in J mol^{-1} K^{-1}.

stirring rate (3 r.p.s. and 10 r.p.s.). Neither pore diffusion nor film diffusion effects could be visualized.

Also in experiments starting from fructose and mannose the reaction rate constants and the degradation constant k'_{-De} have been determined. Table 5.1 gives a survey of the experimental conditions and the kinetic results of the heterogeneous isomerization of glucose on the resin IRA 401 (gel-type) and IRA 904 (macroreticular-type).

We calculated $C_{G_{ie},t=0}$ and $C'_{H_2O_{ie},t=0}$ from the adsorption data (section 4.4) and the pore volume (section 4.3.3). In combination with the capacity (section 4.2.2) and the ionization constant (chapter 3) the internal basicity ($pH_{ie,t=0}$) can be calculated.

From literature data the mutarotation constant k_m is calculated for comparison with the isomerization constants. According to Isbell and Pigman (257), k_m can be calculated from:

$$k_m = k_{\alpha-\beta} + k_{\beta-\alpha} = .0001 + .003\ C_{H_3O^+} + 270\ C_{OH^-} \quad [s^{-1}] \qquad (5.42)$$

with an activation energy E_m of 72 kJ mol^{-1}.
The mutarotation rate can be decreased due to a decreasing water concentration. Kjaer et al. (170) found an order in C'_{H_2O} of 3.7. For this reason $k_m \cdot C'^{3.7}_{H_2O_{ie}}$ is also calculated.

In column (1)-(3) the results are given for the temperatures 323-303 K. Column (4) gives the extrapolated data at 295 K in order to compare them with the results using IRA 938 (column (5)).

In the last column, the thermodynamic parameters (E, ΔH and ΔS) are given, calculated from the data on the corresponding lines in Table 5.1.

The internal concentrations in IRA 401 are almost independent of the temperature. This ensures that the observed influences are direct temperature effects and not indirect concentration effects.

The mutarotation rate $k_m \cdot C'^{3.7}_{H_2O_{ie},t=0}$ is 8000 (IRA 401, 323 K) to 80000 (IRA 904, 295 K) times faster than the isomerization constant k_{GF}.

For the glucose-fructose conversion, we have applied the relations:

$$K_{GF} = k_{GF}/k_{FG} = c_1 \cdot e^{-\frac{E_{GF} - E_{FG}}{R \cdot T}} \tag{5.43}$$

with c_1 is a constant.
As k_{GF} is expressed in (liquid) concentrations, E_{GF} and E_{FG} are energies of activation:

$$\frac{d}{dt}\left(\ln K_{GF}\right) = \frac{E_{GF} - E_{FG}}{R \cdot T^2} = \frac{\Delta U_{GF}}{R \cdot T^2} \tag{5.44}$$

This gives:

$$\Delta U_{GF} = E_{GF} - E_{FG} \tag{5.45}$$

As the pressure is low and the volume of the system remains constant, relation 5.45 can be written as:

$$\Delta H_{GF} \sim \Delta U_{GF} \tag{5.46}$$

And further:

$$\Delta G_{GF} = - R \cdot T \ln K_{GF} \tag{5.47}$$

$$\Delta S_{GF} = \left(\Delta H_{GF} - \Delta G_{GF}\right)/T \tag{5.48}$$

The rate constants for degradation k'_{-De} are given in Table 5.2. The overall degradation constants of the various sugars are calculated with equations 5.24 and 5.26. The auxiliary constants X_I, Y_I and Z_I and the enolate kinetic constants k_I and k'_{-J} are directly calculated with relations 5.18, 5.20, 5.22, 5.27 and 5.28. These data give rise to the following considerations.

The reaction rates from glucose and fructose to mannose are relatively low. Therefore K_{FM} must be much smaller whereas K_{MG} must be

Description	IRA 401				IRA 904	
	323 K	313 K	303 K	295 K	295 K	$E_{IRA\ 401}$
	(1)	(2)	(3)	(4)	(5)	(6)
k'_{-De}	.29	.22	$.18^5$	.15	.25	
Sel_{en}	.71	.78	$.81^5$	.85	.75	
$k_{GDe}.10^3$	.49	.10	.032	.009	.015	108
$k_{FDe}.10^3$	1.22	.33	.073	.022	.044	112
$k_{MDe}.10^3$	.18	.037	.0067	.0016	.0035	132
$X_G.10^3$	.28	.064	.032	.011	.0078	86
$X_F.10^3$	8.0	2.45	.65	.23	.29	99
$X_M.10^3$	33.9	8.05	1.90	.55	.83	114
Y_G	.57	.64	1.02	1.25	.54	
Y_F	1.85	2.81	3.28	4.37	2.40	
Y_M	.066	.096	.10	.13	.068	
$Z_G.10^3$	1.21	.35	.14	.052	.046	85
$Z_F.10^3$	3.02	1.18	.32	.125	.132	90
$Z_M.10^3$	.46	.13	.03	.009	.011	109
$k_G.10^3$	1.69	.45	.17	.061	.058	91
$k_F.10^3$	4.24	1.52	.40	.15	.18	94
$k_M.10^3$	.64	.17	.036	.011	.014	113
k'_{-G}	.16	.14	.19	.18	.13	
k'_{-F}	.53	.62	.61	.65	.60	
k'_{-M}	.019	.021	.019	.020	.017	

Table 5.2. Effect of temperature and catalyst on the kinetics of the isomerization of glucose, fructose and mannose (continuation of Table 5.1).

much greater than 1.0. For the same reason ΔG_{FM} and ΔG_{MG} should be positive and negative successively. Within the enolate model these observations are caused by one single reason, viz. the low k'_{-M} value.

The high activation energy for the isomerization of mannose to glucose and fructose, gives a strong temperature dependence of K_{FM} and K_{MG} in the form of high values of ΔH_{FM} and ΔH_{MG}. It means that at high temperatures the mannose concentration decreases strongly within the equilibrium concentrations of the isomers. In Figure 5.8 the Arrhenius plot of the isomerization constants are given.

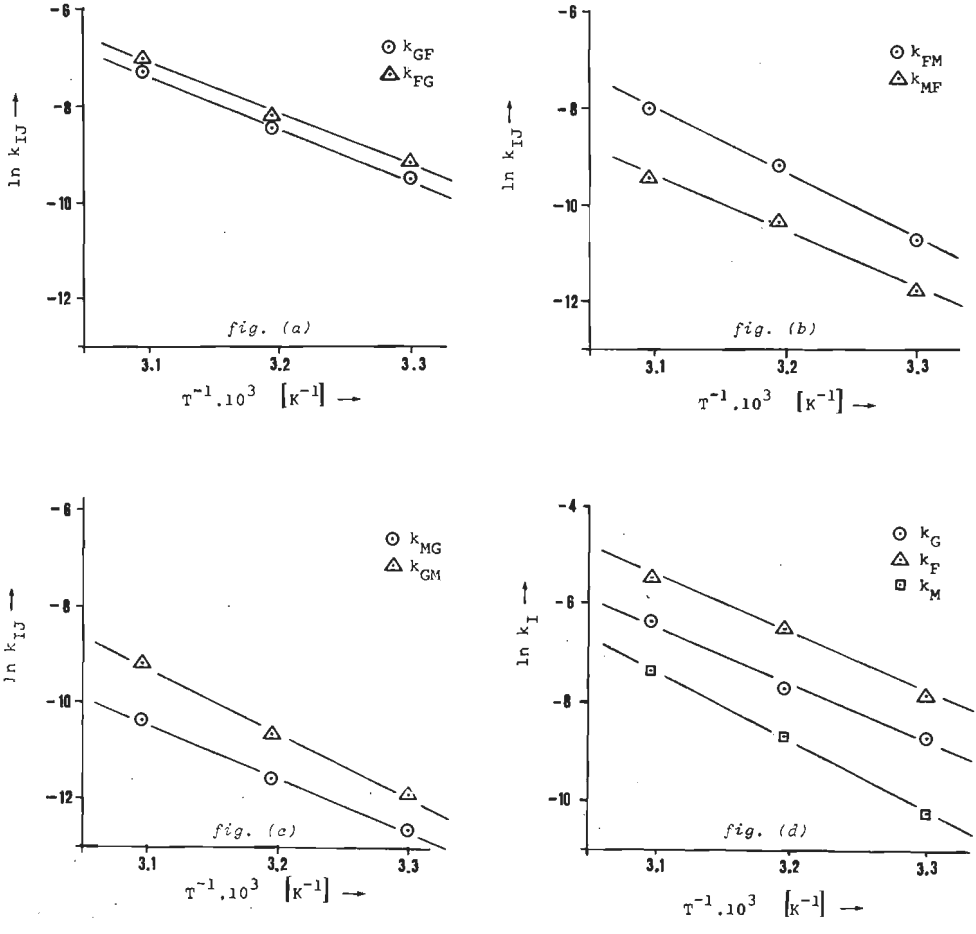

Figure 5.8. Arrhenius plots of the isomerization reaction constants. In Figure 5.8 (a)-(c) the temperature dependency within the overall model is given, while figure 5.8 (d) represents the temperature dependence within the enolate model.

From the activation energies we developed the potential energy picture as given in Figure 5.9.

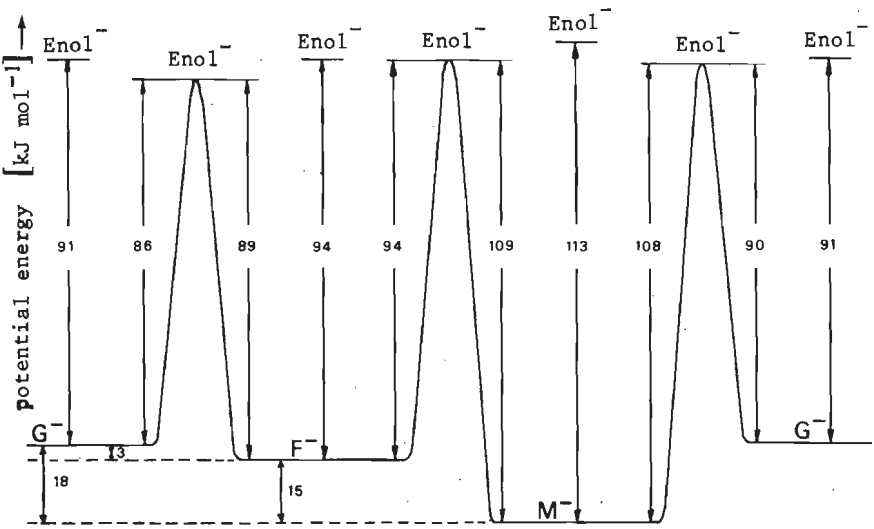

Figure 5.9. Energy picture.

It appears that the activation energies, calculated in the overall system and those calculated for the enolate system are both independent of the starting sugar and yield the same energy level for the activated enolate intermediate. Relative to glucose the energy level of the enolate intermediate is 90 $\pm$ 2.5 kJ mol^{-1}. As this level is independent of the starting sugar, we may say that the description of the interconversion of glucose, fructose and mannose via one single intermediate is in fully agreement with the potential energy distribution.

With decreasing temperature, the degradation k'_{-De} is decreasing (Table 5.2) and the selectivity is increasing (Figure 5.10).

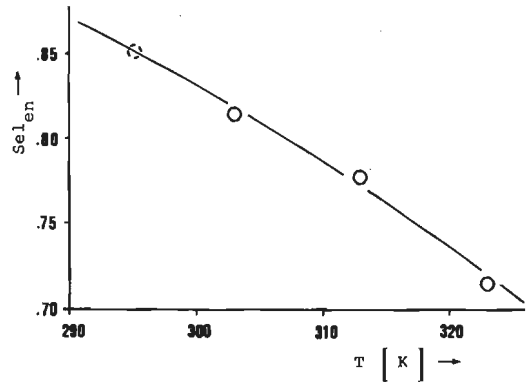

Figure 5.10. Selectivity of the glucose isomerization at standard conditions as a function of the temperature.

5.5.2. *INFLUENCE OF THE CONCENTRATION*

The influence of the initial sugar concentration on the kinetic parameters is determined for glucose only (Table 5.3).

S/ie	37/37	103/41	420/40	3200/410
$C_{G_{sol},t=0}$	22	78	380	2280
$C_{G_{ie},t=0}$	728	1100	1715	2830
$C_{G^-_{ie},t=0}$	717	1075	1590	1570
$C'_{H_2O_{ie},t=0}$	.92	.88	.80	.63
$pH_{ie,t=0}$	13.7	13.5	12.9	11.8
$k_{GF}.10^3$	.22	.28	.26	.24
$k'_{-De}.10^3$	.23	.22	.17	.05
Sel_{en}	.77	.78	.83	.95

Table 5.3. Effect of the sugar concentration on the activity and selectivity of the glucose isomerization reaction.

The isomerization is considered to be first order in the sugar anion concentration. For the conversion of glucose to fructose at $t \to 0$:

$$\frac{d}{dt} C_{F^-_{ie}} = k_{GF} \cdot C_{G^-_{ie}} \tag{5.49}$$

The isomerization constant k_{GF} appeared to be independent of the glucose concentration and the pH inside the ion exchanger:

$$k_{GF,\text{stand. cond.}} = .25 \pm .03 \quad [ks^{-1}]$$

This result proves that the isomerization of glucose is *only* first order in G^- and *independent* of the hydroxyl concentration.

With increasing glucose concentration the degradation decreases and the selectivity increases. Although the mutarotation rate decreases with increasing $C_{G_{ie}}$, the selectivity effect cannot be ascribed to this as the mutarotation rate $k_m \cdot \left(C'_{H_2O_{ie},t=0}\right)^{3.7}$ is 50000 $\left(C_{G_{ie}} = 730 \text{ mol m}^{-3}\right)$ to 200 $\left(C_{G_{ie}} = 2830 \text{ mol m}^{-3}\right)$ times faster than the isomerization rate. If we plot the data of Table 5.3, we obtain the Figures 5.11 (a) through (d).

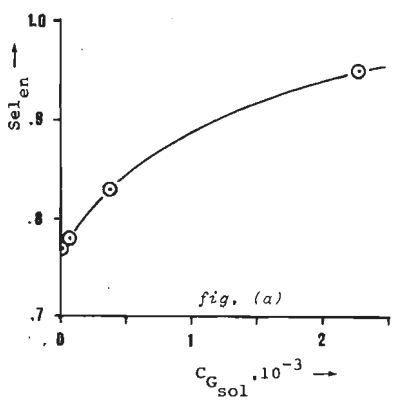

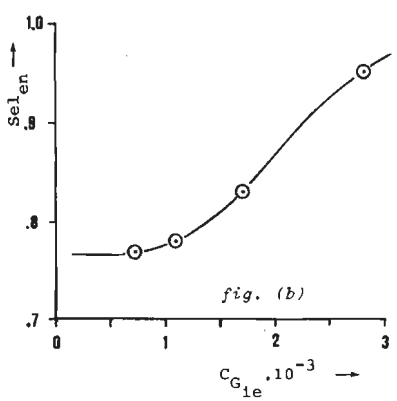

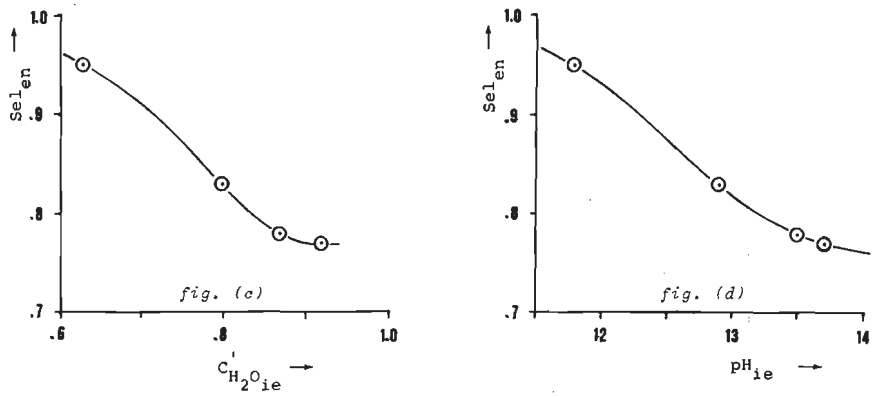

Figure 5.11. Selectivity of the glucose isomerization at standard conditions versus:
(a): glucose concentration in solution;
(b): glucose concentration in the exchanger;
(c): water concentration in the exchanger;
(d): pH in the exchanger.

It is not presumed that all plots show causal relations. The increase in selectivity can in principle be ascribed to an increase of the glucose concentration in the exchanger or to a decrease of the internal pH. The decreased water concentration is directly related with the increased glucose concentration. As we see from column (4) and (5) of Table 5.1 and 5.2 that for two different ion exchangers an increase in selectivity from 0.75 to 0.85 is accompanied by an increase of the internal glucose concentration, while the pH_{ie} remains constant, and because this effect shows the same relation as presented by column (1) and (3) of Table 5.3, we favour the explanation that increased selectivities are coupled to increased glucose concentration (or decreased water concentration). Although the mechanism of the degradation reactions is very complex, the concentration effect at high glucose concentrations (C_G > 1000 mol m^{-3}) must be ascribed to a conformation effect consequent on a decrease of the amount of water molecules in the direct surrounding of the reacting enediol anion.

The causality between the pH_{ie} and other influences, as the presence of quaternary ammonium groups inside the resin, and the selectivity cannot be quantified from our experimental results. At high glucose concentrations they are not supposed to have a dominating influence. For the homogeneous isomerization an influence of the hydroxyl concentration on the degradation is mentioned (165). For this reason it is likely that besides the concentration effect the pH_{ie} will influence the selectivity too.

Up to now the selectivity has been calculated from the fructose concentration curve (section 5.4.2). In order to obtain the concentration dependency, the selectivity is also measured from initial data (section 5.4.1) and the results of both methods are compared (Table 5.4).

experiment:	selectivity (Sel_{en})	
S/ie	from fructose curve (Table 5.3)	from initial data
	(1)	(2)
36/ 36	.77	.83
100/ 40	.78	.92
400/ 40	.83	> 1.00
3000/400	.95	.99

Table 5.4. Effect of the method of determining the selectivity.

In section 5.4.2 was mentioned already that the selectivity calculated from the fructose concentration curve, will give too low a value because of the approximation in the mannose concentration. With the exception of the 400/40 experiment both methods show the same trend with increasing concentration.

5.5.3. INFLUENCE OF THE TYPE OF ION EXCHANGER

In section 5.5.2 the difference in selectivity between the gel-type resin IRA 401 and the macroreticular-type IRA 904 has been discussed already. In Table 5.5 a comparison of the kinetics of the isomerization is given for three different basic ion exchangers and the homogeneous catalyst NaOH

To compare the isomerization constants of the various catalysts, we have normalized the sum of the isomerization constants according to:

$$k'_{-G} + k'_{-F} + k'_{-M} = .85 \qquad (5.50)$$

In column (5) to (7) the data are given, relative to Amberlite IRA 401.

There is a gradual change in the properties of the isomerization with the different catalysts:

$$\text{IRA 401} \longrightarrow \text{IRA 904} \longrightarrow \text{Bio-Rad} \longrightarrow \text{NaOH}$$

In this sequence the isomerization constants k_{IJ} are strongly decreasing. When the enolate constants k_I and k_{-I} are considered we see that the conversion rates of the enolate with glucose and mannose decreases to one quarter while k_F and k_{-F} are strongly increasing. As the pH_{ie} is not essentially different, these effects must be ascribed to the concentration change in the reaction system.

When these results are applied to the relation between the selectivity and the internal concentration, we expect the selectivity to decrease in the given sequence of catalysts, at least under the experimental conditions, stated in Table 5.5.

For the heterogeneous isomerization we saw already that mutarotation is much faster than isomerization. For the homogeneous isomerization at the conditions of MacLaurin and Green the mutarotation is even 500000 times faster.

Gleason and Barker (315) found different values for the relative enolization rate constants of ribose in Na_2CO_3 and KOH. As these rate constants are directly related to the degradation, the influence of

Description	IRA 401	IRA 904	Bio-Rad	NaOH	IRA 904 / IRA 401	Bio-Rad / IRA 401	NaOH / IRA 401
	(1)	(2)	(3)	(4)	(5)	(6)	(7)
$C_{S_{(ie)},t=0}$	1260	440	50	2	.35	.04	.002
$C'_{H_2O_{ie},t=0}$	.86	.95	.99	1.00	1.10	1.15	1.16
$pH_{(ie),t=0}$	13.8[5]	13.7[7]	13.6	14.0	.99	.98	1.01
$k_{GF}.10^3$	.0394	.0350	.0217	.0098	.89	.55	.25
$k_{FG}.10^3$	.0271	.0235	.0146	.0107	.87	.54	.39
$k_{FM}.10^3$	.0029	.0030	.0026	.0017	1.03	.90	.59
$k_{MF}.10^3$	.0070	.0085	.0062	.0031	1.21	.89	.44
$k_{MG}.10^3$	.0020	.0019	.0008	.00014	.95	.40	.07
$k_{GM}.10^3$	.0012	.0010	.0005	.00007	.83	.42	.06
$k_G.10^3$	.061	.052	.029	.012	.85	.48	.20
$k_F.10^3$	.147	.154	.153	.293	1.05	1.04	1.99
$k_M.10^3$	.011	.012	.008	.0030	1.09	.73	.27
k'_{-G}	.18	.15	.096	.037	.83	.53	.21
k'_{-F}	.65	.68	.74	.81	1.05	1.14	1.25
k'_{-M}	.020	.019	.017	.006	.95	.85	.30

Table 5.5. Influence of the type of catalyst on the kinetic constants at 295 K. In column (3) the isomerization constants, measured by Rendleman and Hodge at 300 K (81) are given after correction to 295 K using the activation energies from Table 5.1. The k_{MG}, which was not measured, is calculated with relation 5.16. Column (4) give MacLaurin and Green's data (225) for the homogeneous isomerization. The deviation from relation 5.16 is corrected in k_{GM}. In the columns (5)-(7) the properties relative to IRA 401 are given.

HCO_3^- and CO_3^{2-} as counterions for IRA 401 has been studied. The selectivity increased somewhat but the catalytic activity was very low. In the next section the enolization rates are discussed in more detail.

5.5.4. RELATIVE ENOLIZATION RATES

As we mentioned already, the relative enolization rate constants are related to the degradation. From the enolate equations (section 5.2.2) we can derive, e.g. for fructose relative to glucose:

$$\frac{k_F}{k_G} = \frac{k_{FM}}{k_{GM}} = \frac{k_{FDe}}{k_{GDe}} \qquad (5.51)$$

Isbell et al. (294), de Wilt and Kuster (285), Hepner (316) and de Wit (165) have reported these relative enolization rate constants. We calculated these from our experimental data and from the isomerization constants measured by Rendleman and Hodge (81) and MacLaurin and Green (225). In Table 5.6 a survey is given.

Catalyst	Temp.	Relative constants within enolate model				
	K	k_F/k_G	k'_{-F}/k'_{-G}	k_M/k_G	k'_{-M}/k'_{-G}	k'_{-De}/k'_{-G}
IRA 401	323	2.5	3.3	.38	.12	1.8
IRA 401	313	3.4	4.4	.38	.15	1.6
IRA 401	303	2.4	3.2	.21	.10	1.0
IRA 401	295	2.5	3.6	.18	.11	0.8
IRA 904	295	3.1	4.6	.24	.13	1.9
Bio-Rad	295	5.2	7.7	.29	.18	
NaOH, 1N	295	24.2	22.2	.31	.16	

Table 5.6. Relative reaction rate constants within the enolate model.

The relative reaction constants increase for the different catalysts in the sequence IRA 401→IRA 904→Bio-Rad → NaOH. This sequence is the same as discussed already for the selectivity.

In Figure 5.12 the relative enolization rates are given in an Arrhenius type plot.

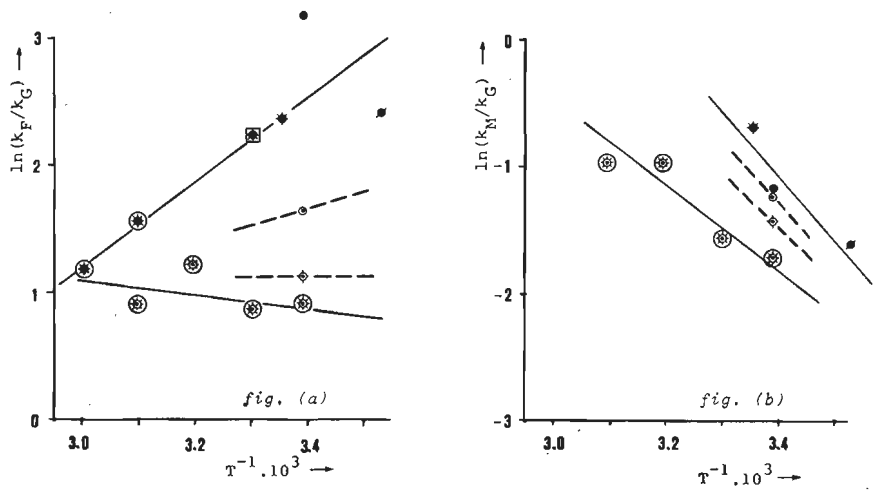

Figure 5.12. Enolization rates of fructose (fig. (a)) and mannose (fig. (b)) with:

our data: ◎ *IRA 401* ⊙ *IRA 904* ◉ *Bio-Rad* ● *NaOH*

literature data: ✱ *de Wilt et al.* ◆ *Hepner* ✸ *Isbell et al.* ✹ *de Wit*

The mentioned temperature dependence of the enolization in IRA 401 is clear. The literature data for the homogeneous reaction (de Wilt et al., Isbell et al., Hepner, MacLaurin et al. and de Wit) also give a more or less linear relation. In 1971 Isbell (317) stated that the data of de Wilt did not agree with his results. However, when the temperature influence on these relative rate constants is taken into account, the difference between de Wilt's and Isbell's data disappear.

5.5.5. FORMATION OF DEGRADATION PRODUCTS

The homogeneous degradation of glucose under N_2-atmosphere has been recently described by de Wit (165), who identified 11 different acidic products. According to his results the pH (11-14.3) and the type of cation influences the product distribution more slightly than the temperature (323-363 K) or the glucose concentration (15-150 mol m^{-3}).

To study the products of the degradation of the sugars glucose, fructose and mannose under N_2, we added a 3-fold excess of KCl to the mixture at the end of isomerization runs (section 5.3), determined the rest activity (Ac_r) by titration (section 4.2.2) and analyzed a sample by electrophoresis. In all cases we observed a deficiency in the carbon balance that varied between 2% at 313 K to 5% at 333 K.

As the mechanism of the degradation reactions is very complex, the possible influence of recombination reactions on the final product distribution will be discussed first.

5.5.5.1. INFLUENCE OF RECOMBINATION

The chain length of the degradation products is not only determined by fragmentation but also by recombination. For the homogeneous isomerization this effect is suggested already in literature (292, 328,329).

To show that recombination reactions also occur with anion exchangers, some explorative experiments were carried out with glyceraldehyde as the starting component on Amberlite IRA 904. From the results given in Table 5.7 we see that recombination to the C_6-sugars glucose, fructose and mannose occurs easily. Almost no glyceraldehyde is left after 1 ks at 333 K. The 1,2-enediol of glyceraldehyde gives lactic acid via β-elimination and a benzilic acid rearrangement. The saccharinic acids can be formed similarly from the 1,2 enolate ion of the hexoses.

Product distribution in mol fraction:			
in solution		in the catalyst	
glucose	.30	formic acid	.04
fructose	.05	acetic acid, glycolic acid	.05
mannose	.15	lactic acid	.62
arabinose, ribose	.20	glyceric acid	.03
galactose	.05	dihydroxybutyric acid	.06
glyceraldehyd	.05	deoxypentonic acid	.04
others	.20	saccharinic acids	.16

Table 5.7. Product distribution from reaction of glyceraldehyde with IRA 904.

5.5.5.2. INFLUENCE OF THE REACTION RATE

For the standard experiment the influence of the reaction time is studied. In Table 5.8 the product distribution in mol fraction and the degree of coverage θ in the ion exchanger are given. The degree of coverage represents the absolute quantity of acids per equivalent ion exchanger. To express the varying quantity of hydroxyl ions in the exchanger during an experiment we use the expression pH_{ie} and calculate the values according to:

$$pH_{ie} = pK_w + \log C_{OH^-_{ie}} + 3 \qquad (5.52)$$

$$pH_{ie} = pK_w + \log C_{OH^-_{ie},t=0} + \log Ac_r + 3 \qquad (5.53)$$

with Ac_r = rest activity.

Until 100 ks (pH_{ie} decreases from 13.5 to 12.7) the rates of formation for lactic acid and saccharinic acid are decreasing. From 100 ks

Description	Product distribution							
	after 7 ks		after 100 ks		after 200 ks		data de Wit: .035 M glucose with KOH at 353 K	
	fraction mol/mol	coverage mol/eq	fraction mol/mol	coverage mol/eq	fraction mol/mol	coverage mol/eq		
	(1)	(2)	(3)	(4)	(5)	(6)	(7)	(8)
rest activity	70 %		16 %		1 %		-	-
final $pH_{(ie)}$	13.4		12.7		11.5		13.7	11.0
formic acid	.05	.02	.09	.08	.12	.12	.03	.14
acetic acid	.07	.02	.10	.08	.15	.15	.10	.15
glycolic acid	.04	.01	.05	.04	.07	.07	.02	.17
lactic acid	.55	.16	.43	.36	.35	.34	.65	.20
glyceric acid	.03	.01	.06	.05	.07	.07	-	.01
dihydroxybutyric acid	.06	.02	.07	.06	.08	.08	.09	.15
deoxypentonic acid	.03	.01	.05	.04	.04	.04	-	.02
saccharinic acid	.17	.05	.15	.13	.12	.12	.10	.16
other acids	-	-	-	-	-	-	.01	-
total	1.00	.30	1.00	.84	1.00	.99	1.00	1.00

Table 5.8. Product distribution as a function of the reaction time for the standard experiment (glucose on IRA 401 at 313 K with S/ie = 100/40), compared with homogeneous data.

to 200 ks (pH_{ie} from 12.7 to 11.5) no further lactic and saccharinic acid are formed in contrast with the other acids.

From an oxygen balance of the isomerization and degradation products we found a few percent oxygen excess, implying that some oxidative degradation must have occurred. To study this, the ion exchanger was filtered from the solution after 7 ks of reaction (column (1) and (2), Table 5.8) and the wet filter cake was contacted with air for 50 ks. A strong increase of formic and glyceric acid and the formation of substantial quantities of arabonic acid were observed. This is in agreement with Samuelson and Stolpe (284) and de Wilt and Kuster (285). As no arabonic acid was found in our experiments (under N_2), we conclude that for the present experiments oxidative degradation can be neglected.

The influence of the product distribution on the pH has been shown for the homogeneous isomerization by de Wit (165). As he measured an influence of the pH, we have calculated the internal pH (pH_{ie}).

The influence of the pH_{ie} can be compared with pH effects in homogeneous isomerizations from de Wit, as presented in column (7) and (8) of Table 5.8. As no quantitative concentrations have been given by de Wit, the comparison can only be of a qualitative nature. With the exception of the saccharinic acids, the changes as a function of pH_{ie} are in agreement with the homogeneous data. At the beginning of the experiment the rupture of the C_3-C_4 bond, leading to the lactic acid production, is the most important reaction. When the reaction shows down due to a lower internal pH, the fragmentation to C_1 and C_2-acids increases relative to the benzilic acid rearrangement.

For a detailed discussion of the complex degradation reaction network, the reader is referred to the scheme given in the thesis of de Wit (165).

5.5.5.3. INFLUENCE OF THE TYPE OF SUGAR

To study the influence of the type of sugar, the standard experiment is also carried out with fructose and mannose for about 10 ks. It is not very useful to compare product distributions for different sugars at the same reaction time because their reaction rate constants are different. In this respect the product of the first order enolization constant k_I (Table 5.2) and the reaction time is a better dimensionless parameter. Therefore in Table 5.9 we have classified the hexose experiments at each temperature according to increasing $k_I \cdot t$.

In experiment (1) to (5) the final pH_{ie} and the rest capacity increase independent of the type of sugar. It also appears that the relative reaction time $k_I \cdot t$ dominates the product distribution. In Figure 5.13 (a) and (b) the mol fraction and the quantity, relative to the capacity (θ), are given as a function of the relative reaction time.

The experiments (6) and (7) at 323 K and (8) and (9) at 333 K show the same relations as discussed for the experiments at 313 K.

Temperature		313 K					323 K		333 K	
experiment nr.		(1)	(2)	(3)	(4)	(5)	(6)	(7)	(8)	(9)
relative time: $k_I \cdot t$		2	3	11	40	80	2	11	8	400
time: t [ks]		12	7	7	100	200	3	3	2	100
sugar		M	G	F	G	G	M	F	G	G
final pH_{ie}		13.4	13.4	13.0	12.7	11.5	13.0	12.8	12.6	11.2
rest activity		.75	.70	.45	.16	.01	.75	.55	.45	.02
mol fraction [mol mol^{-1}]	formic acid	.04	.05	.09	.09	.12	.07	.10	.12	.10
	acetic acid	.09	.07	.11	.10	.15	.10	.11	.14	.18
	glycolic acid		.04	.04	.05	.07		.04		
	lactic acid	.56	.55	.49	.43	.35	.51	.44	.37	.28
	glyceric acid	-	.03		.06	.07				.07
	dihydroxybutyric acid	.08	.06	.07	.07	.08	.07	.06	.08	.08
	deoxypentonic acid	.04	.03	.05	.05	.04	.03	.05	.04	.07
	saccharinic acids	.19	.17	.14	.15	.12	.22	.18	.23	.21
	total	1.00	1.00	1.00	1.00	1.00	1.00	1.00	1.00	1.00
coverage θ [mol eq^{-1}]	formic acid	.01	.02	.05	.08	.12	.02	.05	.06	.10
	acetic acid	.02	.02	.06	.08	.15	.03	.05	.08	.18
	glycolic acid		.01	.02	.04	.07		.02		
	lactic acid	.14	.16	.27	.36	.34	.12	.20	.21	.27
	glyceric acid	-	.01		.05	.07				.07
	dihydroxybutyric acid	.02	.02	.04	.06	.08	.02	.03	.05	.08
	deoxypentonic acid	.01	.01	.03	.04	.04	.01	.02	.02	.07
	saccharinic acids	.05	.05	.08	.13	.12	.05	.08	.13	.20
	total	.25	.30	.55	.84	.99	.25	.45	.55	.98

Table 5.9. Distribution of degradation products for glucose, fructose and mannose as a function of the relative time $k_I \cdot t$.

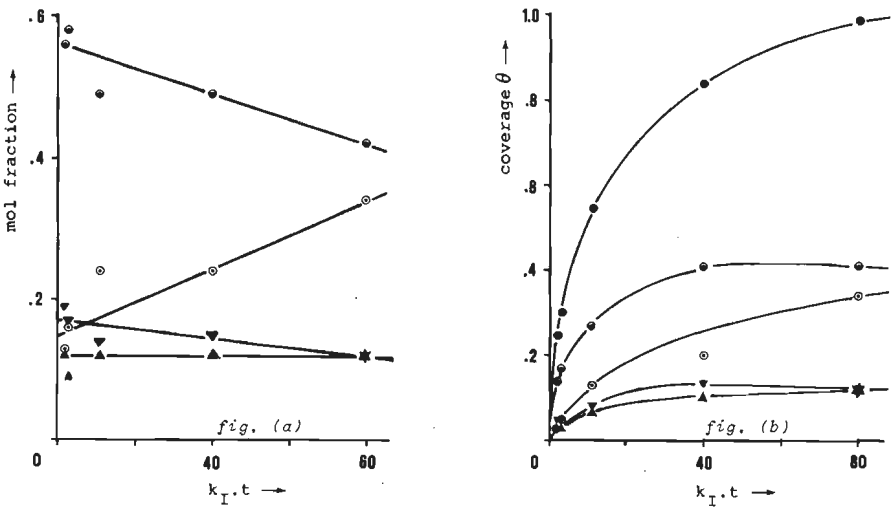

Figure 5.13. Mol fraction (fig. (a)) and coverage (fig. (b)) of the degradation products as a function of time with:
⊙ *$C_{1,2}$-acids;* ◒ *C_3-acids;* ▲ *$C_{4,5}$-acids,* ▼ *C_6-acids and* ● *C_{1-6}-acids.*

5.5.5.4. INFLUENCE OF THE TEMPERATURE

As the degradation as a function of the relative reaction time is independent of the type of sugar, the experiments (6)-(9) (Table 5.9) can be compared directly with column (1) to (5). In Figures 5.14 (a) and (b) the temperature dependency for the C_3 and the C_6 acid formation is shown. At higher temperatures less C_3-acids and more C_6-acids are formed due to an enhanced β-elimination with a benzilic acid rearrangement, relative to the retro-aldolization and aldolization.

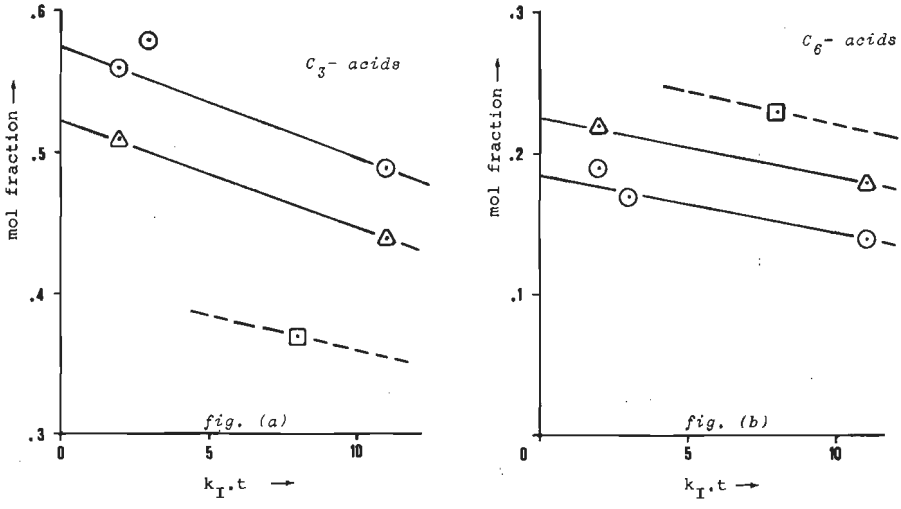

Figure 5.14. Influence temperature on the mol fraction of C_3-acids (fig. (a)) and C_6-acids (fig. (b)) with: ⊙ T = 313 K, ▲ T = 323 K, ⊡ T = 333 K.

5.5.6. FINAL CONCLUSIONS ON THE ISOMERIZATION OF GLUCOSE

- The isomerization of glucose, fructose and mannose can be described satisfactorily with the enolate model as follows inter alia from the energy level of the activated complex and from the observation that the product distribution of the degradation products, are independent of the type of sugar.
- The isomerization is first order in the sugar anion concentration and totally independent of the concentration molecular sugar or the concentration hydroxyl ions.
- The selectivity increases with increasing hexose or decreasing water concentration. To an unknown, but probably minor, extent the pH and the quaternary ammonium groups inside the catalyst may have an influence on the reaction too. At higher temperature the selectivity decreases.
- The mutarotation is under all experimental circumstances much faster than the isomerization and degradation.

- The decrease in selectivity in the series IRA 401 - IRA 904 - Bio-Rad - NaOH can be ascribed to a decrease of the hexose concentration in the catalytic alkaline environment.
- The increased selectivity with increasing glucose concentration, combined with the possibility to influence the physical properties of the catalyst, makes the isomerization process with ion exchangers economically more attractive than the homogeneous isomerization process.

5.6. RESULTS FOR THE ISOMERIZATION OF LACTOSE

The disaccharide lactose (O-β-D-galactopyranosyl-(1→4)-D-glucopyranose) can be considered as glucose with a galactose substituted on C_4. The kinetics of the isomerization of lactose do not differ from those, described for the glucose isomerization. The lactose-lactulose-epilactose interconversion, in which the glucose part of lactose transforms into fructose and mannose respectively, is also supposed to proceed via an enolate ion. The formation of epilactose is not taken into account furthermore. The kinetic model and the relations described in section 5.2 and 5.4 are also valid for the lactose isomerization. However, the main degradation product is galactose, due to glycosyl splitting, as the isomerization of glucose to talose and tagatose is very slow. Consequently, the gross selectivity to lactulose and the conversion for the lactose isomerization can be described by:

$$Sel_{gr} = \frac{C_{Lu_{sol}}}{C_{Lu_{sol}} + C_{Ga_{sol}}} \tag{5.54}$$

$$Conv = \frac{C_{Lu_{sol}} + C_{GA_{sol}}}{C_{La_{sol},t=0}} \tag{5.55}$$

For $t \rightarrow 0$ we get:

$$Sel_{gr,t\rightarrow 0} = \frac{k_{LaLu}}{k_{LaLu} + k_{LaGa}} \tag{5.56}$$

As the disaccharides are large molecules, diffusion can play a more important role. For this reason the standard experiment is carried out with the macroreticular ion exchanger Amberlite IRA 904. The concenctrations of sugar and exchanger for the lactose standard experiment are 600 and 40 mol m^{-3} respectively (S/ie = 600/40). The ionization constants of lactose and lactulose are given in chapter 3. In section 4.4 the adsorption of lactose and lactulose is given. The change of the pore volume due to this adsorption $\left(\frac{dPV}{d\theta}\right)$ is about twice as much as for glucose (Table 5.2, page 74). More information about physical properties like solubility can be found in the literature (319-323).

5.6.1. INFLUENCE OF THE TYPE OF CATALYST

For the isomerization of glucose the catalyst influences the selectivity. For this reason the gross selectivity in the isomerization of lactose was determined as a function of the conversion for several types of ion exchange resins. At 313 K as well as at 333 K the macroreticular resins IRA 904 and IRA 938 gave the highest selectivity. Among all resins, discussed in section 4.3.3 and appendix 2, these two exchangers have exceptionally high porosities.

To study the influence of the pore diffusion, the particle size is reduced about ten fold to $\bar{d}_p = .05 \pm .03$ mm. In Table 5.10 the results are given for the gel-type resin IRA 401 and the macroreticular resin IRA 904 at 313 K. The increased reaction rate constants k_{LaLu} and k_{LaGa} with smaller particles IRA 401 points to a pore diffusion limitation inside IRA 401. With IRA 904 as a catalyst no indication for pore diffusion is found.

If we assume no pore diffusion limitation in the ground particles of both ion exchangers column (2) and (4), it must be concluded that the gross selectivity, $Sel_{gr,t\to 0}$, shows that IRA 401 gives a higher selectivity than IRA 904. This is in agreement with the results of the glucose isomerization.

For the lactose isomerization we found that the carbonate form of Amberlite IRA 904 at 363 K shows a higher selectivity and the same activity than in the hydroxyl form at 313 K. This effect is more important because high temperatures, and thus high concentrations by an increased solubility, can be applied.

Description	IRA 401		IRA 904	
	(1)	(2)	(3)	(4)
$\bar{d}_p$ [mm]	.47	.05	.50	.05
$k_{LaLu}.10^3$	.21	.41	.54	.51
$k_{LaGa}.10^3$	.05	.022	.063	.052
$Sel_{gr,t\to 0}$	.80	.95	.90	.91

Table 5.10. Influence of the particle size on the isomerization of lactose at 313 K.

5.6.2. *INFLUENCE OF THE TEMPERATURE*

The temperature dependence of k_{LaLu} and k_{LuLa} are shown in the Arrhenius plot in Figure 5.15.

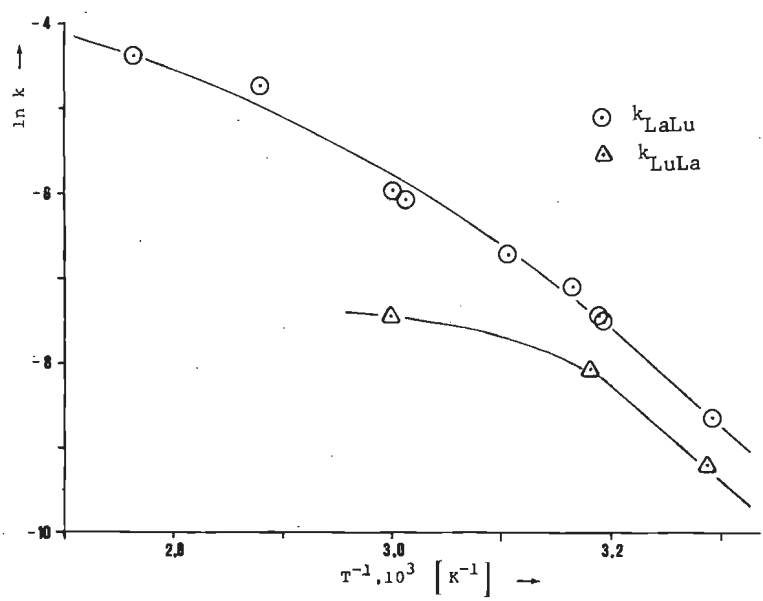

Figure 5.15. Arrhenius plot of k_{LaLu} and k_{LuLa}.

For temperatures T > 313 K the observed overall isomerization constants k_{LaLu} and k_{LuLa} deviate from the Arrhenius relation. The influence of the molecular size on the diffusion is considerable. Although a macroreticular resin is used for the lactose isomerization, a diffusion limitation starts already at a temperature above 313 K (cf. 323 K for glucose on ITA 401). The activation energies for T < 313 K for k_{LaLu} and k_{LuLa} are both about 90 kJ mol^{-1}. Comparison of the kinetic data at 303 K and 313 K with the data of the glucose isomerization with IRA 401 (Table 5.1) are given in Table 5.11.

T [K]	$k_{GF} \cdot 10^3$ [s^{-1}]	$k_{LaLu} \cdot 10^3$ [s^{-1}]	$k_{FG} \cdot 10^3$ [s^{-1}]	$k_{LuLa} \cdot 10^3$ [s^{-1}]	K_{GF}	K_{LaLu}
303	.105	.16	.074	.086	1.4	1.9
313	.28	.54	.215	.27	1.3	2.0

Table 5.11. Comparison isomerization glucose and lactose.

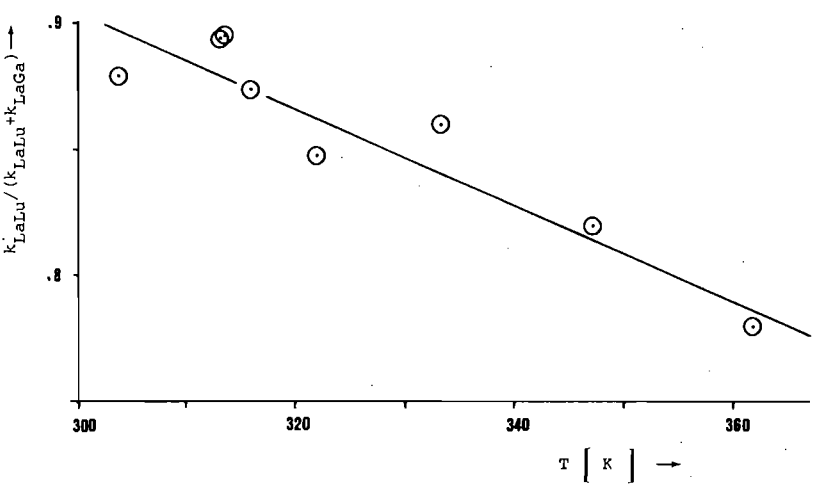

Figure 5.16. Selectivity of the lactose isomerization with IRA 904 as a function of the temperature.

The data show that the isomerization as well as the equilibrium constants for the lactose isomerization are higher than for glucose.

The ratio $k_{LaLu} / \left(k_{LaLu} + k_{LaGa}\right)$ is a measure of the selectivity. In Figure 5.16 this ratio is shown as a function of the temperature. The decrease in the selectivity with increasing temperature is in agreement with the observation in the glucose isomerization (section 5.1.1).

5.6.3. INFLUENCE OF THE CONCENTRATION

S/ie	100/40	600/40
$C_{S_{opl},t=0}$	90	570
$C_{S_{ie},t=0}$	250	570
$C'_{H_2O_{ie},t=0}$	.94	.87
$pH_{ie,t=0}$	13.43	13.15
$k_{LaLu}.10^3$	.60	.54
$k_{LuLa}.10^3$	.20	.27
$k_{LaGa}.10^3$	.15	.064
$k_{LuGa}.10^3$	.67	.51
K_{LaLu}	3.0	2.0
$k_{La}.10^3$	.79	.64
$k_{Lu}.10^3$	3.5	5.1
k'_{-La}	.06	.05
k'_{-Lu}	.75	.85
k'_{-Ga}	.19	.10
Sel_{en}	.81	.90

At two different concentrations, lactose and lactulose isomerization experiments have been carried out. In Table 5.12 the data, corrected to 313 K, are given. With the relations as discussed in section 5.2.2, the kinetic constants within the enolate model can be calculated.

The enolate selectivity Sel_{en} for the lactose isomerization is calculated directly from the measured degradation constants. For this reason it is not possible to compare these data with Sel_{en} for the glucose isomerization.

The increase of Sel_{en} with the sugar concentration is in agreement with this effect for the glucose isomerization.

Table 5.12. Influence of the concentration in the lactose isomerization on IRA 904 at 313 K.

5.6.4. FORMATION OF DEGRADATION PRODUCTS

The degradation of oligosaccharides has been studied by several authors (307-313). The homogeneous degradation of lactose gives the hydrolysis products galactose and α- and β-isosaccharinic acids.

In Table 5.13 the product distribution of the degradation of lactose in IRA 904 is compared with that of glucose at a comparable $k_I \cdot t$ value.

name acid	mol ratio	
	lactose	hexose
formic acid	.21	.06
acetic acid / glycolic acid	.05	.15
lactic acid	.03	.33
glyceric acid	.01	.02
dihydroxybutyric acid	.12	.10
deoxypentonic acid	.04	.04
meta-saccharinic acid	.11	.24
iso-saccharinic acid	.43	.06

lactose:
S/ie = 200/40
T = 333 K
$k_I \cdot t$ = 23

Table 5.13. Product distribution in lactose degradation, compared with the product distribution from glucose.

From the amounts of formic acid and iso-saccharinic acid we can conclude that the degradation of lactose and lactulose probably will proceed via the same intermediate 4-deoxy-2,3-hexodiulose.

Recent literature data (300-303) show that 4-deoxy-2,3-hexodiulose, an intermediate for the degradation via an 2,3 enolate mechanism for hexoses, can give 3,4-dideoxypentonic acid. However, we were unable to verify these results.

5.6.5. *FINAL CONCLUSIONS ON THE ISOMERIZATION OF LACTOSE*

- The isomerization of lactose to lactulose in the presence of basic ion exchangers can be described analogous to the glucose isomerization. The interconversion is only a function of the temperature and the concentration of the sugar anions inside the resin. The pH_{ie} has no influence on the isomerization.
- Degradation of lactose and lactulose occurs mainly via an 2,3-enolate intermediate and 4-deoxy-2,3-hexodiulose to formic acid and iso-saccharinic acid.
- The increased selectivity with increasing lactose concentration at higher temperatures will give an economically attractive process. To prevent diffusion limitation a less active catalyst as a weakly basic ion exchanger can be used.
- The isomerization with ion exchangers is specially commercially attractive for those processes which cannot be carried out enzymaticly e.g. the conversion of lactose to lactulose and maltose to maltulose.

LITERATURE

1. Hale, W.J., The Farm Chemurgy, The Stratford Co., Boston, Mass. (1934)
2. Clark, J.P., Kirk-Othmer Enc. Chem. Techn., 5, 553-564 (1979)
3. Mc.Ketta, J.J., Enc. Chem. Proc., 7, 303-304 (1978)
4. Hall, D.O., Biomass for Energy, UK-ISES, 1-14 (1979)
5. Rapport van de Club van Rome, Het Spectrum, Utrecht, Aula-Pocket 500 (1972)
6. Kohn, Ph.M., Chem. Engng., 31, 63-65 (1977)
7. Van der Baan, H.S., Chemisch Weekblad, m123 (1976)
8. Maisel, D.S., Tappi, 61, (1), 51-53 (1978)
9. Luteijn, D., Chemisch Weekblad, 39, 1 (1978)
10. Van Krevelen, D.W., Chemisch Weekblad, m723-m728 (1978)
11. Davies, D.S., Chemistry and Industry, 771-775 (1975)
12. Princen, L.H., Crop Resources, 4133-4147 (1977)
13. Coombs, J., Parker, K.J., Biomass for Energy, UK-ISES, 69-89 (1979)
14. Selby, K., Industrial Aspects of Biochemistry, 787-812 (1974)
15. Marton, J., Science, 199, 1041 (1978)
16. Bol, W., Chemisch Weekblad, 23-25 (7-6-1974)
17. Tillman, D.A., Wood as an Energy Resource, N.Y., Acad. Press (1978)
18. Interdisciplinaire Adviesgroep, A.I.D.-Energy (1977)
19. Turbak, A.F., Kirk-Othmer Enc. of Chem. Techn., 5, 71 (1979)
20. Wilke, C.R., Cellulose as a Chemical and Energy Resource, New York, Interscience (1975)
21. Rowell, R.M. and Young, R.A., Modified Cellulosics, New York, Academic Press (1978)
22. Funk, H.F., Appl. Pol. Symp., 28, 145-153 (1975)
23. Heikens, D., Chemisch Weekblad, m17 (1979)
24. Jullander, I., Appl. Pol. Symp. 28, 55-60 (1975)

25. Birch, G.G., Parker, K.J., Sugar: Science and Technology, London, Applied Science Publishers LTD (1979)
26. Parker, K.J., La Sucr. Belge, 93, 15-27 (1974)
27. Benninga, H., Chemisch Weekblad, m133-m135 (1976)
28. Vlitos, A.J., Sucr. Fr., 3, 109-117 (1975)
29. Kampen, W.H., Procestechniek, 34, 500-505 (1979)
30. Von Bernhard, W., Menrad, H. and König, A., Starch 31, 254 (1979)
31. Gochnarg, I., Biomass for Energy, UK-ISES, 30-50 (1979)
32. Swinkels, J., Woldendorp, P., Chemisch Weekblad, 3, m136-m138 (1976)
33. Kohn, Ph.M., Chem. Engng. 19, 36-38 (1977)
34. Otey, O.F., Westhoff, R.P., Russell, C.R., I&EC Prod. Res. & Development, 16, 305-308 (1977)
35. Kempf, W., Starch, 30, 254-256 (1978)
36. Suzuki, S., Starch, 30, 217-223 (1978)
37. Gramera, R.E., Starch, 30, 20-23 (1978)
38. Dirkx, J.M.H., Thesis Eindhoven (1977)
39. Vellenga, K., Thesis Groningen (1978)
40. Kuster, B.F.M., Thesis Eindhoven (1975)
41. Nickerson, T.A., Food Technol., 14, 40-60 (1978)
42. Van der Steen, H.C., Internal report of University of Technology Eindhoven, Department of Chemical Engineering (1974)
43. Fruin, J.C., Scallet, B.L., Food Technol., 11, 40-45 (1975)
44. Kirk-Othmer, Enc. of Chem. Techn., 19, 594-595 (1966)
45. Doty, T.E., Vanninen, E., Food Technology, 11, 34-38 (1975)
46. Henry, R.E., The Bakers Digest, 50, (2), 25-26 (1976)
47. Singleton, C.B., The outlook for isoglucose, Ratzeburg, F.O. Light, 7-36 (1978)
48. Schmidt, E., The outlook for isoglucose, Ratzeburg, F.O. Light, 37-58 (1978)
49. Editorial staff, Starch, 31, 71 (1979)
50. Pijnenburg, H.C.M., Kuster, B.F.M., van der Baan, H.S., Starch, 30, 199-205 (1978)
51. Gruette, F.K., Haenel, H., Mueller-Benthow, W., Nutr., Proc. Int. Congr., 8th, 451-453 (1969)

52. Repertorium Pharmaceutische Specialité's, 12, (24), 186 and 436; De Toorts, Haarlem (1979)
53. Van der Steen, H.C., Internal report of the Eindhoven University of Technology, Departm. of Chem. Engng. (1975)
54. Roels, J.A., Intermediair, 15, (41), 53-61 (1979)
55. Lobry de Bruyn, C.A., Alberda van Ekenstein, W., Rec. Trav. Chim. Pays-Bas, 14, 204-216 (1895); 15, 93-96 (1896); 16, 257-261 (1897)
56. Speck, J.B., Adv. Carbohyd. Chem., 13, 63-103 (1958)
57. MacAllister, R., Adv. Carbohyd. Chem., 36, 15-56 (1979)
58. Marchall, R.O., Kooi, E.R., Science, 125, 648-649 (1957)
59. Boonstra, D.J., Vellenga, K., de Wilt, H.G.J., Chemisch Weekblad, m196 (1976)
60. Mendicino, J.F., J. Am. Chem. Soc., 82, 4975-4979 (1960)
61. Kainuma, K., Tadokoro, K., Suzuki, S., Nippon Nogei Kagaku Kaishi, J. Agr. Chem. Soc., 40, 35-40 (1966)
62. Barker, S.A., Hatt, B.W., Somers, P.J., Carbohyd. Res., 26, 41-53 (1973)
63. Barker, S.A., Somers, P.J., Hatt, B.W., Ger. Offen Pat. 2,229,064 (1973)
64. Barker, S.A., Hatt, B.W., Somers, P.J., Carbohyd. Res., 26, 55-64 (1973)
65. Barker, S.A., et al., U.S. Pat. 3,875,140 (1975)
66. Barker, S.A., et al., Ger. Offen Pat. 2,627,111 (1976)
67. Bociek, S., Franks, F., J. Chem. Soc., Farad. Trans. 1, 75, 262-270 (1979)
68. Haack, E., Braun, F., Kohler, K., Brit. Pat. 949,293 (1961)
69. Haack, E., Braun, F., Kohler, K., U.S. Pat. 3,256,270 (1966)
70. Nitta, Y., Nakajima, Y., et al., Jap. Pat. 67-3487 (1967)
71. Parrisch, F.W., U.S. Pat. 3,431,253 (1969)
72. Guth, J.H., Tumerman, L., U.S. Pat. 3,546,209 (1970)
73. Hodge, J.E., Rendleman, J.A., Nelson, E.C., Cereal Sci. Today, 17, 180-188 (1972)
74. Machida, I., et al., Jap. Pat. 73-49,938 (1973)
75. Tumerman, L., et al., U.S. Pat. 3,822,249 (1974)
76. Haack, E., Braun, F., Kohler, K., Ger. Pat. 1,163,307 (1961)
77. Rendleman, J.A., Hodge, J.E., Carbohyd. Res., 44, 155-167 (1976)

78. Shaw, A.J., Diss. Abstr. Int. B, 38, 808 (1977)
79. Shaw, A.J., Tsao, G.T., Carbohyd. Res., 60, 327-335 (1978)
80. Shaw, A.J., Tsao, G.T., Carbohyd. Res., 60, 376-382 (1978)
81. Rendleman, J.A., Hodge, J.E., Carbohyd. Res., 75, 83-99 (1979)
82. Rebenfeld, L., Pascu, E., J. Am. Chem. Soc., 75, 4370 (1953)
83. De Wit, G., Kieboom, A.P.G., Van Bekkum, H., Carbohyd. Res., 74, 157-175 (1979)
84. Beenackers, J.A.W.M., Lecture at "Die Stärketagung", Detmold (1979)
85. Ohms, J.I., Zec, J., Benson, J.V., Patterson, J.A., Anal. Biochem., 20, 51-57 (1967)
86. Kesler, R.B., Anal. Chem., 39, 1416-1422 (1967)
87. Walborg, E.F., Lantz, R.S., Anal. Biochem., 22, 123-133 (1968)
88. Walborg, E.F., Kondo, L.E., Anal. Biochem., 37, 320-329 (1970)
89. Floridi, A., J. Chromatogr., 59, 61-70 (1971)
90. Verhaar, L.A.Th., Dirkx, J.M.H., Carbohyd. Res., 59, 1 (1977)
91. Jandera, P., Churácek, J., J. Chromatogr., 98, 55 (1974)
92. Voelter, W., Bauer, H., J. Chromatogr., 126, 693 (1976)
93. Verhaar, L.A.Th., Van der Aalst, M.J.M., Beenackers, J.A.W.M., Kuster, B.F.M., J. Chromatogr., 170, 363-370 (1979)
94. Kennedy, J.F., Chaplin, M.F., Carbohyd. Res., 40, 227-233 (1975)
95. Everaerts, F.M., Routs, R.J., J. Chromatogr., 58, 181 (1971)
96. Everaerts, F.M., Thesis, Eindhoven University of Technology (1968)
97. Everaerts, F.M., Beckers, J.L., Verheggen, Th.P.E.M., Isotachophoresis, J. of Chrom. Library, 6, Elsevier Sc. Publ. Co. (1976)
98. Whistler, R.L., BeMiller, J.N., Methods in Carbohyd. Chem. II, 480 (1963)
99. Minderhout, J.K., M.Sc. Thesis, Delft University of Technology (1976)
100. De Wit, G., M.Sc. Thesis, Delft University of Technology (1976)
101. Sato, Y., Miyake, T., Sakai, S., Mitsuhashi, M., Ger. Offen. Pat. 2,038,230 (1969)
102. Peligot, E., Compt. Rend., 7, 106 (1838)
103. Peligot, E., Ann., 30, 69 (1839)
104. Pigman, W., Isbell, H.S., Adv. Carbohyd. Chem., 23, 11-57 (1968)
105. Isbell, H.S., Pigman, W., Adv. Carbohyd. Chem. Biochem., 24, 13-65 (1969)

106. Pigman, W., "The carbohydrates", Academic Press Inc., New York (1957)
107. Isbell, H.S., Wade, C.W.R., J. Res. Natl. Bur. Stand. Sect., A71, 137 (1967)
108. Isbell, H.S., Frush, H.L., Wade, C.W.R., Hunter, H., Carbohyd. Res., 9, 163 (1969)
109. Maier, G.D., Kusiak, J.W., Baily, J.M., Carbohyd. Res., 53, 1-11 (1977)
110. Kiyohisa, F., Makromol. Chem., 179, 625-632 (1978)
111. Cher Soon, C., Hsing Hua, H., J. Chem. Soc., Perkin Trans., 2, 474-478 (1978)
112. Gram, F., Hveding, J.A., Rein, A., Acta Chem. Scand., 27, 3616-3624 (1973)
113. Kiyohisa, F., Aust. J. Chem., 30, 685-7 (1977)
114. Livingstone, G., Franks, F., Aspinal, L.J., J. Sol. Chem., 6, 203-216 (1977)
115. Cox, B.G., Natarajan, R., J. Chem. Soc., Perkin Trans., 2, 2021-2024 (1977)
116. Mercer, D.G., O'Driscoll, K.F., J. Mol. Cat., 4, 217-224 (1978)
117. De Wit, G., Kieboom, A.P.G., van Bekkum, H., Trav. Chim. Pays-Bas, 98, 355-361 (1979)
118. Hudson, C.S., Dale, J.K., J. Am. Chem. Soc., 39, 320-328 (1917)
119. Los, J.M., Simpson, L.B., Rec. Trav. Chim., 76, 267-285 (1957)
120. Smolenski, K., Kozlowski, W., Rocz. Chem. Annals of Chemistry, 16, 270 (1936)
121. Smolenski, K., Kozlowski, W., Rocz. Chem. Annals of Chemistry, 16, 281 (1936)
122. Capon, B., Overend, W.G., Advan. Carbohyd. Chem., 15, 32 (1960)
123. Casu, B., Reggiani, M., Gallo, G.G., Vigerani, A., Tetrahedron, 22, 3061 (1966)
124. Lygina, V.Ya., Lygin, E.S., Izv. Vyssh. Ucheb. Zaveb., Pishch. Tekhnol. (Bull. Inst. Higher Educ. Food Technol.), 5, 34-36 (1970)
125. Madsen, T., Z. Phes. Chem., 36, 290 (1901)
126. Hirsch, P., Schlags, R., Z. Physik. Chem.-A, 141, 387 (1929)
127. Urban, F., Shaffer, P.A., J. Biol. Chem., 94, 697 (1931-1932)
128. Souchay, P., Schaal, R., Bull. Soc. Chim. Fr., 819 (1950)

129. Kilde, G.C., Wynne-Jones, W.F.K., Trans. Far. Soc., 49, 243 (1953)
130. Los, J.M., Simpson, L.B., Rec. Trav. Chim. Pays-Bas, 73, 941-958 (1954)
131. Ramaiah, N.A., Kativar, S.S., Proc. Ann. Conv. Sugar Technol. Ass. India, 29, 77 (1961)
132. Guillot, G., Rumpe, P., Compt. Rend., 259, 4064 (1964)
133. Bunton, C.A., Chaimorich, H., J. Am. Chem. Soc., 88, 4082 (1966)
134. Izatt, R.M., Rytting, J.H., Hansen, L.D., Christensen, J.J., J. Am. Chem. Soc., 88, 12 (1966)
135. De Wilt, H.G.J., Thesis, Eindhoven University of Technology (1969)
136. Christensen, J.J., Rytting, J.H., Izatt, R.M., J. Chem. Soc.-B, 9, 1646-1648 (1970)
137. Degani, Ch., Carbohyd. Res., 18, 329 (1971)
138. Thamsen, J., Acta Chemica Scandinavica, 6, 270-284 (1952)
139. Michaelis, L., Rona, P., Biochem. Z., 49, 232 (1913)
140. Denbigh, K., 'The principles of chemical equilibrium', Cambridge University Press (1971)
141. De Wilt, H.G.J., Lindhout, I., Carbohyd. Res., 23, 333-341 (1973)
142. Robinson, R.A., Stokes, R.H., Electrolyte Solutions, 2nd Ed., London (1959)
143. Shiio, H., J. Am. Chem. Soc., 80, 70-73 (1958)
144. Yasunaga, T., Usui, I., Iwato, K., Miura, M., Bull. Chem. Soc. Japan., 37, 1658-1660 (1964)
145. Tait, M.J., Suggett, A., Franks, F., Ablett, S., Quinkenden, P.A., J. Sol. Chem., 1, 131-151 (1972)
146. Franks, F., Reid, D.S., Suggett, A., J. Sol. Chem., 2, (2/3), 99-118 (1973)
147. Harvey, J.M., Symons, M.C.R., Richard, J., Nature, 261, 435-436 (1976)
148. Suggett, A., J. Sol. Chem., 5, 33-47 (1976)
149. Miyahara, Y., Kagaku, 29, 365 (1959)
150. Stokes, R.H., Robinson, R.A., J. Sol. Chem., 2, 173-191 (1973)
151. Flory, P.J., J. Chem. Phys., 9, 660 (1941); *ibid.*, 10, 51 (1942)
152. Kozak, J.J., et al., J. Chem. Phys., 48, 675 (1968)

153. Rendleman, Jr., J.A., Adv. Chem. Ser., 117, 51-69 (1973)
154. "Tabellenboekje ten dienste van laboratoria', K.N.C.V. (1962)
155. Yagil, G., Anbar, M., J. Am. Chem. Soc., 85, 2376-2380 (1963)
156. Anbar, M., Bobtelsky, M., Samnel, D., Silver, B., Yagil G., J. Am. Chem. Soc., 85, 2380-2384 (1963)
157. Yagil, G., J. Phys. Chem., 71, 1045-1052 (1967)
158. Yagil, G., J. Phys. Chem., 73, 1610-1612 (1968)
159. Yagil, G., Israel Journal of Chemistry, 9, 329-350 (1971)
160. Yagil, G., J. Chem. Soc. Chem. Comm., 672-673 (1977)
161. Bonner, O.D., Breazeale, W.H., J. Chem. Engng. Data, 10, 325-327 (1965)
162. Rao, V.S.R., Foster, J.F., J. Phys. Chem., 69, 636 (1965)
163. Schwabe, K., Croat. Chem. Acta., 44, 127-137 (1972)
164. Christensen, J.J., Izatt, R.M., Hansen, L.D., J. Am. Chem. Soc., 89, 213-222 (1967)
165. De Wit, G., Thesis, Delft University of Technology (1979)
166. Allen, C.R., Wright, P.C., J. Chem. Ed., 41, 251 (1964)
167. Gurney, R.W., Ionic processes in solution, New York (1953)
168. King, E.J., Int. Enc. Chem. Phys., 15, (4) (1965)
169. Huggins, M.L., J. Chem. Phys., 9, 440 (1941); *ibid.*, 46, 151 (1942); Ann. N.Y. Acad. Sci., 43, 1 (1942)
170. Kjaer, A.M., Sorensen, P.E., Ulstrup, J., J. Chem. Soc., Perkin Trans. II, 1, 51-59 (1978)
171. Kunin, R., Ion Exchange Resins, Huntington, N.Y. (1972)
172. Kolarz, B., Chem. Stosow., 19, 71-79 (1975)
173. Kolarz, B., Chem. Stosow., 20, 3-4 (1976)
174. Oehme, Ch., Martinola, F., Chemistry and Industry, 823-826 (1973)
175. Venderbosch, H.W., KEMA, Arnhem, private communications
176. Petrarin, I., Dragan, S., Petrarin, P., Rev. Chim., 21, 207-212 (1970)
177. Fejes, P., ASEA (Allm. Sv. Elek. AB) Res., 10, 127-141 (1969)
178. Subbotina, N.P., Gromoglasov, A.A., Pavlova, L.A., Tr. Mosk. Energ. Inst., 80, 140-149 (1971)
179. Kuyama, H., Takamisawa, Y., Higosaki, N., Nippon Kagaku Kaishi, 10, 2020-2022 (1974)
180. Gerritsen, L.A., Thesis, Delft University of Technology (1979)

181. Paleos, J., Rohm and Haas Company, private communications (1979)
182. Tilsley, G.M., Chem. and Ind., March, 142-148 (1979)
183. Christofides, C., Smits, J., Chem. and Ind., March, 149-153 (1979)
184. Setinek, K., Chem. Prum,, 26, 535-538 (1976)
185. Pokrovskaya, A.I., Martsinkerich, R.V., Soldatov, V.S., Veste Akad. Navuk Belarus SSR, Ser. Khim. Navuk., 5, 38-42 (1973)
186. Langmuir, J., J. Am. Chem. Soc., 40, 1361 (1918)
187. Boyd, G.E., Adamson, A.W., J. Am. Chem. Soc., 69, 2818-2829 (1947)
188. Beranek, L., Cat. Rev.-Sci. Eng., 16, 1-35 (1977)
189. Freundlich, H., Trans. Far. Soc., 28, 195-201 (1932)
190. Zeldovitch, J.B., Acta Physicochimica, U.S.S.R., 1, 961 (1935)
191. Appel, J., Surf. Sci., 39, 237-244 (1973)
192. Fujii, S., Kawasaki, K., Komoto, M., Nippon Shokuhin Kogyo Gakkai-Shi (J. Food. Sci. Technol.), 20, 449-455 (1973)
193. Fujii, S., Kawasaki, K., Komoto, M., Seito Gijutsu Kenkyukaishi (Proc. Res. Soc. Jap. Sugar Ref. Technol.), 25, 39-46 (1975)
194. Halsey, G., Taylor, H.S., J. Chem. Phys., 15, 624 (1947)
195. Sips, R., J. Chem. Phys., 16, 490-495 (1948)
196. Sips, R., J. Chem. Phys., 18, 1024-1026 (1950)
197. Hill, T.L., J. Chem. Phys., 17, 762 (1949)
198. Rudnitsky, L.A., Alexeger, A.M., J. Cat., 37, 232 (1975)
199. Michaeli, I., Katchalsky, A., J. Polym. Sci., 23, 683-696 (1957)
200. Svetlov, A.K., Demenkova, T.N., Zh. Fiz. Khim. (J. Phys. Chem. U.S.S.R.), 47, 1716-1719 (1973)
201. Martinola, F., Siegers, G., V.G.B. Kraftwerktechn., 55, 40-47 (1975)
202. London, M., Fuld, J., Crane, E., Marymont Jr., J.H., Arch. Biochem. Biophys. 122, 439-448 (1967)
203. Pigman, W., Horton, D., The Carbohydrates, Vol. 1A, 2nd Ed., Acad. Press, New York (1972)
204. Peterson, S., Ann. N.Y. Acad. Sci., 57, 144-158 (1953)
205. Boyd, G.E., Adamson, A.W., Meyers Jr., L.S., J. Am. Chem. Soc., 69, 2836-2848 (1947)
206. Reichenberg, D., J. Am. Chem. Soc., 75, 589-597 (1953)
207. Znamenskii, Yu.P., Zh. Fiz. Khim. (J. Phys. Chem. U.S.S.R.), 49, 2384-2386 (1975)

208. Gladden, J.K., Dole, M., J. Am. Chem. Soc., 75, 3900-3904 (1953)
209. Helfferich, F., Plesset, M.S., J. Chem. Phys., 28, 418-424 (1958)
210. Helfferich, F., Plesset, M.S., J. Chem. Phys., 29, 697 (1958)
211. Helfferich, F., Ionenaustauscher I, Grundlagen, Verlag Chemie, GmbH, Weinheim (1959)
212. Marinsky, J.A., Ion Exchange I, Marcel Dekker Inc., N.Y. (1966)
213. Turner, J.C.R., Church, M.R., Johnson, A.S.W., Snowdon, C.B., Chem. Eng. Sci., 21, 317-325 (1966)
214. Timmerman, E.O., Z. Phys. Chem. (Frankfurt am Main), 70, 195-218 (1970)
215. Katoaka, T., Yoshida, H., Sanada, H., J. Chem. Eng. Jpn., 7, 105-109 (1974)
216. Mackie, J.S., Meares, P., Proc. Roy. Soc., A 232, 498-509 (1955)
217. Yasuda, A., Lamze, C.E., Ykenberry, L.D., Makromol. Chem., 118, 19 (1968)
218. Fernandez-Prini, R., Philipp, M., J. Phys. Chem., 80, 2041-2046 (1976)
219. Doolittle, A.K., Technology of solvents and plasticizers, John Wiley, N.Y., 769 (1954)
220. Doolittle, A.K., J. Appl. Phys., 22, 1471 (1951)
221. Cohen, M.H., Turnbull, D., J. Chem. Phys., 31, 1164 (1959)
222. Crank, J., Park, G.S., Diffusion in polymers, Acad. Press, London, 120, 373 (1968)
223. Lagos, A.E., Kitchener, J.A., Trans. Far. Soc., 56, 1245-1251 (1960)
224. Wong, C.P., Schrag, J.L., Fermy, J.D., J. Polym. Sci., Part A-2, 9, 1725 (1971)
225. Mc.Laurin, J., Green, J.W., Can. J. Chem. 47, 3947-3956 (1969)
226. Isbell, H.S., Linek, K., Hepner, K.E., Carbohyd. Res., 19, 319-327 (1971)
227. Bamford, C.H., Collins, J.R., Proc. Roy. Soc., A204, 62-84 (1950)
228. Bamford, C.H., Bamford, D., Collins, J.R., Proc. Roy. Soc., A204, 85-98 (1950)
229. Bamford, C.H., Collins, J.R., Proc. Roy. Soc., A228, 100-119 (1955)

230. Garrett, E.R., Young, J.F., J. Org. Chem., 35, 3502-3509 (1970)
231. Kooijman, C., Vellenga, K., de Wilt, H.G.J., Carbohyd. Res., 54, 33-44 (1977)
232. Gottfried, J.B., Benjamin, D.G., Ind. Eng. Chem., 44, 141-145 (1952)
233. Snowden, J.C., Schaffer, R., J. Am. Chem. Soc., 74, 499-504 (1952); *ibid.*, 74, 505-507 (1952)
234. Malyoth, G., Stein, H.W., Angew. Chem., 64, 399 (1952)
235. Schneider, F., Erleman, G.A., Naturwissenschaften, 39, 160 (1952)
236. Strocchi, P.M., Gliozzi, E., Ann. Chim., 43, 104-112 (1953)
237. Suzuki, S., Kainuma, K., Jap. Pat. 23,998 (1963)
238. Kainuma, K., Suzuki, S., Nippon Nogei Kagaku Kaishi, 38, 556-561 (1964)
239. Kainuma, K., Suzuki, S., Starch, 18, 135-141 (1966); *ibid.*, 19, 60-65 (1967); *ibid.*, 19, 66-70 (1967)
240. Scallet, B.L., Ehrenthal, I., U.S. Pat. 3,285,776 (1966)
241. Scallet, B.L., Ehrenthal, I., U.S. Pat. 3,305,395 (1967)
242. Scallet, B.L., Ehrenthal, I., U.S. Pat. 3,383,245 (1968)
243. Feather, M.S., Carbohyd. Res., 7, 86-88 (1968)
244. Sallam, M.A.E., Carbohyd. Res., 63, 127-130 (1978)
245. Doner, L.W., Carbohyd. Res., 70, 209-216 (1979)
246. Work in progress, Laboratory of Carbohydrate Technology, Eindhoven University of Technology (1980)
247. Hanack, M., Conformation theory, 155, Acad. Press, New York (1965)
248. Tumerman, L., Guth, J.H., U.S. Pat. 3,850,905 (1974)
249. Carubelli, R., U.S. Pat. 3,505,309 (1970)
250. Galup, J.S., Span. Pat. 397,810 (1974)
251. Nagasawa, T., Jap. Pat. 77 00,091 (1971)
252. Machida, I., Jap. Pat. 74 19,255 (1970)
253. Hayashibara Company, Britt. Pat. 1325727 (1973)
254. Turton, C.N., Pascu, E., J. Am. Chem. Soc., 77, 1059-1061 (1955)
255. Snowden, J.C., Thompson, R.R., J. Am. Chem. Soc., 80, 1435-1437 (1958)
256. Blair, M.C., Snowden, J.C., J. Am. Chem. Soc., 77, 3323-3325 (1955)

257. Isbell, H.S., Pigman, W., J. Res. Nat. Bur. Stand., 20, 773 (1938)
258. Montgomery, E.M., Hudson, C.S., J. Am. Chem. Soc., 52, 2101-2106 (1930)
259. Hough, L., Jones, J.K.N., Richards, E.L., J. Chem. Soc., 3854-3857 (1952); *ibid.*, 2005-2009 (1953)
260. Bots, J.P.L., Rec. Trav. Chim., 76, 515-518 (1957)
261. Nagasawa, T., Fr. Demande 2,139,789 (1973); *ibid.*, Ger. Offen 2,153,106 (1972); *ibid.*, U.S. Pat. 3,716,408 (1973)
262. Nagasawa, T., Ger. Offen. 2,224,680 (1973); *ibid.*, Jap. Kokai 72 39,545 (1972); *ibid.*, Jap. Kokai 77 00,091 (1977)
263. Zagrodzki, S., Krol, B., Rocz. Techn. Chem. Zywn., 15, 189-200 (1969)
264. Toyofuku, H., Sumi, Y., Jap. Kokai 75 29,760 (1975)
265. McLaurin, J., Green, J.W., Can. J. Chem., 47, 3957-3964 (1969)
266. Corbett, W.M., Kenner, J., J. Chem. Soc., 1431-1435 (1955)
267. Arigad, G., Biochem. J., 73, 587 (1959)
268. Pazur, J.H., Kleppe, K., J. Biol. Chem., 237, 1002 (1962)
269. Schmid, H., Monatsh. Chem., 100, 1654-1661 (1969)
270. Buhler, D.R., Thomas, R.C., Christensen, B.E., Wang, C.H., J. Am. Chem. Soc., 77, 481 (1955)
271. Langlois, D.P., Larson, R.F., U.S. Pat. 2,746,889 (1956)
272. Snowden, J.C., J. Am. Chem. Soc., 76, 4487-4488 (1954)
273. Thompson, R.R., Diss. Abstr., 17.752 (1957)
274. Täufel, K., Steinbach, K.J., Grunert, K.S., Nährung, 5, 66-83 (1961)
275. Hattori, Y., Fujii, E., Nagasawa, E., Sugiyama, B., Dempunto Gijutsu Kentyu Kaiho, 27, 26-30 (1963)
276. Kurimura, T., Endo, Y., D.G.K.K., 27, 13-17 (1963)
277. Carubelli, R., Carbohyd. Res., 2, 480 (1966)
278. Katz, E., Ehrenthal, I., Scallet, B.L., U.S. Pat. 3,690,948 (1972)
279. Katz, E., Ehrenthal, I., Scallet, B.L., U.S. Pat. 3,684,574 (1972)
280. Mitsubishi Chemical Industries, Jap. Pat. DOS 2527506 (Int. Cl. C07H,3/02) (1974)

281. Murphy, P.T., Richards, G.N., Senogles, E., Carbohyd. Res., 7, 460-467 (1968)
282. Okazaki, K., Kohno, S., Yamatsu, I., Sugiyama, K., Ueyama, S., U.S. Pat. 3,558,355 (1971)
283. Demaimay, M., Baron, C., Le Lait, 575-576, 234-245 (1978)
284. Samuelson, O., Stolpe, L., Acta Chem. Scand., 27, 3061 (1973)
285. De Wilt, H.G.J., Kuster, B.F.M., Carbohyd. Res., 19, 5 (1971)
286. De Wit, G., Chem. Weekblad, m139-m141 (1976)
287. Evans, W.M.L., Chem. Rev., 31, 537-560 (1942)
288. Pigman, W., Anet, E.F.L.J., Adv. Carbohyd. Res., 19, 175-181 (1964)
289. Feast, A.A.J., Lindberg, B., Theander, O., Acta Chem. Scand., 19, 1127-1134 (1965)
290. Telegdy-Kovats, L., Orsi, F., Räsky, K., Die Nährung, 14, 9-12 (1970)
291. Lai, Y.Z., Carbohyd. Res., 28, 154-157 (1973)
292. Feather, M.S., Harris, J.F., Adv. Carbohyd. Chem. Biochem., 28, 161-224 (1973)
293. Koizumi, K., Hashimoto, K., Miyako, M., Sawada, C., Yakugaku Zasshi, 94, 232-237 (1974)
294. Isbell, H.S., Frush, H.L., Wade, C.W.R., Hunter, C.E., Carbohyd. Res., 9, 163-175 (1969)
295. Martinez, N., Kara-Murza, S.G., Rev. CENIC, Cienc. Fis., 7, 141-151 (1976)
296. Moulik, S.P., Basu, D., Bhattacharya, P.K., Carbohyd. Res., 63, 165-172 (1978)
297. Whistler, R.L., BeMiller, J.N., Adv. Carbohyd. Chem., 13, 289 (1958)
298. Telegdy-Kovats, L., Orsi, F., Rasky, K., Elelmiszerviszgalati Kozlem, 4, 193-195 (1969)
299. Fleming, M., Parker, K.J., Williams, J.C., The Sugar Journal, april (1971)
300. Koetz, R., Neukom, H., Carbohyd. Res., 42, 365-368 (1975)
301. Lindström, L.A., Samuelson, O., Acta Chem. Scand., B31, 479-484 (1977)
302. Johansson, M., Samuelson, O., J. Appl. Pol. Sci., 22, 615-623 (1978)

303. Lindström, L.A., Carbohyd. Res., 69, 269-271 (1979)
304. Phillips, J.D., Pollard, A., Nature, 171, 41-42 (1953)
305. Hulme, A.C., Nature, 171, 610-611 (1953)
306. Rebenfeld, L., Pascu, E., J. Am. Chem. Soc., 75, 4370-4371 (1953)
307. Stanek, J., Cerneý, M., Pacák, J., The oligosaccharides, Acad. Press, 241 (1965)
308. Lischka, H., Theoret. Chim. Acta., 31, 39 (1973)
309. Corbett, W.M., Kenner, J., J. Am. Chem. Soc., 2245-2247 (1953)
310. Corbett, W.M., Kenner, J., J. Am. Chem. Soc., 1789-1791 (1954)
311. Corbett, W.M., Kenner, J., J. Am. Chem. Soc., 1431-1435 (1955)
312. Ziderman, I., Bel-Aych, J., Basch, A., Lewin, M., Carbohyd. Res., 43, 255-263 (1975)
313. Löwendahl, L., Samuelson, O., Acta Chem. Scand., B30, (8) 691-694 (1976)
314. Antkowiak, W.Z., Gessner, W.P., Milecki, J., Bulletin de l'Académie Polonaise des Sciences, 23 (2), 129-133 (1975)
315. Gleason, W.B., Barker, R., Can. J. Chem., 49, 1425 (1971)
316. Hepner, K.E., Thesis, The American University of Washington, D.C. (1972)
317. Isbell, H.S., ACS Symposium on Carbohyd. Chem., Washington D.C. (1971)
318. Kreyzing, E., Adv. Eng. Math., 4th ed., John Wiley & Sons, New York (1979)
319. Cakebead, S.H., Confectionary Production, 37 (5), 274-278 (1971)
320. Nickerson, T.A., More, E.E., J. of Food Sci., 37, 60-61 (1972)
321. Oosten, B.J., Rec. Trav. Chem. Pays-Bas, 86, 673-674 (1967)
322. Hickson, R.L., Adv. in Carbohyd. Chem., 16 (1961)
323. Wallenfels, K., Malhotra, O.P., Adv. Carbohyd. Chem., 16, 239-298 (1961)
324. Diercksen, G.H.F., Theoret. Chem. Acta., 21, 335 (1971)
325. Newton, M.D., Ehren, S., J. Am. Chem. Soc., 92, 4971 (1971)
326. Kraemer, W.P., Diercksen, G.H.F., Chem. Phys. Letters, 5, 463 (1970)
327. Kraemer, W.P., Diercksen, G.H.F., Theoret. Chem. Acta., 23, 398 (1972)
328. Snowden, J.C., Kuenne, D.J., J. Am. Chem. Soc., 75, 2788 (1953)

329. Snowden, J.C., Blair, M.G., Kuenne, D.J. J. Am. Chem. Soc., 79, 6450 (1957)

330. Hönig, H., Weidmann, H., Carbohyd. Res., 73, 260-266 (1979)

APPENDIX 1

Structure formulae

The D-family of aldoses and 2-ketoses from Pigman and Horton (203).

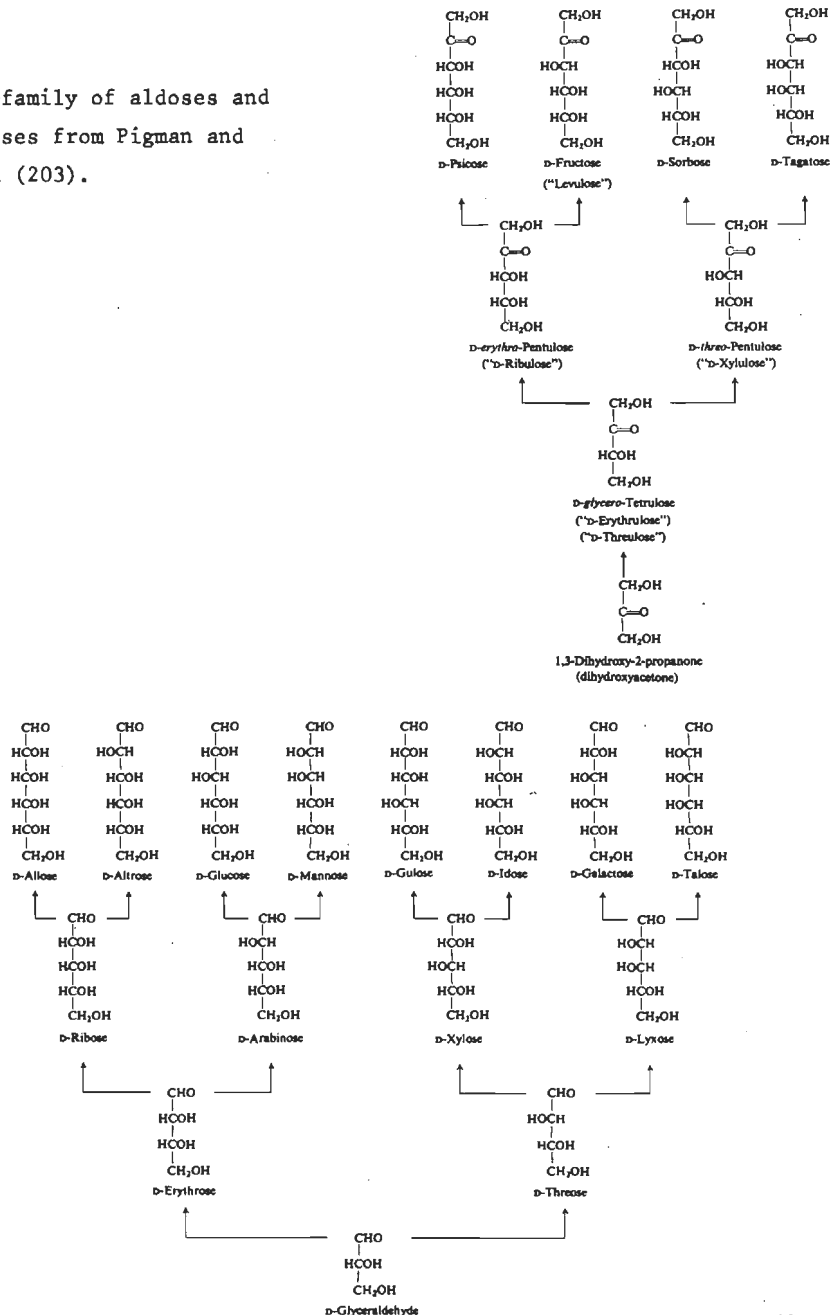

Structure formulae of sugar acid:

formic acid

acetic acid

glycolic acid

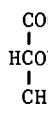

lactic acid

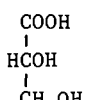

glyceric acid

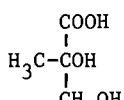

2-methyl-glyceric acid

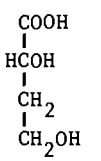

2,4-dihydroxy-butyric acid

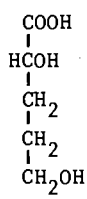

3,4-dideoxy-pentonic acid

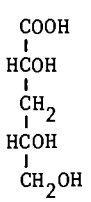

3-deoxy-pentonic acid

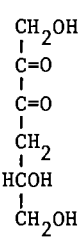

4-deoxy-2,3-hexodiulose

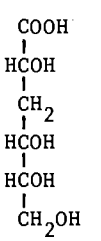

meta-saccharinic acid

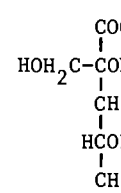

iso-saccharinic acid

APPENDIX 2

Specifications of resins

type[1]	name	wet density [kg dm^{-3}]	moisture [%]	exchange cap. wet [eq dm^{-3}]	exchange cap. dry [eq kg^{-1}]	T_{max}[2] [°C]	$C^{pol}_{NR_4^+}$[3] [eq dm^{-3}]	$C^{part}_{NR_4^+}$[3] [eq dm^{-3}]
(1)	(2)	(3)	(4)	(5)	(6)	(7)	(8)	(9)
SB-I-G	Amberlite IRA 401	.69	59-65	1.0	4.3	60	3.4	1.23
SB-I-G	Lewatit M 504	.7-.75	55-60	1.3		70	4.6	1.34
SB-I-G	Asmit 261		68[4]	.8	4.0	80		
SB-I-G	Imac S-5-50		53[4]	1.2	3.6	50	3.3	1.27
SB-I-MP	Amberlite IRA 900	.67	58-64	1.0	4.2	60	4.1	1.11
SB-I-MP	Amberlite IRA 904	.67	55-62	.7	2.6	60	1.9	.64
SB-I-MP	Amberlite IRA 938	.64	69-77	1.0	3.8	60	3.5	.62
SB-I-MP	Lewatit MP 500	.65-.7	55-60	1.2		70	4.2	1.12
SB-I-MP	Zerolit MPF	.72		1.1		60		
SB-I-MP	Duolite A 171 SC	.73	60			100[4]		
SB-I-MP	Dowex MSA-1		56-64	1.0	3.8-4.2	50		
SB-II-G	Amberlite IRA 410	.70	38-44	1.4	3.7	40	3.7	1.79
SB-II-G	Imac S-5-42		54[4]	1.1	3.4	40	3.9	1.58
SB-II-G	Sephadex QAE-A 25				3.0			
SB-II-MP	Amberlite IRA 910	.67	55-60	1.0	3.8	40		
SB-II-MP	Lewatit CA 9223	.75-.85		1.2		40	4.7	1.68
WB-MP	Amberlite IRA 93	.61	53-60	1.4	4.2	100		
WB-MP	Lewatit MP 64	.6-.7	60-65	1.5				
WB-MP	Imac A 20 S		60	1.5	4.9	65		

Remarks: 1) SB = strongly basic; WB = weakly basic;
I = type I resin; II = type II resin;
G = gel type; MP = macroporous.

2) recommended maximum operating temperature for the hydroxyl form.

3) concentration active groups related to the polymer volume $C^{pol}_{NR_4^+}$ and to the particle volume $C^{part}_{NR_4^+}$, calculated from the experimental data of Table 4.2.

4) valid for the chloride form.

APPENDIX 3

Overall-enolate model relations

In Figure 5.2 a scheme is given of the kinetic model of the isomerization of glucose, fructose and mannose. In this appendix relations between the overall model and the enolate model will be derived.

The differential equation for glucose within the *enolate model* is:

$$\frac{dC_G^-}{dt} = k_{-G} \cdot C_{Enol}^- - k_G \cdot C_G^- \qquad \text{(III-1)}$$

The concentration of the enolate ion can be calculated from equation 5.14:

$$C_{Enol}^- = \frac{k_G}{\Sigma\, k_{-J}} \cdot C_G + \frac{k_F}{\Sigma\, k_{-J}} \cdot C_F + \frac{k_M}{\Sigma\, k_{-J}} \cdot C_M \qquad \text{(III-2)}$$

Substitution of equations 5.15 and III.2 in equation III.1 gives:

$$\frac{dC_G^-}{dt} = k'_{-G} \cdot k_G \cdot C_G^- + k'_{-G} \cdot k_F \cdot C_F^- + k'_{-G} \cdot k_M \cdot C_M^- - k_G \cdot C_G \qquad \text{(III-3)}$$

The differential equation for glucose within the *overall model* is:

$$\frac{dC_G^-}{dt} = k_{FG} \cdot C_F^- + k_{MG} \cdot C_M^- - \Sigma\, k_{GJ} \cdot C_G^- \qquad \text{(III-4)}$$

Equalization of the equations III.3 and III.4 gives:

$$k_{FG} = k_F \cdot k'_{-G};\ k_{MG} = k_M \cdot k'_{-G};\ \Sigma\, k_{GJ} = k_G \left(1 - k'_{-G}\right) \qquad \text{(III-5)}$$

From the differential equations of F^-, M^- and De^- within both models more relations can be derived at a similar way:

$$\left.\begin{array}{lll} k_{GF} = k_G \cdot k'_{-F} & k_{FG} = k_F \cdot k'_{-G} & k_{MG} = k_M \cdot k'_{-G} \\ k_{GM} = k_G \cdot k'_{-M} & k_{FM} = k_F \cdot k'_{-M} & k_{MF} = k_M \cdot k'_{-F} \\ k_{GDe} = k_G \cdot k'_{-De} & k_{FDe} = k_F \cdot k'_{-De} & k_{MDe} = k_M \cdot k'_{-De} \end{array}\right\} \text{(III-6)}$$

$$\frac{}{\Sigma\, k_{GJ} + k_G\left(1 - k'_{-G}\right)} \quad \frac{}{\Sigma\, k_{FJ} = k_F\left(1 - k'_{-F}\right)} \quad \frac{}{\Sigma\, k_{MJ} = k_M\left(1 - k'_{-M}\right)}$$

(III-7)

In general

$$k_{IJ} = k_I \cdot k'_{-J} \qquad \text{(III-8)}$$

$$\sum_J k_{IJ} = k_I\,(1 - k'_{-I}) \qquad \text{(III-9)}$$

From the equations III-6,8 we can derive for glucose:

$$k_G = \frac{k_{GF}}{k'_{-F}} = \frac{k_{GM}}{k'_{-M}} = \frac{k_{GDe}}{k'_{-De}} = \frac{\Sigma\, k_{GJ}}{1-k'_{-G}} \qquad \text{(III-10)}$$

In general:

$$k_I = \frac{k_{I\hat{I}}}{k'_{-\hat{I}}} = \frac{k_{IDe}}{k'_{-De}} = \frac{\sum_J k_{IJ}}{1 - k'_{-I}} \qquad \text{(III-11)}$$

with $\hat{I}$= G, F, M; $\hat{I} \neq I$

From equation III-10:

$$k'_{-G} = 1 - \frac{\Sigma\, k_{GJ}}{k_G} \qquad \text{(III-12)}$$

From equation III-6:

$$k'_{-G} = \frac{k_{FG}}{k_F} = \frac{k_{MG}}{k_M} = \frac{k_{FG}}{k_{FDe}} \cdot k'_{-De} = \frac{k_{MG}}{k_{MDe}} \cdot k'_{-De} = Y_G \cdot k'_{-De} \qquad \text{(III-13)}$$

with

$$Y_G = \frac{k_{FG}}{k_{FDe}} = \frac{k_{MG}}{k_{MDe}} \qquad \text{(III-14)}$$

In general:

$$k'_{-I} = 1 - \frac{\sum^{J} k_{IJ}}{k_I} \qquad \text{(III-15)}$$

$$k'_{-I} = Y_I \, k'_{-De} \qquad \text{(III-16)}$$

$$Y_I = \frac{\hat{k_{II}}}{\hat{k_{IDe}}} \qquad \text{(III-17)}$$

From equation 5.16 and III-16 we calculate:

$$k'_{-De} = 1 - k'_{-G} - k'_{-F} - k'_{-M} = 1 - k'_{-De}\left(Y_G + Y_F + Y_M\right) \qquad \text{(III-18)}$$

$$k'_{-De} = \frac{1}{Y_G + Y_F + Y_M + 1} = \frac{1}{\Sigma\, Y_I + 1} \qquad \text{(III-19)}$$

Substitution of equation III-19 in equation III-16 gives:

$$k'_{-I} = \frac{Y_I}{\Sigma\, Y_I + 1} \qquad \text{(III-20)}$$

Equation III-19 in III-10 gives:

$$k_G = \frac{k_{GDe}}{k'_{-De}} = k_{GDe}\left(Y_G + Y_F + Y_M + 1\right) \qquad \text{(III-21)}$$

$$= k_{GDe} \cdot Y_G + k_{GF} + k_{GM} + k_{GDe} \qquad \text{(III-22)}$$

$$k_G = \Sigma\, k_{GJ} + Y_G \cdot k_{GDe} = \Sigma\, k_{GJ} + X_G \qquad \text{(III-23)}$$

with

$$X_G = k_{FG} \cdot \frac{k_{GDe}}{k_{FDe}} = k_{MG} \cdot \frac{k_{GDe}}{k_{MDe}} \qquad \text{(III-24)}$$

In general:

$$k_I = {}_J\Sigma\, k_{IJ} + X_I \qquad \text{(III-25)}$$

$$X_I = Y_I \cdot k_{IDe} = \hat{k}_{IJ} \cdot \frac{k_{IDe}}{\hat{k}_{IDe}} \qquad \text{(III-26)}$$

From the equations III-6 we derive:

$$\frac{k_{GDe}}{k_{FDe}} = \frac{k_{GM}}{k_{FM}} \qquad \text{and} \qquad \frac{k_{GDe}}{k_{MDe}} = \frac{k_{GF}}{k_{MF}} \qquad \text{(III-27)}$$

Substitution in equation III-24 gives:

$$X_G = \frac{k_{FG} \cdot k_{GDe}}{k_{FDe}} = \frac{k_{MG} \cdot k_{GDe}}{k_{MDe}} = \frac{k_{FG} \cdot k_{GM}}{k_{FM}} = \frac{k_{MG} \cdot k_{GF}}{k_{MF}} \qquad \text{(III-28)}$$

From this relation we derive directly the important relation:

$$\frac{k_{GF}}{k_{FG}} \cdot \frac{k_{FM}}{k_{MF}} \cdot \frac{k_{MG}}{k_{GM}} = K_{GF} \cdot K_{FM} \cdot K_{MG} = 1 \qquad \text{(III-29)}$$

We define a third auxiliary constant Z_I in terms of only isomerization constants ($\hat{k}_{II}$).
For glucose:

$$Z_G = k_{GF} + k_{GM} + X_G = k_{GF} + k_{GM} + k_{FG} \cdot \frac{k_{GM}}{k_{FM}}$$

$$Z_G = k_{GF} + k_{GM} + k_{FG} \cdot \frac{k_{GDe}}{k_{FDe}} = k_{GDe}\left(\frac{k_{GF}}{k_{GDe}} + \frac{k_{GM}}{k_{GDe}} + \frac{k_{FG}}{k_{FDe}}\right)$$

$$= k_{GDe}\left(Y_F + Y_M + Y_G\right) = k_{GDe} \cdot \Sigma\, Y_I \qquad \text{(III-30)}$$

In general:

$$Z_I = k_{IDe} \cdot \Sigma\, Y_I \qquad \text{(III-31)}$$

Combining equation III-31 with III-19 gives:

$$k'_{-De} = \frac{1}{\Sigma\, Y_I + 1} = \frac{k_{IDe}}{k_{IDe} + Z_I} \qquad \text{(III-32)}$$

When the isomerization constants k'_{II} and *one* degradation constant (e.g. k_{FDe}) is known, directly k'_{-De} can be calculated with III-32, provided that Z_I is calculated with equation III-30 from k'_{II}.

The auxiliary constants X_I, Y_I and Z_I can also be calculated from data defined within the enolate model. Substituting the equation III-8 in III-26, III-17 and III-31 gives:

$$X_I = k'_{II} \cdot \frac{k_{IDe}}{k'_{IDe}} = k'_I \cdot k'_{-I} \cdot \frac{k_I \cdot k'_{-De}}{k'_I \cdot k'_{-De}} = k_I \cdot k'_{-I} \qquad \text{(III.33)}$$

$$Y_I = \frac{k'_{II}}{k'_{IDe}} = \frac{k'_I \cdot k'_{-I}}{k'_I \cdot k'_{-De}} = \frac{k'_{-I}}{k'_{-De}} \qquad \text{(III-34)}$$

$$Z_I = k_{IDe}\ \Sigma\, Y_I = k_I \cdot k'_{-De} \cdot \frac{1 - k'_{-De}}{k'_{-De}} = k_I\left(1 - k'_{-De}\right) \qquad \text{(III-35)}$$

To calculate the degradation constants within the overall model (k_{IDe}) from the isomerization constants k'_{II} and the degradation constant k'_{-De}, equation III-35 is substituted in equation III-8:

$$k_{IDe} = k_I \cdot k'_{-De} = Z_I \cdot \frac{k'_{-De}}{1 - k'_{-De}} \qquad \text{(III.36)}$$

In section 5.2.2 a summary of the different relations is given.

LIST OF SYMBOLS

LATIN SYMBOLS

A	peak area	
A_T	Debye-Hückel constant	$kg^{.5}\ mol^{-.5}$
Ac_r	rest activity catalyst	$eq\ eq^{-1}$
B_T	Debye-Hückel constant	$kg^{.5}\ mol^{-.5}\ m^{-1}$
C_i	concentration	$mol\ m^{-3}$
$C_{NR_4^+}$	concentration of sites, related to the volume of the pores	$mol\ m^{-3}$
$C_{NR_4^+}^{part}$	concentration of sites, related to the volume of the total particle	$mol\ m^{-3}$
$C_{NR_4^+}^{pol}$	concentration of sites, related to the volume of the polymer skeleton	$mol\ m^{-3}$
$C_{NR_4^+}^{sol}$	concentration of sites, related to the volume of the solution outside the resin	$mol\ m^{-3}$
C'_{H_2O}	relative water concentration	$mol\ mol^{-1}$
c_i	constant (i = 1,2,...)	
Cap	capacity	eq
Cap'	specific capacity, related to the wet compacted weight	$eq\ kg^{-1}$
D	degradation products (reversible adsorbing)	
D_i	diffusion coefficient	$m^2\ s^{-1}$
De	reversible and irreversible adsorbing degradation products	
d	diameter	m
d_{site}	distance between active sites	nm
E	activation energy	$kJ\ mol^{-1}$
E^-	irreversible adsorbing degradation acids	
$Enol^-$	enediol anion intermediate	
F	fructose	

G	glucose	
Ga	galactose	
Gm	galacto mannose (= epilactose)	
ΔG	change of chemical potential	kJ mol^{-1}
ΔG^*	difference of free energy of pure components	kJ mol^{-1}
ΔG^E	excess free energy	kJ mol^{-1}
H	signal height	mm
ΔH	change of enthalpy	kJ mol^{-1}
h_I	hydration number of sugar I	
I	ionic strength	mol kg^{-1}
K_{AS}	Langmuir adsorption constant	m^3 mol^{-1}
K_{ES}	exchange constant	
K'_{ES}	derived exchange constant	m^3 mol^{-1}
K_{FrS}	Freundlich adsorption constant	$m^{3\alpha'}$ $mol^{-\alpha'}$
K_{SiS}	Sips adsorption constant	$m^{3\alpha}$ $mol^{-\alpha}$
k_{IJ}	reaction velocity constant	s^{-1}
k_I	isomerization constant *to* enolate ion	s^{-1}
k_{-J}	isomerization constant *from* enolate ion	s^{-1}
k'_{-J}	relative isomerization constant *from* enolate ion	s^{-1}
La	lactose	
Lu	lactulose	
M	mannose	
Ml	mannitol	
M_i	mol weight of component i	kg mol^{-1}
m_i	molality of component i	mol kg^{-1}
n_p	number of particles	
P_{IJ}	auxiliary kinetic constant	m^3 mol^{-1}
PV	pore volume relative to the capacity	m^3 eq^{-1}
p	stoichiometric coefficient	
pH	acidity : $pH = 3 - \log C_{H^+}$	
pK_S	pK_a : $pK_S = 3 - \log K_S$	
Q	electrostatic interaction factor	
$\overline{Q}_{ads}$	average heat of adsorption	kJ mol^{-1}
Q_{IJ}	auxiliary kinetic constant	s^{-1}
q	stoichiometric coefficient	

R	gas constant	$J\ mol^{-1}\ K^{-1}$
R_{pore}	radius of the pores	nm
S	sugar (S = SH + S^-): G, F, M, D, La, Lu, Gm, Gu, Sl, Sm	
S^-	ionized sugar	
SH	molecular sugar	
Sl	sorbitol	
Sm	mannitol	
S/ie	ratio of total concentration sugar and sites, both related to the volume outside the resin	
ΔS	change of entropy	$J\ mol^{-1}\ K^{-1}$
Sel	selectivity	
T	temperature	K
ΔU	change in internal energy	$kJ\ mol^{-1}$
V	volume	m^3
V'	specific volume, related to the dry weight	$m^3\ kg^{-1}$
W	weight	kg
X_I	auxiliary reaction constant (I = G, F, M)	s^{-1}
X_{1-3}	unknown products	
x	mol fraction	$mol\ mol^{-1}$
x'	weight fraction	$kg\ kg^{-1}$
x''	volume fraction	$m^3\ m^{-3}$
Y_I	auxiliary reaction constant (I = G, F, M)	
Y_{1-3}	unknown products	
Ya_S	constant of Yasuda for sugar S	
y_i	activity coefficient of component i on molarity scale	
Z_I	auxiliary reaction constant (I = G, F, M)	s^{-1}

GREEK SYMBOLS

α	exponent in the Sips adsorption isotherm
α'	exponent in the Freundlich adsorption isotherm
γ_i	activity coefficient of component i on molality scale
δ	optimalization criterium

θ_i	coverage of component i	mol eq^{-1}
μ_i	chemical potential of component i in the solution	J mol^{-1}
μ_i^*	chemical potential of the pure component	J mol^{-1}
$\mu_{H_2O}^*$	chemical potential of pure water	J mol^{-1}
ν_i	stoichiometric coefficient	
ρ	liquid density	kg m^{-3}
ϕ_i	osmotic coefficient of component i	

SUBSCRIPTS

ads	adsorption
AS	adsorption of sugar S
diff	diffusion
en	enolate
eq	equilibrium
f	filtered
gr	gross
Hg	mercury penetration porosimetric
hyd	hydration
$\underset{\sim}{I}$	G, F, M
$\hat{I}$	G, F, M, but not I
i	component or number
ie	ion exchange resin
ion	ionization
$\underset{\sim}{J}$	G, F, M, D, E
$\hat{J}$	G, F, M, D, E, but not J
ov	overall
p	particle (= pore + polymer)
pol	polymer
pore	pore of
sol	solution outside
tot	total
wc	wet compacted

SUMMARY

Less than 1% of the solar energy that reaches the earth is used for photosynthesis. Of this only 10% would be required to cover the world's present day energy demand. These data show the feasibility to use renewable resources like carbohydrates, as alternatives for energy production and chemical feedstock.

Starch from cereal crops, maize, potatoes and cassava is converted for 10% to glucose. Among the sugars, obtained by hydrolysis, glucose is the most important base material for the chemical industry.

Lactose is prepared in large quantities from whey, a by-product in the manufacture of cheese.

Isomerization of glucose gives fructose and a little mannose. Lactose gives in a similar way lactulose and some epilactose.

A reaction mixture of equal amounts of glucose and fructose, known as isoglucose or isomerose, has a sweetness and taste comparable with sucrose (cane- and beet-sugar), which makes it a good alternative for sucrose in certain applications. The isomerization product lactulose is used in medicine as a laxans. Isomerization products can also be used as a feedstock for other processes such as dehydration or hydrogenation.

The glucose isomerization is catalyzed by alkali and by the enzym glucose isomerase. For the isomerization of lactose as yet no enzym is available.

This thesis deals with the kinetics of the heterogeneous alkaline isomerization with strongly alkaline ion exchangers as a catalyst. An important prior condition for the experimental conditions was that the results should also provide useful information in regard to possible commercial applications.

The homogeneous isomerization is shown to be first order in the concentration of the sugar anion. This concentration is a function of the total sugar concentration, the pH and the ionization constant of the sugar.

For the heterogeneous isomerization an anion exchanger with hydroxyl groups as counter ion is used. When sugar adsorbs, the different molecules and ions are more or less randomly distributed over the available pore volume, either in molecular or in ionic form. Due to the presence of numerous hydroxyl groups, the adsorbed sugar will generally be stronger ionized. Just as for the homogeneous reaction it is supposed that with ion exchangers only the sugar ion isomerizes. In this thesis the heterogeneous isomerization is described as a pseudo homogeneous reaction inside the pores of the ion exchanger.

In order to obtain quick and accurate information on the composition of reaction samples, much attention has been paid to the analysis of sugars and sugar acids. The sugars (mono- and disaccharides) were generally analyzed by ion exchange chromatography. For low conversions a colorimetric analysis for ketoses has been developed. This system allows the determination of ketoses quantitatively in the presence of a more than 5000 fold excess of aldoses. For the analysis of sugar acids isotachophoresis was applied.

When a sugar adsorbs on a strongly basic ion exchanger, the total sugar concentration inside the resin is relatively high. To determine the degree of ionization in such concentration solutions, potentiometric titrations have been carried out over a wide range of glucose concentrations. The ionization can be described with an ionization constant that is independent of the concentration by assuming that at 298 K the glucose molecule is hydrated with 3.5 molecules of water and that the glucose anion is not hydrated. The influence of the temperature on the ionization and the hydration is discussed.

For several ion exchangers the quantity of active groups (the capacity) is determined by titrating the hydroxyl groups in the resin. Combination of these results with the measured pore volume of the resin gives directly the hydroxyl concentration inside a fresh resin. The adsorption of the different types of sugars on various ion exchangers is measured as a function of the external sugar concentration and the temperature. The ionization and hydration model described above makes it possible to calculate the concentrations of the various components inside the resin. The adsorption of sugars on ion exchangers can be described by an adsorption relation as given by Sips.

We found in our kinetic study that diffusion can play an important role. For this reason the internal diffusion coefficient is measured for IRA 401 (gel-type) and IRA 938 (macroreticular-type). A mathematical expression is derived to calculate this internal diffusion coefficient as a function of the temperature, the type of sugar and the type of resin.

The interconversion of glucose, fructose and mannose and their degradation reactions are described in the overall model with 6 isomerization and 3 degradation rate constants. As all these reactions, however, pass via the same enediol anion intermediate, a kinetic model based on this enolate mechanism gives a better description: the enolate model. The various degradation reactions of the overall model are in the enolate model reduced to one single reaction. Mathematical expressions are derived to convert rate constants from one model to the other.

The main aim of this thesis is the determination to the kinetics of the reaction system as a function of the process parameters, in such a way that it enables us to optimize the selectivity of the process.

From our experimental results we can conclude that the isomerization of glucose can be described well with the enolate model. This conclusion is based on the facts that the potential energy level of the enolate ion as well as the product distribution of the degradation products are independent of the type of sugar that is used as starting material. The isomerization in the anion exchanger is first order in the sugar anion concentration and totally independent of the concentration of molecular sugar or the concentration of hydroxyl ions.

The selectivity of the isomerization increases with decreasing temperature and increasing sugar or with a decreasing water concentration. The increase in selectivity of the isomerization with different ion exchangers in the sequence NaOH → Bio-Rad → IRA 904 → IRA 401 can be ascribed too to a decrease of the water concentration.

The high selectivity, combined with the possibility to influence the catalytic properties predictable by changing the properties of the ion exchanger, makes the heterogeneous isomerization in many aspects more attractive than the homogeneous isomerization process.

SAMENVATTING

Minder dan 1% van de zonneënergie die de aarde bereikt, wordt daadwerkelijk door middel van fotosynthese omgezet. Toch zou slechts 10% hiervan al voldoende zijn om het huidige energieverbruik van de wereld te dekken. Deze getallen geven een indruk van de kwantitatieve ruimte die er is voor toepassing van gegroeide grondstoffen, zoals koolhydraten, als alternatieve energiebron, en a fortiori als grondstof voor de chemische industrie.

Zetmeel van graan, mais, aardappelen en cassava wordt voor ongeveer 10% omgezet tot glucose, dat van alle door hydrolyse verkregen suikers de belangrijkste grondstof voor de chemische industrie is.

Daarnaast wordt lactose in grote hoeveelheden geproduceerd uit wei, een nevenproduct bij de kaasbereiding.

Isomerisatie van glucose geeft fructose en een beetje mannose. Lactose geeft in vergelijkbare hoeveelheden lactulose en epilactose.

Een reactiemengsel van gelijke hoeveelheden glucose en fructose, isoglucose of isomerose genaamd, heeft een vergelijkbare zoetheid als sucrose (riet- of bietsuiker). Hierdoor is het voor bepaalde toepassingen geschikt als alternatief voor sucrose. Het isomerisatieproduct lactulose wordt in de geneeskunde gebruikt als laxeermiddel. Isomerisatieproducten kunnen verder gebruikt worden als uitgangsstoffen voor andere processen zoals dehydratatie of hydrogenering.

De isomerisatie van glucose kan worden gekatalyseerd door een base of door het enzym glucose isomerase. Voor de isomerisatie van lactose is nog geen enzym beschikbaar.

In dit proefschrift wordt de kinetiek van de heterogeen alkalische isomerisatie met sterk basische ionenwisselaars als katalysator beschreven. Een belangrijke randvoorwaarde bij de keuze van de experimentele condities was dat de resultaten ook informatie zouden moeten geven voor eventuele commerciële toepassingen.

Er wordt verondersteld dat de homogene isomerisatie eerste orde is

in de suiker ion concentratie. Deze laatste is, behalve van de totale hoeveelheid suiker, afhankelijk van de pH en de ionisatie konstante van het betreffende suiker.

Voor de heterogene isomerisatie worden basische ionenwisselaars gebruikt met hydroxyl groepen als tegenion. De geadsorbeerde suiker is als molecuul of in de ionvorm min of meer homogeen over het beschikbare porievolume verspreid. Door de aanwezigheid van de hydroxyl groepen zullen de geadsorbeerde suikers in vrij sterke mate geïoniseerd zijn. Evenals bij de homogene reactie wordt ook bij het gebruik van ionenwisselaars verondersteld dat alleen het suikerion isomeriseert. In dit proefschrift wordt de heterogeen katalytische isomerisatie beschreven als een pseudo homogene reactie in de poriën van de ionenwisselaar.

Om snel en nauwkeurig gegevens te verkrijgen over de samenstelling van de reactiemonsters, is veel aandacht besteed aan de analyse van suikers en suikerzuren. De suikers (mono- en disacchariden) werden meestal vloeistofchromatografisch geanalyseerd. Voor metingen bij kleine omzettingen werd een speciale colorimetrische analyse voor ketosen ontwikkeld. Deze ketose analyse maakt het mogelijk kwantitatief ketosen te bepalen in een meer dan 5000-voudige overmaat aldosen. Voor de analyse van suikerzuren werd isotachoforese gebruikt.

Adsorptie van suikers aan sterk basische ionenwisselaars geeft in de poriën relatief sterk geconcentreerde suikeroplossingen. Voor het bepalen van de ionisatiegraad in deze geconcentreerde oplossingen zijn over een breed concentratiegebied potentiometrische titraties uitgevoerd. De ionisatie kan onafhankelijk van de concentratie met een konstante ionisatie konstante worden beschreven door voor het glucose molecuul een hydratatiegetal van 3,5 en voor het glucose ion geen hydratatie aan te nemen. De invloed van de temperatuur op de ionisatie en de hydratatie is eveneens beschreven.

Voor verscheidene ionenwisselaars zijn het aantal aktieve groepen (de capaciteit) bepaald door de hydroxyl groepen in de wisselaar te titreren. Uit deze resultaten, gecombineerd met het gemeten porievolume, kan de hydroxyl concentratie in de poriën van een verse wisselaar bepaald worden. De adsorptie van suikers aan diverse wisselaars is gemeten als functie van de uitwendige suiker concentratie en de temperatuur. De uitgewerkte ionisatie- en hydratatietheorie maakt het

mogelijk de concentraties van de verschillende stoffen in de poriën te berekenen. De adsorptie van suikers aan ionenwisselaars kan beschreven worden met de adsorptie relatie van Sips.

Bij de isomerisatie van suikers kan diffusie een belangrijke rol spelen. Om deze reden is de inwendige diffusie coëfficiënt gemeten voor de ionenwisselaars IRA 401 (gel-type) en IRA 938 (macroporeus-type). Een wiskundige relatie is ontwikkeld om deze inwendige diffusie coëfficiënt te berekenen als functie van de temperatuur, het type suiker en het type ionenwisselaar. De isomerisatie van glucose, fructose en mannose met hun degradatie reacties worden in het zogenaamde overall model beschreven met 6 isomerisatie en 3 degradatie snelheidskonstanten. Omdat echter al deze reacties via hetzelfde enolaat ion verlopen, geeft een model, gebaseerd op dit enolaat mechanisme, een betere beschrijving: het enolaat model. Er zijn wiskundige relaties afgeleid om de snelheidskonstanten van het ene model om te rekenen in het andere.

Het belangrijkste doel van dit proefschrift is om de kinetiek van het reactiesysteem te bepalen als functie van diverse procesvariabelen zodat de condities voor een optimale selectiviteit van de reactie kunnen worden vastgesteld.

Uit onze experimentele resultaten is gebleken dat de isomerisatie van glucose goed beschreven kan worden met het enolaat model. Deze conclusie is gebaseerd op het feit dat zowel het potentiële energieniveau van het gevormde enolaat ion als ook de productverdeling van de degradatieproducten onafhankelijk zijn van de suiker, die als uitgangsmateriaal is gekozen. De isomerisatie in de ionenwisselaar is eerste orde in de suiker ion concentratie en onafhankelijk van de concentratie van de moleculaire glucose of de concentratie van de hydroxyl ionen.

De selectiviteit van de isomerisatie reactie neemt toe met afnemende temperatuur en toenemende suiker concentratie of afnemende water concentratie. De toename van de selectiviteit van de isomerisatie voor de verschillende wisselaars in de volgorde NaOH → Bio-Rad → IRA 904 → IRA 401 kan eveneens toegeschreven worden aan een afnemende water concentratie.

De hoge selectiviteit, gecombineerd met de mogelijkheid om de katalytische eigenschappen voorspelbaar te beïnvloeden door de eigen-

schappen van de ionenwisselaar te veranderen, maken de heterogeen alkalische isomerisatie in vele opzichten aantrekkelijker dan de homogene isomerisatie.

LEVENSBERICHT

Johannes A.W.M. Beenackers werd op 12 mei 1948 geboren te Bavel, gemeente Nieuw Ginneken. Na de lagere school volgde hij de opleiding aan de St. Laurentius U.L.O. te Breda, waar hij het diploma A en B behaalde in respectievelijk 1964 en 1965. Daarna volgde hij aan de Hogere Technische School St. Virgilius te Breda de opleiding in de Chemische Techniek. In 1970 werd het diploma behaald. Tijdens het vervullen van de militaire dienstplicht in de periode 1970-1971, begon hij aan de Technische Hogeschool te Eindhoven de studie voor scheikundig ingenieur, welke werd afgesloten in maart 1976 na een afstudeerperiode onder leiding van prof.drs. H.S. van der Baan, hoogleraar in de chemische technologie. Per 1 april 1976 trad hij in dienst van de Technische Hogeschool te Eindhoven als wetenschappelijk ambtenaar bij de vakgroep Chemische Technologie, waar het in dit proefschrift beschreven onderzoek werd verricht. Per 1 juni 1980 zal hij in dienst treden van DSM te Geleen.

DANKWOORD

Het onderzoek, weergegeven in dit proefschrift, is tot stand gekomen dankzij de medewerking van velen. In het bijzonder geldt dit voor de medewerkers en studenten van de vakgroep Chemische Technologie. Aan allen hiervoor mijn hartelijke dank.

De meeste dank ben ik verschuldigd aan M.J.M. van der Aalst. Hij heeft gedurende 2½ jaar, gedeeltelijk binnen een samenwerkingsverband met Philips-Duphar, op een breed gebied bijgedragen tot het goede verloop van het onderzoek.

Veel dank ben ik verschuldigd aan de afstudeerders E.G.R.M. van Boxtel, P.G. Eggels, J.A.M. Driessen, P.C.C. Smits en P.F.H.A. van Dooren, als ook F.Th.H.M. Wijnhoven en J.G.J. Haan die allen met veel inzet en enthousiasme hebben meegewerkt aan het onderzoek. Eveneens dank ik de vele praktikanten en stagiaires die een bijdrage hebben geleverd tot het onderzoek.

De discussies met diverse medewerkers van Philips-Duphar hebben bijgedragen tot een verdieping van het inzicht in de praktische toepasbaarheid van de in het proefschrift beschreven reaktiesysteem. Mijn hartelijke dank hiervoor.

Verder ben ik veel dank verschuldigd aan de medewerkers binnen de werkgroep Koolhydraten. De heer B.F.M. Kuster dank ik voor de interessante discussies die wij gevoerd hebben over het onderzoek. De heer M.P.A. van der Heyden ben ik veel dank verschuldigd, niet alleen voor de technische werkzaamheden maar ook voor de vele andere taken die hij binnen de werkgroep op zich had genomen. De heer L.A.Th. Verhaar dank ik voor zijn bijdrage op het gebied van de vloeistofchromatografie.

De heer H.C.B. Ladan heeft de foto's gemaakt met behulp van een elektronenmicroscoop. De vakgroep Instrumentele Analyse heeft de analyse van monsters met isotachoforese verzorgd. De kwikporositeitsmetingen zijn uitgevoerd door N. van Westen van de TH Delft. Aan allen mijn hartelijke dank.

De Centraal Technische Dienst, en in het bijzonder de glasblazerij, ben ik dank verschuldigd voor het accuraat uitvoeren van de vaak zeer moeilijke opdrachten.

Mijn dank gaat verder uit naar de heer R.J.M. van der Wey, die de tekeningen in dit proefschrift heeft verzorgd. Mevr. E.J.W.J. Eichhorn-Meijers ben ik in het bijzonder dank verschuldigd voor het feit dat zij binnen zeer korte tijd het proefschrift op een zeer conciëntieuze wijze heeft getypt.

Gaarne maak ik van deze gelegenheid gebruik om ook familie, vrienden en bekenden te danken voor hun indirekte bijdragen tot de totstandkoming van dit proefschrift.

STELLINGEN

1. De bewering van Mathlouthi, Luu and Luu dat in sterk geconcentreerde waterige suikeroplossingen boven een bepaalde concentratie de suikermolekulen zich bevrijden van hun oplosmiddel en hierdoor zuiver water doen ontstaan, is in strijd met de thermodynamica.

   Mathlouthi, M., Luu, C., Luu, O.V., Acad. Sc. Paris, T. 289, Nr. 3, 81-84 (1979)

2. Bij de oxidatie van thiolen met polymeer-gebonden cobaltporphyrines als katalysator neemt Rollmann ten onrechte de bijdrage van zure bijprodukten aan de deaktivering van de katalysator niet in beschouwing.

   Rollmann, L.D., J. Am. Chem. Soc., 97, 2132-2136 (1975)
   Schutten, J.H., Beelen, T.P.M., J. Mol. Catalysis, aangeboden voor publikatie

3. De methode van Dautzenberg et al. naar de bepaling van kinetische parameters voor de Fischer-Tropsch synthese is, gezien de bevindingen van Madon, aan twijfel onderhevig.

   Dautzenberg, F.M., Helle, J.N., van Santen, R.A., Verbeek, H., J. of Catal., 50, 8-14 (1977)
   Madon, R.J., J. of Catal., 57, 183-186 (1979)

4. De door Dirkx et al. gegeven relatieve snelheidskonstanten bij de oxidatie van gluconzuur dienen slechts als gemiddelde waarden tijdens de betreffende experimenten te worden beschouwd.

   Dirkx, J.M.H., van der Baan, H.S., van den Broek, M.A.J. J., Carbohydr. Res., 59, 63-72 (1977)

5. De door Klinken en van Dongen beschreven verdunningsmethode is een bruikbare techniek om de kinetiek van een heterogeen gekatalyseerde reaktie in een trickle bed reaktor te bestuderen. Indien ook homogene reakties kunnen optreden dient men echter terdege rekening te houden met een toename van de invloed van homogene omzettingen met toenemende katalysatorbedverdunning.

van Klinken, J., van Dongen, R.H., Chem. Eng. Sci., 35, 59-66 (1980)

6. Kumar and Ruckenstein tonen aan dat de ontleding van $Bi_2Mo_2O_9$ (β-bismuthmolybdaat) naar Bi_2MoO_6 (γ-vorm) thermisch verloopt. Het is echter diskutabel of deze thermische reduktie bij aanwezigheid van olefinen een belangrijke rol speelt.

Kumar, J., Ruckenstein, E., J. of Solid State Chem., 31, 41-46 (1980)

7. Katalysatorarchitektuur is erop gericht katalysatoren te maken die de hoge selektiviteit van enzymen paren aan de grote bestendigheid der konventionele katalysatoren, waarbij bovendien nog een juiste positie tussen de grote specifisiteit der eerste en de redelijke universaliteit der laatste gekozen kan worden.

Projektgroep Katalysatorarchitektuur THE

8. Omdat volgens de IUPAC-normeringen een concentratie uitgedrukt moet worden is mol m^{-3}, verdient het aanbeveling de definitie van de zuurgraad pH hierbij aan te passen. Een neutrale oplossing heeft in de nieuwe eenheden een pH van 4.

IUPAC (International Union of Pure and Applied Chemistry), Manual of symbols and technology for physicochemical quantities and units, aangepast op 7 juli 1969; Pure and Appl. Chem., 21, 1-44 (1970)

9. De invoering van K (Kelvin) and Pa (Pascal) als maat voor temperatuur en druk kan sterk versneld worden wanneer de fabrikanten van temperatuur- en drukmeters hun produkten aan de meest recente normeringen zouden aanpassen.

IUPAC, Pure and Appl. Chem., 21, 1-44 (1970)

10. Het uitdrukken van reaktiesnelheidskonstanten voor katalytische reakties in reciproke seconden verdient meer te worden toegepast.

11. Men dient zich af te vragen wat de motieven van de overheid zijn om in een regenachtig land als Nederland de niet-kostwinner slechts bromfietsvergoeding te geven, terwijl zijn kollega als kostwinner in aanmerking komt voor autokostenvergoeding wanneer geen openbaar vervoer aanwezig is tussen woonplaats en standplaats.

Bezoldiging Burgerlijk Overheidspersoneel; De verplaatsingskostenbeschikking 1962, art. 12 en De reis- en pensionkostenbeschikking ongehuwd burgerlijk rijkspersoneel, par. 3, losbladige uitgave, Samson, Alphen a.d. Rijn

12. Het verdient aanbeveling de proefboringen naar geneeskrachtige zoutoplossingen (te Nieuwerschans) en de proefboringen naar eventuele opslagplaatsen van radioaktief afval in zoutlagen zodanig op elkaar af te stemmen dat ook op de lange termijn het kuuroord een positieve bijdrage kan blijven leveren aan de gezondheid van de baders.

Eindhoven, 2 mei 1980 J.A.W.M. Beenackers